INVESTIGATION OF SYNERGISTIC NO_X REDUCTION FROM COFIRING AND AIR STAGED COMBUSTION OF COAL AND LOW ASH DAIRY BIOMASS IN A 30 KILOWATT LOW NO_X FURNACE

A Dissertation

by

BENJAMIN DANIEL LAWRENCE

Submitted to the Office of Graduate Studies of
Texas A&M University
In partial fulfillment of the requirements for the degree of

DOCTOR OF PHILOSOPHY

Chair of Committee,	Kalyan Annamalai
Committee Members,	Sergio Capareda
	Tim Jacobs
	Gerald Morrison
Head of Department,	Andreas Polycarpou

August 2013

Major Subject: Mechanical Engineering

ABSTRACT

Alternate, cost effective disposal methods must be developed for reducing phosphorous and nitrogen loading from land application of animal waste. Cofiring coal with animal waste, termed dairy biomass (DB), is the proposed thermo-chemical method to address this concern. DB is evaluated as a cofired fuel with Wyoming Powder River Basin (PRB) sub-bituminous coal in a small-scale 29 kW_t low NO_x burner (LNB) facility. Fuel properties, of PRB and DB revealed the following: a higher heating value of 29590 kJ/kg for dry ash free (DAF) coal and 21450 kJ/kg for DAF DB. A new method called Respiratory Quotient (RQ), defined as ratio of carbon dioxide moles to oxygen moles consumed in combustion, used widely in biology, was recently introduced to engineering literature to rank global warming potential (GWP) of fuels. A higher RQ means higher CO_2 emission and higher GWP. PRB had an RQ of 0.90 and DB had an RQ of 0.92. For comparison purposes, methane has an RQ of 0.50. For unknown fuel composition, gas analyses can be adapted to estimate RQ values.

The LNB was modified and cofiring experiments were performed at various equivalence ratios (ϕ) with pure coal and blends of PRB-DB. Standard emissions from solid fuel combustion were measured; then NO_x on a heat basis (g/GJ), fuel burnt fraction, and fuel nitrogen conversion percentage were estimated. The gas analyses yielded burnt fraction ranging from 89% to 100% and confirmed an RQ of 0.90 to 0.94, which is almost the same as the RQ based on fuel composition. At the 0.90 equivalence

ratio, unstaged pure coal produced 653 ppm (377 g/GJ) of NO_x. At the same equivalence ratio, a 90-10 PRB:LADB blended fuel produced 687 ppm (397 g/GJ) of NO_x. By staging 20% of the total combustion air as tertiary air (which raised the equivalence ratio of the main burner to 1.12), NO_x was reduced to 545 ppm (304 g/GJ) for the 90-10 blended fuel. Analysis of variance showed that variances were statistically significant because of real differences between the independent variables (equivalence ratio, percent LADB in the fuel, and staging intensity).

DEDICATION

This work is dedicated to my grandparents, each of whom inspired me in their own unique way. This work is the tree that has grown from the seeds they planted long, long ago. My only hope is that it will provide shade for others.

ACKNOWLEDGEMENTS

No scientific work occurs in a vacuum and although my name might appear on the title page, I must acknowledge everyone who has come before me and assisted me along the way.

First acknowledgement must go to God, the Heavenly Father. I always have and always will consider all of my scientific endeavors as an attempt to better understand the universe you created. I pray that I am a worthy steward of the responsibilities you have given me.

I wish to give thanks to all of my professors at Kansas State and Texas A&M. I appreciate the countless hours you put in guiding my education. If I have absorbed 10% of the knowledge you attempted to pass on to me, I consider it a success. Particular thanks must be extended to my committee. Thank you for the guidance and answers to my never-ending questions.

I give thanks to my family and friends who supported me through the entire process. I would be lying if I said that there weren't many doubts along the way. I am sure that there were many times when giving up on me was the easy choice. Thank you for staying with me.

Special thanks are extended to Siva Thanapal. You have done almost all of the leg work for me while I have been away from campus. I do not take for granted how valuable you have been. I am very blessed to have you as a colleague. I am even more blessed to have you as a friend.

I give thanks to my daughter. Watching you grow and learn has inspired me in how I go about growing and learning. Every day I am shocked and amazed to see the world through your eyes. Your perception humbles me. I can't wait to see what lessons you still have in store for me.

Lastly, and most importantly, I thank my wife for all the sacrifices she made along the way. You have supported me and loved me more than I deserved. As impossible as it might be to believe, it is actually finished, Babe. I know I could not have done it without you.

NOMENCLATURE

AgB	Agricultural Waste Based Biomass
AnB	Animal Waste Based Biomass
ANOVA	Analysis of Variance
BF	Burnt Fraction
BTU	British Thermal Unit
C	Carbon
CAFO	Concentrated Animal Feeding Operation
CB	Cattle Biomass
CCOFA	Close Coupled Over Fire Air
CFB	Circulating Fluidized Bed
CH_4	Methane
CO	Carbon Monoxide
CO_2	Carbon Dioxide
DAF	Dry Ash Free
DB	Dairy Biomass
dc	Critical Diameter
EA	Excess Air
EPA	Environmental Protection Agency
FB	Feedlot Biomass
FC	Fixed Carbon or Fully Composted (context dependent)

g	Gram
GC	Gas Chromatograph
GJ	Gigajoule
H	Hydrogen Atom
H_2S	Dihydrogen Sulfide
HCN	Hydrogen Cyanide
HHV	Higher Heating Value
K	kelvin
kg	Kilogram
kJ	Kilojoule
LADB	Low Ash Dairy Biomass
LB	Litter Biomass
lb	Pound
LNB	Low NO_x Burner
LOI	Loss on Ignition
min	Minute
mmBTU	Million BTUs
MJ	Megajoule
MS	Mass Spectrometer
MW	Megawatt
N	Nitrogen Atom
N_2	Atmospheric Nitrogen (diatomic)

N_{CONV}	Nitrogen Conversion Efficiency
NH_3	Ammonia
NO	Nitrogen Monoxide
NO_2	Nitrogen Dioxide
NO_x	NO + NO_2
O	Oxygen Atom
O_2	Atmospheric Oxygen (diatomic)
$O_{2,A}$	Ambient Oxygen Concentration (20.9%)
OFA	Over-Fire Air
PC	Partially Composted
PRB	Powder River Basin (a subbituminous coal)
PL	Poultry Litter
PM	Particulate Matter
q	Respiratory Ratio
r	N_2/O_2 in oxidant
RM	Raw Manure
RQ	Respiration Quotient
S	Sulfur
SCR	Selective Catalytic Reduction
SNCR	Selective Non-catalytic Reduction
SO_2	Sulfur Dioxide
SOFA	Separated Over-Fire Air

SO_x	Sulfur Oxides
TCEQ	Texas Commission on Environmental Quality
TGA	Thermogravimetric Analyzer
TMDL	Total Maximum Daily Load
$T_X L$	Te_x as Lignite
USDA	United States Department of Agriculture
VM	Volatile Matter
Y_C	Carbon Mass Fraction

SYMBOLS

R_{90}	Mass Percentage Remaining in a 90 μm Sieve
°C	Degree Centigrade
ϕ	Equivalence Ratio
μm	Micrometer or Micron
ν_{O2}	Oxygen Required for Stoichiometric Combustion

TABLE OF CONTENTS

Page

LIST OF FIGURES

FIGURE Page

FIGURE Page

FIGURE Page

LIST OF TABLES

1. INTRODUCTION

Large coal-fired plants in the United States produce about 310 GW of electricity requiring almost 930 GW of thermal energy input with a plant efficiency of 33%. In addition to producing global warming CO_2 gas, they also emit pollutants such as NO_x and SO_2. Cofiring is defined as combustion of two dissimilar fuels being burned together simultaneously. Cofiring is a cost effective method in reducing fossil fuel costs and in promoting the use of alternate fuels. Cofiring can provide up to 15% of heat input and has been successfully demonstrated at over 150 installations worldwide (Baxter, 2004). Boiler efficiency has not suffered when the portion of cofired fuel is of the order 5-10%. According to Laux et al. (2011) biomass fuels can be cofired by

- premixing two solid fuels (as done in these experiments) when biomass contributes <10% of the total heat input,
- by firing coal in the central fuel nozzle with biomass in the coaxial nozzle, and
- by firing biomass separately in a single boiler when heat input is more than 10%. Firing biomass separately is less desirable because of complexities in air tuning.

Biomass can be classified as AgB or AnB. In traditional pulverized coal-fired boilers, coal is milled to a fine powder (approximately 70% smaller than 75 microns) and fired in a suspension-fired boiler. Hence, utility companies expect that biomass needs to be ground to a similar pulverization.

Recently, the interest in renewable fuels has increased because of global warming concerns and current regulations limiting the amount of hazardous pollutants released into the atmosphere. Biomass has been touted as a renewable fuel source that could reduce greenhouse CO_2 emissions. However, this statement needs to be examined more closely. The use of biomass itself does not directly reduce CO_2 per MJ of fuel burned (Annamalai and Puri, 2005). Baxter (2004) demonstrated that the direct emissions of CO_2 in g/MJ from coal and biomass are similar even though the H/C ratio is higher for biomass than it is for coal. CO_2 emissions for coal and biomass are the same because they have similar heat-based carbon loading. In theory, a higher H/C ratio implies a lower carbon content and hence lower CO_2 formation on a mass basis. However, in addition to having a higher H/C ratio biomass has a higher O/C ratio, which lowers the heat value. Thus, more fuel is required to maintain a constant heat rate. Therefore, the emission of CO_2 on a heat basis is normally unaffected by cofiring. The advantages of cofiring with biomass include a reduction of fueling and capital cost, fossil CO_2 reduction due to biomass's classification as a renewable fuel, and NO_x reduction when firing low nitrogen agricultural biomass fuels. The issues with cofiring are high nitrogen content of biomass fuels, potential fouling, and catalytic components of the cofired fuel. Most of the early research has concentrated on agricultural biomass, which typically contains low nitrogen (exceptions include Alfalfa and rice hulls) and sulfur. The current research deals with cofiring of high nitrogen animal waste biomass fuels.

Intensive animal feeding operations (dairy, cattle, and poultry farms) are the cornerstone of the agricultural economy in Texas and neighboring states in the Southern Great Plains. These operations create large amounts of animal waste that must be safely disposed of in order to avoid environmental degradation. Potentially harvestable biomass from cattle farms from all of the confined feeding operations in the U. S. easily exceeds 100 million tons per year on a dry basis with 6-12 million dry tons in the Texas Panhandle alone. If cattle manure is not beneficially utilized as fertilizer or properly disposed of, these by-products may become sources of air, water, or soil pollution and CH_4 gas emissions in U.S. farm areas, including the Southern Great Plains. Methane is listed as a greenhouse gas. When cattle biomass dries, the cattle's feet grind the dry manure, which creates a dust emission with particulate matter ranging from 8.5 to 12 microns. The PM 10 regulation requires that particulate matter less than 10 μm generated by concentrated animal feeding operations (CAFO) be reduced to less than 150 $\mu g/m^3$. Total suspended particles in feedlot dust can range from 150 $\mu g/m^3$ to 400 $\mu g/m^3$ (Sweeten, 1979).

Cattle manure is the product of undigested feed and can be used as a fuel by mixing it with coal and firing it in an existing coal suspension fired combustion system. Due to its potential use as a fuel source, cattle manure will be henceforth termed as CB. Compared to coal, CB fuels are higher in moisture, nitrogen, sulfur, and ash as well as lower in heat content. Nitrogen and sulfur are of particular concern because combustion can oxidize fuel-bound nitrogen to NO_x (called fuel NO_x) and sulfur to SO_2.

NO_x, a byproduct of the coal combustion process, is a pollutant that is harmful to the environment and human health. Total NO_x formed in combustion is the sum of fuel NO_x and oxidation of atmospheric nitrogen, called thermal NO_x. Because of its associated hazards, NO_x is an EPA regulated emission.

In staged combustion injection of a portion combustion, air is delayed until downstream of the initial flame. This creates a fuel-rich zone that drives the formation of molecular nitrogen and inhibits fuel NO_x production. In addition, lower flame temperatures inhibit thermal NO_x production. With the addition of tertiary air at the end of the flame, front combustion is completed in the over-fire burn zone.

This work focuses on studying the effects of cofiring coal with DB, which contains more nitrogen than coal. The objective is to determine the comparative performance of a burner when it is fired with coal and then cofired with blends of Coal:DB. Furthermore, the research demonstrates the effects of staged combustion used in conjunction with cofiring of AnB fuels.

PRB was used as the baseline fuel for the parametric studies. In addition to baseline experiments, PRB was also cofired with LADB. High ash DB was not considered as a fuel because of its high ash content. The ash accumulates inside the furnace causing significant ash fouling and slagging problems that damage measurement devices and cause significant clogging in the gas sample ports. Goughnour (2006) demonstrated that cofiring high ash partially composted feedlot biomass completely clogged the small-scale reactor. This study used the following PRB:LADB fuel blends: 95:5, 90:10, and 85:15. The equivalence ratio varied from 0.85 to 1.05 in 0.05

increments. Air was staged through either the lip or arm staging apparatus from 0% to 30% in 10% increments. Oxygen, carbon dioxide, carbon monoxide, and NO_x emissions were measured. In addition, a new method of gas analysis called the RQ method was introduced and used for gas analysis.

2. LITERATURE REVIEW

2.1 Introduction

It has been well established that cofiring coal and agricultural biomass can be used as a NO_x control technique. In particular, Tillman (2000) demonstrated that cofiring reduced NO_x at a greater rate than the amount of biomass added to the coal due to the high volatile content of the biomass rapidly consuming oxygen at the flame front (see Figure 2.1). In addition, using animal waste as a fuel source for heat and power is not a novel technology. Wilder (1932) described burning cow manure for home heating and cooking in 1869. It is worthwhile to research what information is already known on the technology in order to add to the general body of knowledge.

2.2 Coal Combustion

NO_x is created during combustion from both atmospheric nitrogen and from fuel-bound nitrogen bonding with oxygen to form NO and NO_2. NO_x produced from oxidation of atmospheric N_2 is called thermal NO_x (to emphasize its strong temperature dependence). Thermal NO_x production does not become significant until combustion temperatures reach 1800 K. At this temperature, there is sufficient energy to break the relatively stable N_2 triple bond and form N radicals. Prompt NO_x is formed directly at the flame front in fuel rich environments when N_2 from air is converted to HCN in the presence of hydrocarbons. HCN is then either converted to N_2 or combined with O radicals to form NO_x. Prompt NO_x accounts for less than 10% of total NO_x emissions

from combustion (Heywood, 1998, Lyon and Hardy, 1986). Finally, solid fuels (coal, CB, and AB) also contain N in the fuel, which may directly release nitrogen containing volatiles such as HCN and NH_3. This volatile nitrogen can be converted to NO and N_2. Some NO will later be fully oxidized to NO_2. The sum of NO and NO_2 comprise NO_x emissions from combustion. The NO_x produced via fuel-bound N, called fuel NO_x, accounts for approximately 75% of the total NO_x formed during solid fuel combustion. Thus, the total NO_x is composed of prompt, thermal, and fuel NO_x. The EPA regulates NO_x and SO_x emissions on a case-by-case basis. Typical regulations are that emissions cannot exceed 260 g/GJ (0.45 lb/mmBTU). Emissions regulations are becoming increasingly more restrictive.

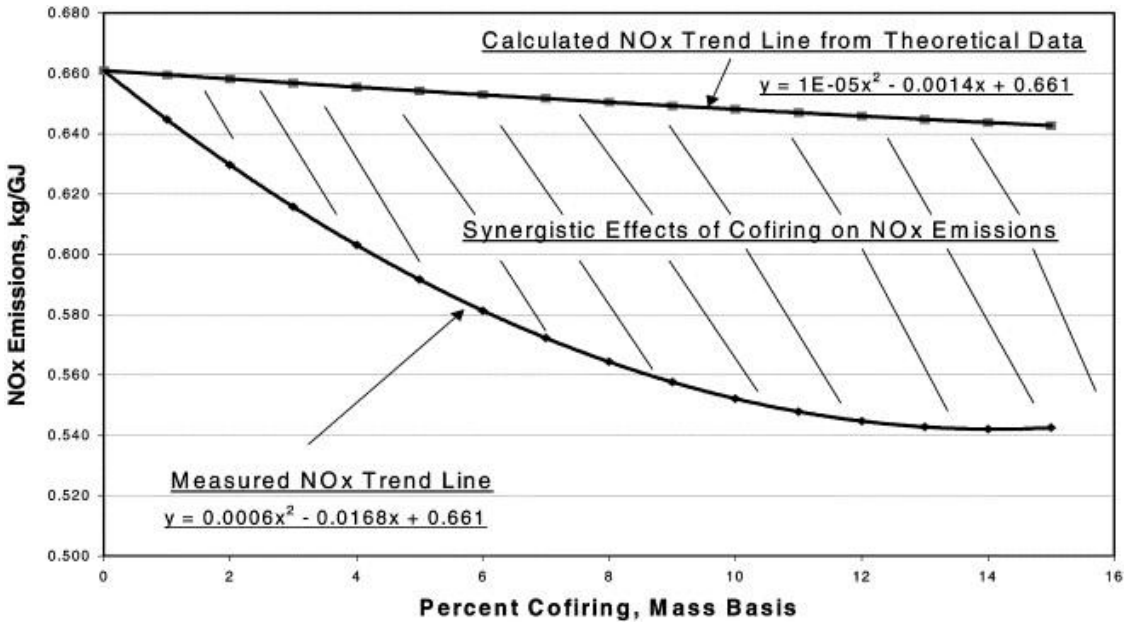

Figure 2.1 NO_x reduction from cofiring low nitrogen biomass with coal. Note that the amount of NO_x reduction is greater than predicted by reduction of nitrogen loading. Adapted from Tillman (2000).

There are two general technologies used to reduce NO_x emissions in coal-fired power plants: primary NO_x controls and secondary NO_x controls. The most common primary controls (near the main burner zone) are LNBs, OFA (which could be a CCOFA, SOFA, or both), or a combination of both. Secondary NO_x controls condition the combustion gases exiting from the primary burn region of the boiler, typically converting the NO_x produced in the main burn region to N_2. In the United States, the most common secondary NO_x controls are reburn, SCRs, and SNCRs. SCRs use NH_3 or urea and layers of catalysts positioned downstream to promote a low temperature reaction to achieve better than 90% NO_x reduction. SNCRs use high temperature urea to achieve approximately 35% NO_x reduction in plants over 50 MW. Although selective reduction (SCR or SNCR) is currently more common than reburn, there is a danger of ammonia exposure when using these technologies. Moreover, SCR systems are very expensive, mostly because of the cost of catalyst replacements and ammonia importation and processing (Srivastava et al. 2005, EPA, 2005).

In reburn systems, the flue gases enter a secondary stage of combustion (as depicted in Figure 2.2) in which a fuel rich mixture reacts with the combustion gases to reduce NO_x. Typically, OFA is then injected into the boiler to complete the combustion process. The most common reburn fuels are natural gas and micro-pulverized coal. Conventional gas reburn systems can reduce NO_x emissions by 50-60%. Less common amine enhanced fuel lean gas reburn systems have been shown to reduce NO_x emissions by up to 70%. Including decommissioned installations, approximately 30 coal-fired units in the U.S. have reburn systems. Nearly all natural gas reburn systems have been

decommissioned due to high natural gas prices. Thus, only a small number (approximately four) of coal-fired units in the U.S. consistently use any type of reburning system (Srivastava et al. 2005).

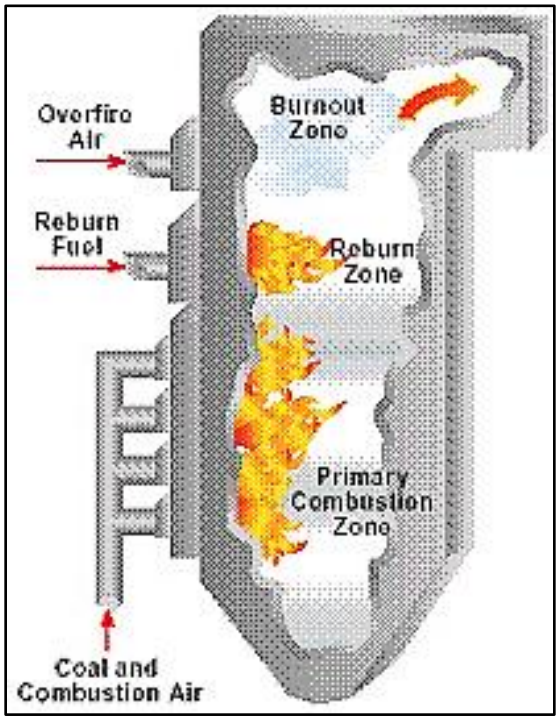

Figure 2.2 Schematic of a canonical reburn system with OFA.

In an LNB system, a fuel gun supplies primary air with coal. Primary air accounts for approximately 20% of the total air and is used to convey the pulverized coal into the burner. In addition to primary air, secondary air is also injected into the main combustion zone to provide oxygen for the combustion reaction. Secondary air is typically swirled and accounts for approximately 60% of the total air. After the main

combustion zone, tertiary air (also called OFA) is injected. Tertiary air may be swirled and accounts for the remainder of the total air as depicted in Figure 2.3. Because the main combustion zone is fuel rich, the nitrogen released from the fuel does not see available oxygen to bond with; hence, it is forced to bond with itself and form N_2. Furthermore, the highest temperatures of the flame are not achieved until later stages, resulting in reduced thermal NO_x. Advanced LNB systems such as combined CCOFAs and SOFAs, and rotating opposed fire air can reduce emissions by 60%.

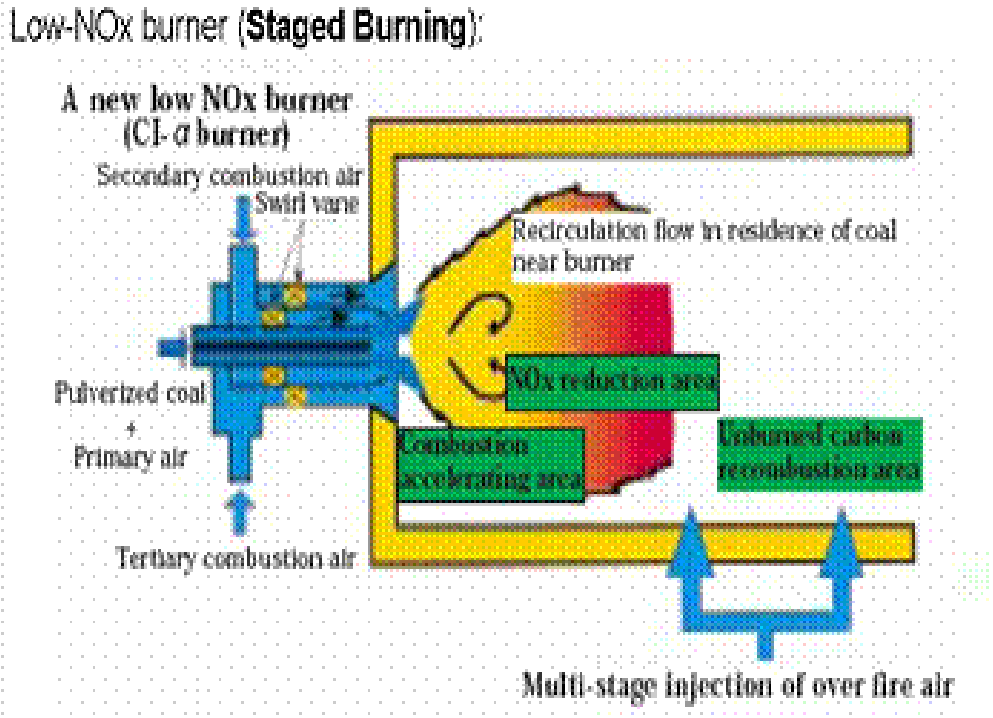

Figure 2.3 Schematic of a canonical LNB.

Li et al. (2009) studied a 300 MW utility boiler that was retrofit with CCOFA and SOFA for improved NO_x emissions. They described the process the utility used to tune the airflow patterns to maximize NO_x reduction with minimal impact on combustion performance. The boiler studied was a tangentially fired boiler with five levels of primary air, six levels of secondary air, two CCOFAs, and one SOFA. The boiler was designed to fire Chinese bituminous coal. Figure 2.4 shows the schematic of the boiler layout and Table 2.1 presents its fuel properties.

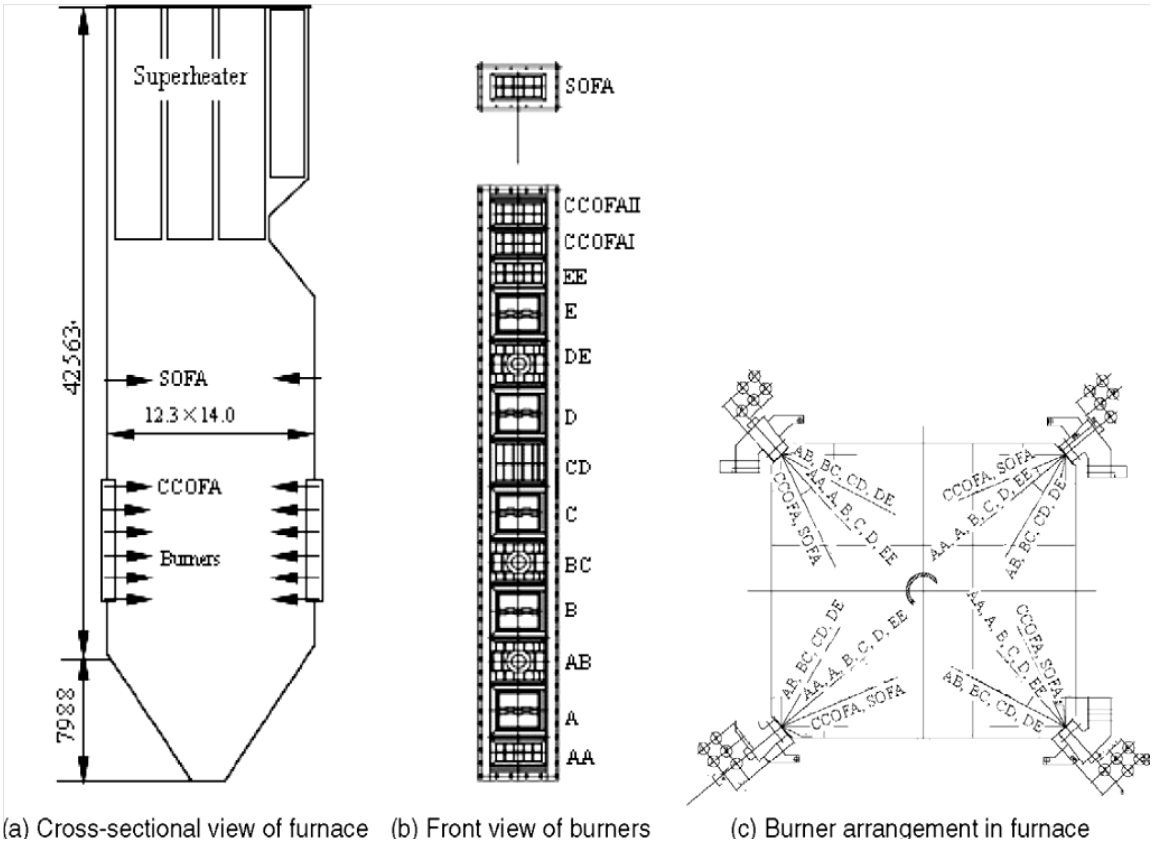

(a) Cross-sectional view of furnace (b) Front view of burners (c) Burner arrangement in furnace

Figure 2.4 Schematic of boiler used by Li et al., 2009.

Table 2.1 Fuel properties of bituminous coal fired by Li et al. (2009)

Proximate Analysis, weight percentage (as air-dried)				
Moisture	Volatile Matter	Fixed Carbon	Ash	HHV (BTU/lb)
12.5	15.66	25.91	45.93	9532
Ultimate Analysis, weight percentage (as air-dried)				
Carbon	Hydrogen	Oxygen	Nitrogen	Sulfur
58.46	3.28	8.68	0.98	0.44

Li et al. (2009) went through a wide variety of percent excess air ratios, secondary air distribution patterns, OFA patterns, and coal sizes in order to determine the optimal scheme for NO_x reduction with minimal impact of boiler performance (as measured by CO emission, unburnt carbon in fly ash, and boiler efficiency). The first operating condition studied was the stoichiometric ratio. Figure 2.5 illustrates the effect of percent excess air ratio on unburnt carbon in the fly ash and on CO. As expected, increasing the amount of excess air increased the combustion performance, which manifested itself in the form of less unburnt carbon and less CO emitted. This improvement in combustion came at a cost. Increasing the amount of excess air also increased the amount of NO_x formed due to increased oxygen available to bond with fuel-bound nitrogen. Figure 2.6 shows this trend. Li et al. (2009) used the information in Figures 2.5 and 2.6 to determine that 1.22 was the best excess air ratio to use in subsequent experiments.

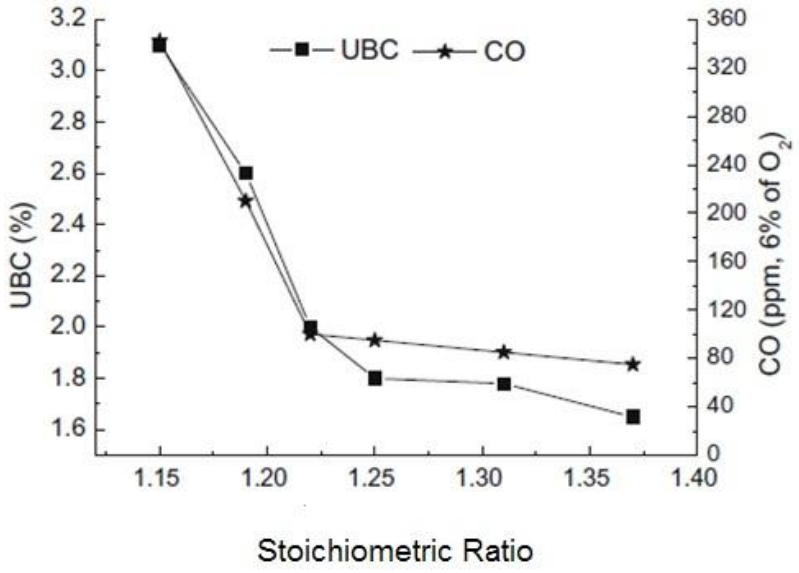

Figure 2.5 Effect of excess air on combustion performance as measured by unburnt carbon in ash and carbon monoxide concentration. Note that after 1.22, there is little improvement in combustion performance with increased excess air ratio. (Adapted from Li et al., 2009.)

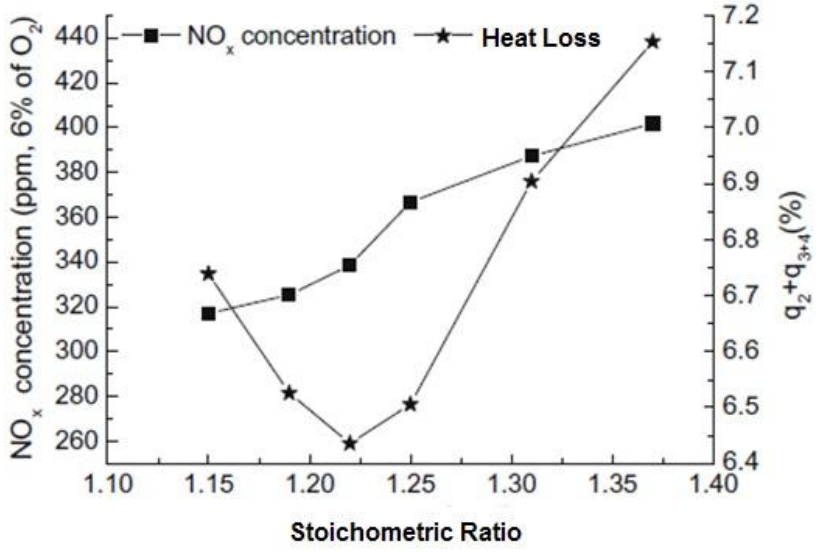

Figure 2.6 Effect of excess air on NO_x concentration and boiler heat losses. Based on this data and the data in Figure 2.5, the operators decided 1.22 was the optimal excess air ratio going forward. (Adapted from Li et al., 2009.)

Following the decision regarding this excess air ratio, the next operating condition investigated was the distribution of secondary air throughout the boiler. Li et al. (2009) used several different percentages for damper opening positions and different percentages at different elevations to investigate the effects on NO_x and boiler performance. The conclusion they drew from parameterizing secondary air distribution was that it was best to have the largest percentage of secondary air enter the boiler at the bottom two registers, a lesser percentage enter at the two intermediate registers, and the least percentage enter at the two top registers. They hypothesized that the best NO_x reduction could be obtained by having sufficient air present in the base to allow NO_x to form, and then destroying that NO_x as it traveled up the boiler into a reducing atmosphere that increased in intensity with elevation.

After determining the appropriate secondary air distribution, Li et al. turned their attention to the distribution of air throughout the OFA. This was where they found they could simultaneously decrease NO_x and improve boiler thermal efficiency. They found that the optimal operating condition occurred when an intermediate amount of air entered through the two CCOFAs and an intermediate amount entered through the SOFA. Figure 2.7 presents their findings regarding the parameterization of the OFA distribution. Li et al. also explained how the percentages for each damper opening correspond to each case. They concluded that Case 11 had the optimal operating conditions. This case had both CCOFAs open at 20% and the SOFA open at 50%. This case gave a minimized NO_x emission with an acceptable boiler thermal efficiency. As shown in Figure 2.7, the OFA operation had a significant impact on NO_x and on boiler

thermal efficiency. Additional research reaffirming this general rule will be discussed later.

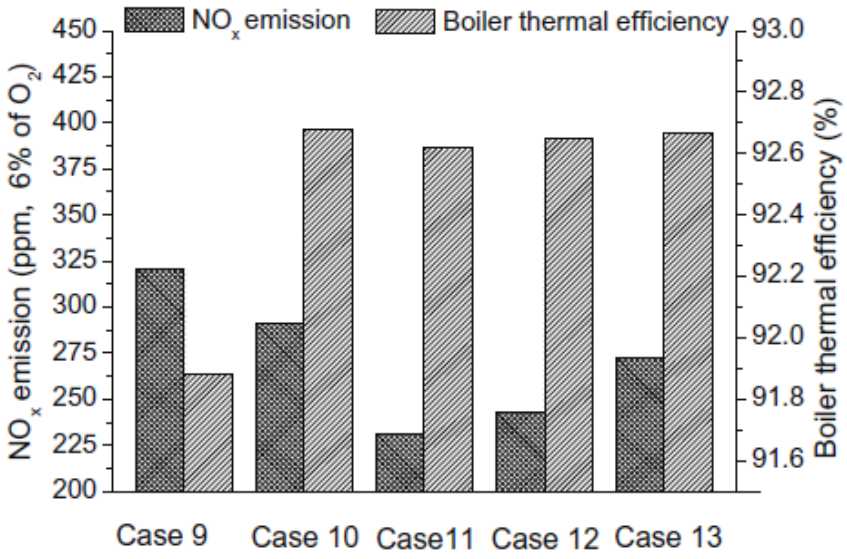

Figure 2.7 Effect of parameterizing over-fire air distribution on NO_x and boiler thermal efficiency. The authors decided on Case 11 (as described in the article) being the optimal operating conditions. (Adapted from Li et al., 2009.)

The last variable the authors investigated was the effect of fuel particle size on NO_x and combustion performance as measured by unburnt carbon in the fly ash and boiler thermal efficiency. Li et al. (2009) used the R_{90} method to quantify coal particle size. R_{90} measures the weight percentage remaining in a 90 μm sieve following shaking. A smaller R_{90} value means less mass remaining in the sieve, which means the particle size is smaller. They investigated samples with R_{90} values of 14%, 11%, and 9%. They

found that the 9% R_{90} coal allowed them to obtain a boiler thermal efficiency and unburnt carbon in fly ash percent that was acceptably close to the pre-retrofit level.

Maier et al. (1994) also performed extensive work using R_{90} classified coal to investigate airflow and particle size on NO_x emission. Figure 2.8 presents the work of Maier et al. (1994) investigating the effect of particle size on NO_x emission. They used the mass percent of sample remaining in a 90 μm sieve (labeled as R 0.09 in Figure 2.8) to quantify particle size distribution. Moving to the left on the abscissa of Figure 2.8 indicates smaller mass percentage remaining on a 90 μm sieve, and thus decreasing particle size distribution. Maier et al. (1994) use the term tertiary air for the air that is more commonly called OFA. As can be seen in Figure 2.8, when the secondary air velocity was 25 m/s and the tertiary air velocity was 80 m/s, the maximum NO_x emission occurred at an R0.09 value of ~10%. When the secondary air velocity was 40 m/s and the tertiary air velocity was 40 m/s (reduced tertiary air), the maximum NO_x emission occurred at an R0.09 value of ~9%. At this operating condition, NO_x emissions are approximately double what they are at 80 m/s tertiary air. Thus, secondary air and over-fire air operating conditions have a significant impact on NO_x, which is consistent with the findings of Li et al. (2009).

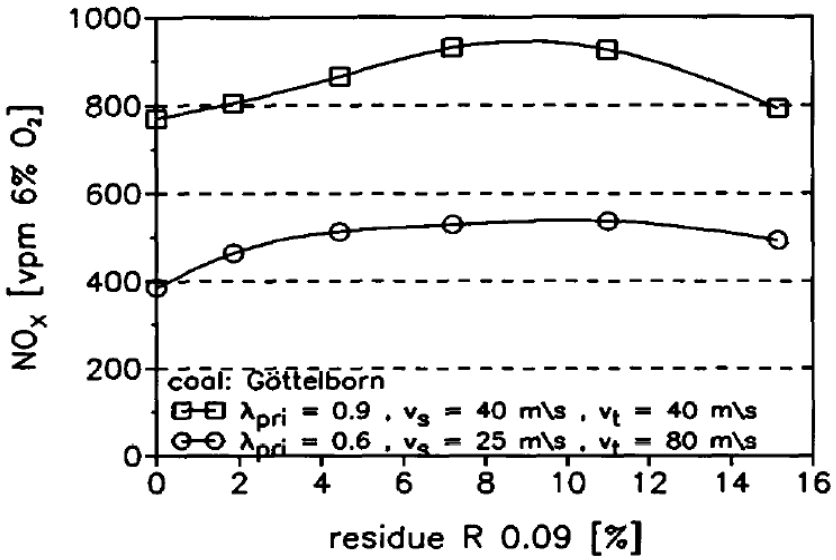

Figure 2.8 Effect of particle size on NO_x emission. Note that initial reductions in particle size lead to increased NO_x emission, but subsequent reductions in particle size lead to decreased NO_x emission. (Adapted from Maier et al., 1994.)

Maier et al. (1994) consistently obtained the results regarding secondary and tertiary air presented in Figure 2.8. NO_x emission is reduced at high tertiary air percentages. The low secondary air velocities decrease the turbulent mixing of the coal and air and thus the NO_x reactions are retarded. The exact opposite condition is desired in the over-fire air region. Here, a high amount of turbulent mixing is desired to promote char oxidation to CO_2 to deprive liberated nitrogen radicals of oxygen and thus inhibit NO_x formation.

Duxbury and Welford (1989) also investigated the effect of particle size on NO_x emissions for a pulverized, bituminous coal fired in a shell boiler modified from fluidized bed combustion operation. The authors stated that decreasing coal particle size increased NO_x emissions. They also reported other researchers had discovered that firing

a high-volatile (31.8%) coal caused NO_x emissions to decrease with increasing coal fineness. There are numerous competing reactions at work. As particle size decreases, char oxidation rate increases increasing oxygen consumption rate. However, char nitrogen is also liberated faster. Lastly, high volatile coals rapidly release volatiles, which also consume oxygen rapidly.

Jiang et al. (2008) stated, "Particle size impacts NO_x emission from coal combustion significantly." Micro-pulverized coal reduces NO_x emission. Thus, there appear to be conflicting results regarding the impact of particle size on NO_x emission. This apparent paradox is resolved by the concept of the critical diameter introduced by Hao and Jin (2010). Hao and Jin proposed that for fuel particles larger than the critical diameter, decreasing particle size increases NO_x emission, and for particle sizes smaller than the critical diameter, decreasing particle diameter decreases NO_x emission. They referred to this critical diameter as dc. Their research has shown that the numeric value of dc depends on coal rank, nitrogen content, volatile content, combustion technique, and combustion air operating parameters. Not only does the nitrogen content affect NO_x emission, but also the form (i.e. NH_3 vs. HCN) of fuel-bound nitrogen is important. Table 2.2 gives the proximate and ultimate analyses of the four coals that Hao and Jin investigated. Note that as the coal number increases, coal rank also increases while the volatile content decreases. This is the same numbering system used for all figures adapted from Hao and Jin. They performed experiments on each coal using six different coal sizes. The nominal sizes of the coals investigated were 15, 30, 50, 60, 70, and 80

μm. Figure 2.9 presents the impact of particle size on NO emission for the bituminous coal (coal #2) investigated.

Table 2.2 Fuel analyses of coal investigated by Hao and Jin (2010)

Coal	Rank	Proximate Analysis				Ultimate Analysis				
		Moisture	Volatile	Fixed Carbon	Ash	Carbon	Hydrogen	Oxygen	Nitrogen	Sulfur
#1	Lignite	8.40	39.70	29.80	22.10	49.90	3.40	14.22	0.60	1.38
#2	Bituminous	1.76	23.06	45.07	30.11	53.68	3.31	9.66	0.51	0.97
#3	Lean	0.50	12.80	62.80	23.90	65.60	3.18	3.02	1.85	1.95
#4	Anthracite	2.81	7.00	70.75	19.44	71.53	1.94	2.49	0.93	0.85

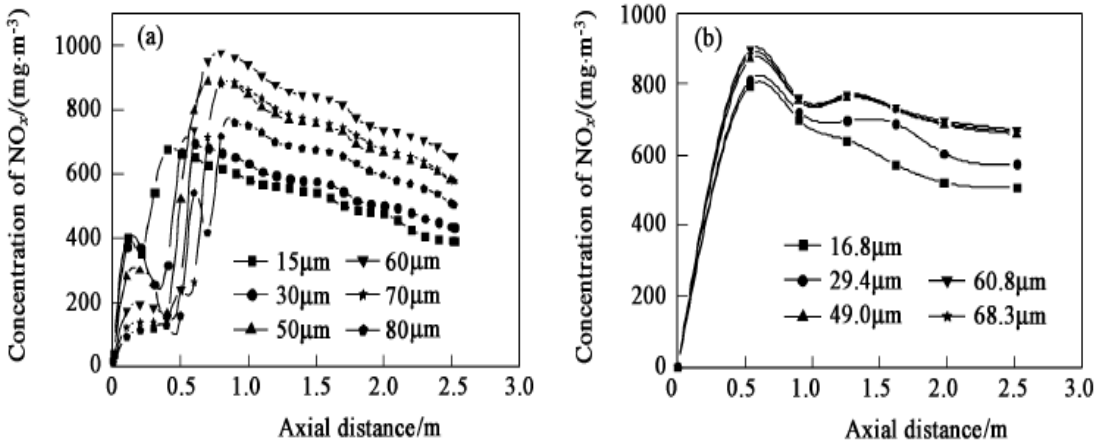

Figure 2.9 Effect of particle size on NO_x emission from numerical modeling (a) and experimentation (b). Note that the coal used was the bituminous coal (#2) shown in Table 2. (Adapted from Hao and Jin, 2010.)

It is important to note that in Figure 2.9 and Figure 2.10, (a) results are from numeric modeling and (b) refers to results from experimentation. Experimental results should always be considered more valid because they come from real data. As can be

seen in Figure 2.9(a) when decreasing the coal particle size from 80 to 60 μm, NO_x emission increases at the furnace exit. Then, continuing to decrease the fuel particle size causes NO_x emission to decreases. Figure 2.9(b) shows similar results; that decreasing particle size below 60 μm reduces NO_x emission. Figure 2.9 gives NO_x concentration for several axial positions along the furnace. NO_x concentration at the furnace exit is most important. This information is given in Figure 2.10 for all coal investigated. Figure 2.10 shows another example of critical diameter behavior. All four coals show critical diameter behavior across all ranks. Figure 2.10 also shows that the location of this local maximum is different for different coals.

As shown by the experiments performed by Hao and Jin (2010), the size of the critical diameter can be ordered by decreasing diameter as anthracite, lean, lignite, bituminous. In general, the lower the rank of the coal the smaller the size of the critical diameter; bituminous is the exception. Note that Figure 2.8 shows similar critical diameter behavior.

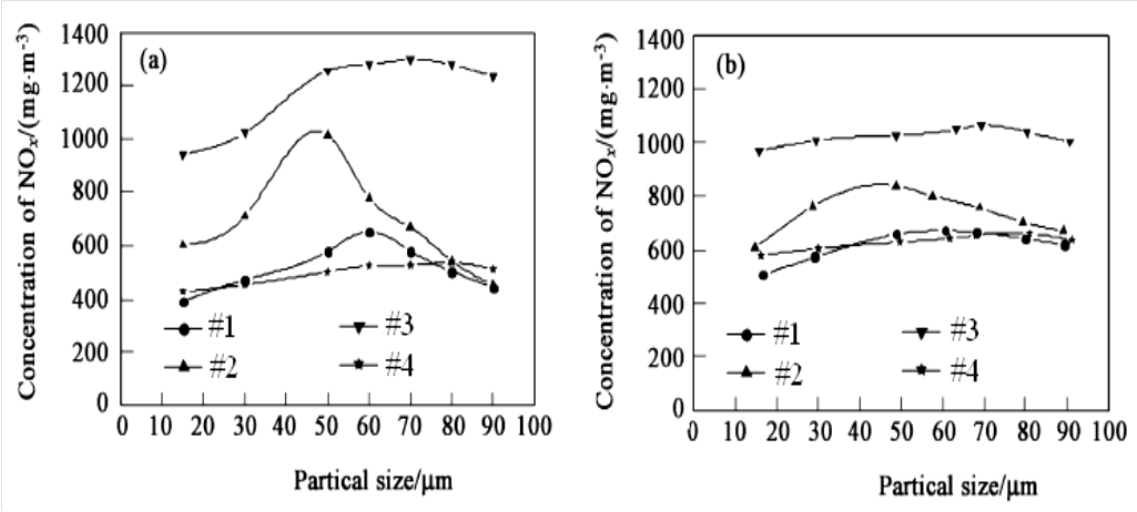

Figure 2.10 Effect of coal rank and particle size on NO_x emission. Adapted from Hao and Jin (2010) (a) models and (b) experiments. Note that the same numbering system is used as in Table 2.2 (increasing number increases coal rank).

The work of Jiang et al. (2008) comes from TGA-GCMS experiments in which fuel samples were heated in an oven at heating rates of 5, 10, and 20°C/min, and mass and emissions as a function of temperature was recorded. Obviously, these heating rates are much, much lower than normal coal particles encounter in a utility boiler. Figure 2.11 shows the emissions of NO_2 and NO for various coal particle sizes heated at 20°C/min in 20% ambient O_2. The figure illustrates that the smallest particle size sample (7.0 μm) also had the smallest NO_2 and NO emission.

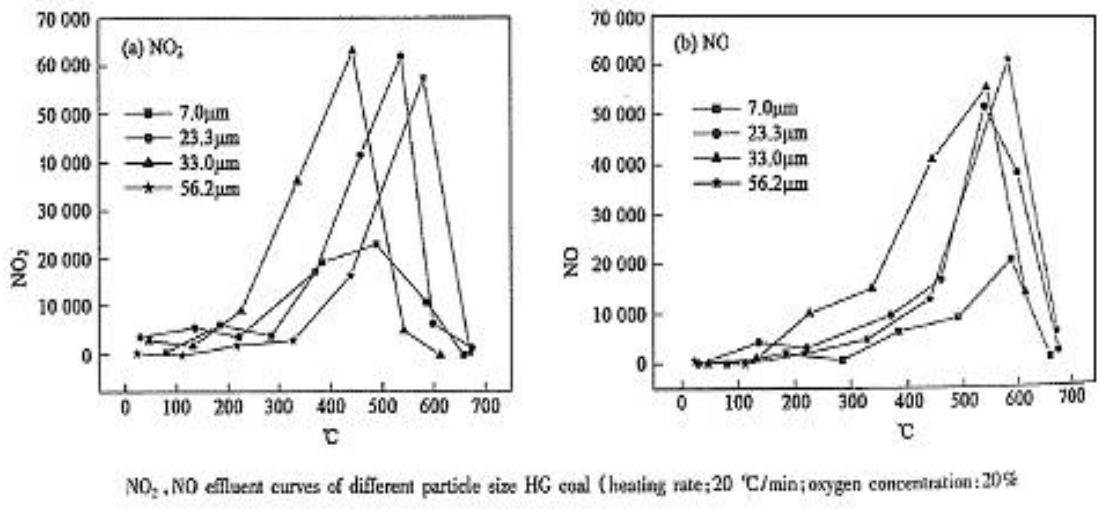

Figure 2.11 Effect of coal particle size on NO_x emissions from TGA experiments. (Adapted from Jiang et al., 2008.)

A trend can be observed when examining Figure 2.11(a). Decreasing the particle size from 56.2 μm to 33.0 μm increases the peak NO_2 emission. However, further decreasing the particle size from 33.0 μm to 23.3 μm and then to 7.0 μm reduces the peak NO_2 emissions. NO_2 results obtained by Jiang et al. (2008) demonstrate critical diameter behavior with the critical diameter being 33.0 μm. The 7.0 μm coal particles also produced the least amount of NO. It is unfortunate that Jiang et al. (2008) placed NO and NO_2 on separate graphs. Attempting to combine the traces together successfully to obtain a NO_x trace is virtually impossible.

The local maximum behavior of NO_x as a function of coal particle size is reinforced by the work of Shen et al. (2011). Their experiments were conducted in a drop tube furnace, in which only primary (motive) air was used to convey the fuel to the furnace and OFA for complete combustion. They experimented with two Chinese

bituminous coals investigating coal particle size, primary air zone stoichiometric ratio, and over-fire air location effects on NO_x, CO, and unburnt carbon. Figure 2.12 shows the local maximum behavior of particle size on NO_x. As Figure 2.12 shows, for a range of primary air zone stoichiometric ratios, decreasing particle size leads to an increase in NO_x until ~17.5 μm and then continued reduction in particle size leads to a decrease in NO_x. It is important to note that the work was done in a drop tube furnace and so the numerical values obtained are different from what a full scale furnace would probably observe. The qualitative behavior seems to be similar. The same statement can be made for the TGA work of Jiang et al. (2008).

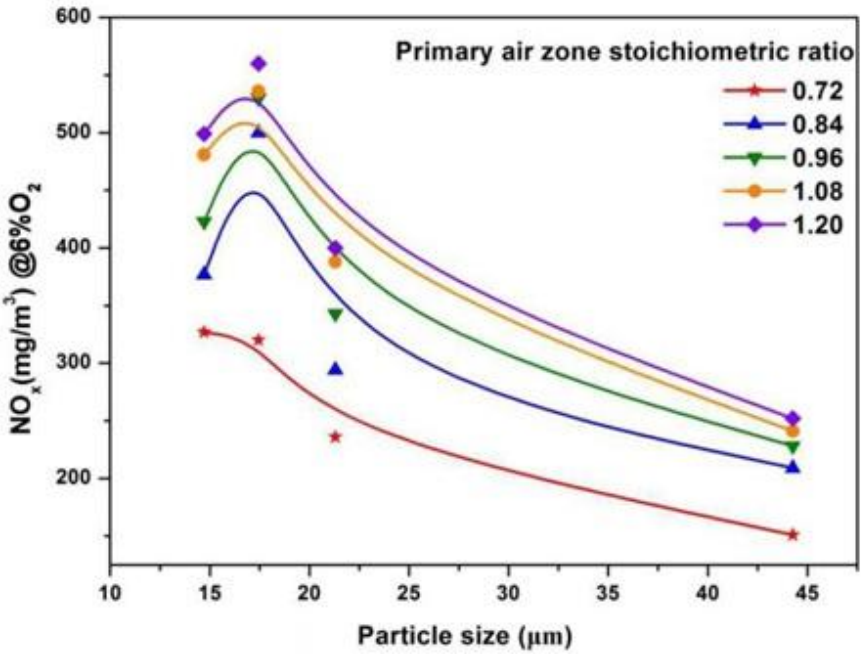

Figure 2.12 Effect of fuel particle size and primary air zone stoichiometric ratio on NO_x emission. Note that there is a point of maximum NO_x emission at ~17.5 mm. (Adapted from Shen et al., 2011.)

Figure 2.13 presents the effect of particle size and OFA location on NO_x emission. As can be seen in Figure 2.13, the local maximum behavior is repetable and manifests itself for every OFA location. The data presented in Figure 2.13 is for a primary air zone stoichiometric ratio of 0.84. As expected, as the OFA port was moved further downstream, the NO_x emission decreased. In the extreme case, NO_x was significantly reduced by moving the OFA far downstream; further demonstration of the importance of OFA on NO_x.

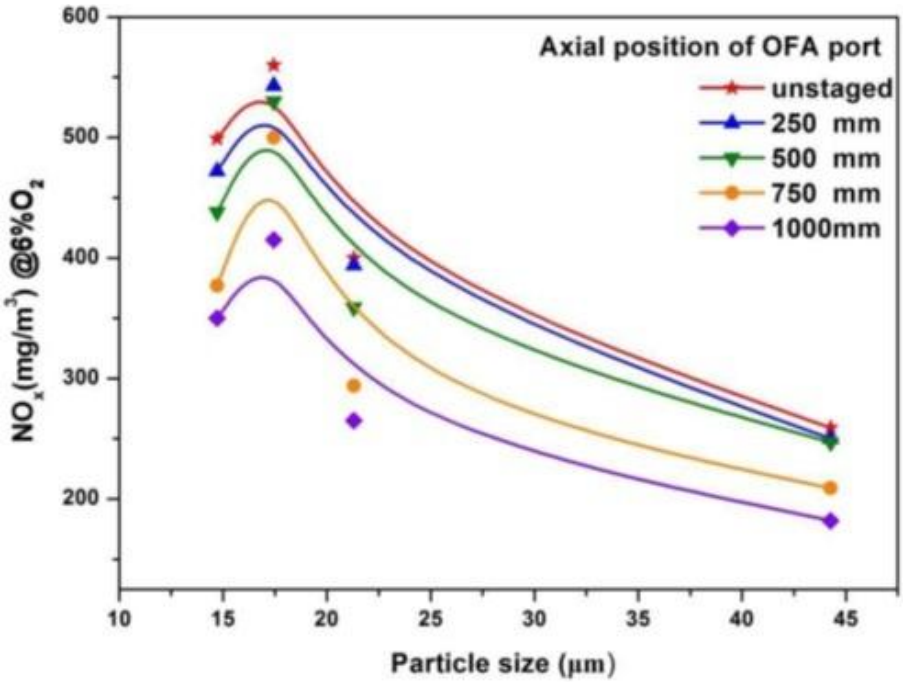

Figure 2.13 Effect of particle size and OFA location on NO_x emission. Note that the local maximum behavior with respect to particle size exists for all OFA port locations. The primary air zone stoichiometric ratio is 0.84. (Adapted from Shen et al., 2011).

As shown in Figure 2.13, the conclusion Shen et al. (2011) drew was that they could obtain good NO_x reduction with a minor compromise on combustion efficiency with the OFA port set at 750 mm. This was the operating condition they used to generate Figure 2.14, which shows how particle size and primary air zone stoichiometric ratio affects NO_x. Each grouping of data points (in order of decreasing particle size: purple, green, blue, red) represent a different particle size. When going from 44.26 μm to 21.30 μm to 17.44 μm, NO_x emission increases. However, when going from 17.44 μm to 14.71 μm, NO_x emission decreases. This trend is observed for almost all of the data points. The one exception for 17.44 and 14.71 μm coal particles is at the primary air zone stoichiometric ratio of 0.72. At this point, the NO_x emissions are close enough to be within experimental uncertainty. As expected, decreasing the primary air zone stoichiometric ratio decreased NO_x emission because less primary air was available to oxidize nitrogen to NO_x.

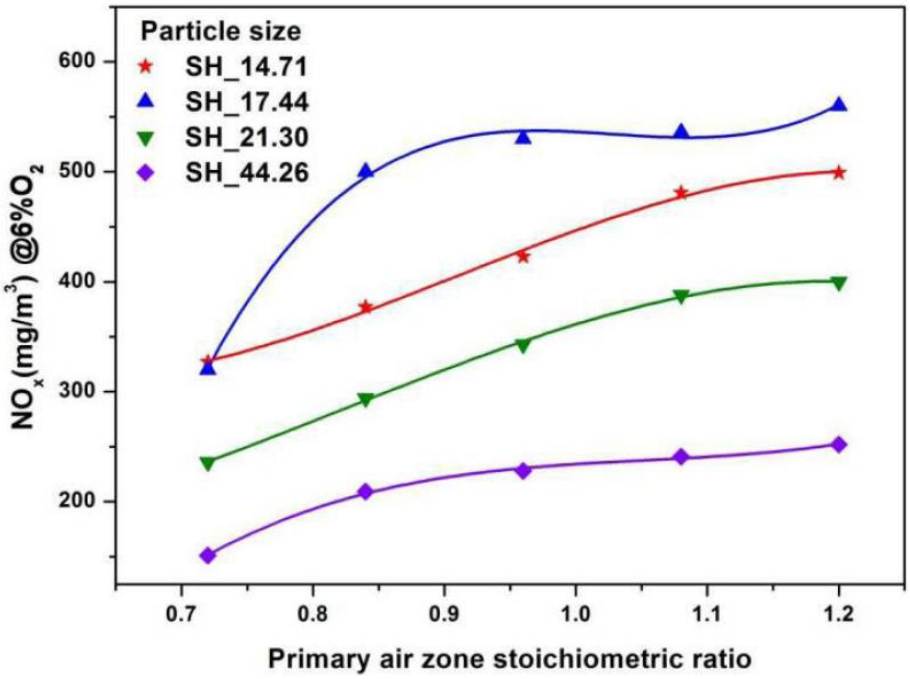

Figure 2.14 Effect of particle size and primary air stoichiometric ratio on NO_x emission. Note that the most NO_x is emitted from 17.44 μm coal particles for almost all primary air zone stoichiometric ratios. Particles larger than this size and particles smaller than this size emit less NO_x. (Adapted from Shen et al., 2011).

In order to meet future NO_x regulations, Partlow et al. (2011) performed many modifications at the Gibbons Creek Plant from 2001-2002. One of the first steps was replacing antique lignite pulverizers with state-of-the-art pulverizers. By doing so, they increased coal fineness from 60% through a 200 mesh screen to 70% through a 200 mesh screen, lowered LOI, improved combustion efficiency, and reduced NO_x by 20%.

All of the literature appears to confirm the idea that there is a critical diameter particle size that maximizes NO_x emission. Increasing the particle size to something larger than this diameter or decreasing the particle size to something smaller than this diameter will decrease NO_x emission, relative to the NO_x emission at the critical

diameter. The literature further supports the idea that the location of this critical diameter is affected by coal properties, combustion technique, and combustion parameters (i.e. fuel flow rate, airflow rate, air injection location, airflow partitioning, etc.). In addition, past research shows that these parameters also affect the amount of NO_x formed at the critical diameter. In other words, there is a hill that the NO_x emissions must climb when decreasing particle size. Once the hill has been crested, further decreases in particle size will yield a decrease in NO_x.

Table 2.3 provides a summary of the references used in this section. It summarizes the experimentation apparatus used, the type of coal investigated, the particle sizes investigated, critical diameter (if applicable), and general comments.

Table 2.3 Summary of references and major findings related to fuel particle size and NO_x

Reference	Experiment	Coal Investigated	Particle Sizes	Critical Diameter	Comments
Duxbury and Welford, 1989	Shell Boiler	Bituminous	N/A	N/A	No_x with decreasing particle size
Maier et al., 1994	Coal Combustion Facility	Not Specified	15%, 11%, 7%, 5%, 2%, 0% (R_{90})	N/A	Particle size did not affect NO_x. An excellent reference on NO_x tuning.
Jiang et al., 2008	TGA	Not Specified	56.2; 33.0; 23.3; 7.0 (μm)	33.0 μm for No_2	7.0 μm coal produced significantly less NO_x.
Hao and Jin, 2010	Down Fired Furnace	Lignite	68.3; 60.8; 49.0; 29.4; 16.8 (μm)	60 μm	Bituminous coal was most profoundly affected by particle size.
	Down Fired Furnace	Bituminous	68.3; 60.8; 49.0; 29.4; 16.8 (μm)	45 μm	
	Down Fired Furnace	Lean	68.3; 60.8; 49.0; 29.4; 16.8 (μm)	70 μm	
	Down Fired Furnace	Anthracite	68.3; 60.8; 49.0; 29.4; 16.8 (μm)	80 μm	
Shen et al., 2011	Drop Tube Furnace	Bituminous	44.26; 21.30; 17.44; 14.71 (μm)	17.44 μm	Over-fire air was of equal importance.

2.3 Biomass

Biomass provides approximately 4% of the energy in the United States. According to a report by Shell Petroleum, biomass could satisfy between 25-50 % of the world's energy demand by the middle of the 21st century. Biomass can be classified into two broad categories: agricultural and animal waste based fuels.

Traditionally, CB from feedlots in West Texas, DB from dairies in Central Texas, and LB from chicken ranches in East and Central Texas has been used as fertilizer on crop or pasture land. However, there are environmental concerns regarding over-application leading to excess phosphorus loading. This concern has led to TMDLs for some streams (e.g., the North Bosque River system) and land areas. While land application of CB as fertilizer has been the expedient solution, manure has a relatively low nutrient content. Beyond a certain radius, manure cannot compete economically with commercial fertilizer as a nutrient source. Further, the production of manure from all species in a region may exceed farmland availability for application considering declining groundwater tables for crop irrigation and water quality concerns. Storage of CB contributes to air quality and greenhouse gas concerns with the release of CH_4, NH_3, H_2S, amines, volatile organic fatty acids, mercaptans, esters, and other chemicals. The emissions from stored manure and other environmental wastes reportedly accounts for about 8% of United States greenhouse gas methane emissions. Moore and Hart (1997) detail the problems associated with dairy manure management systems and proposed solutions. Figure 2.15 presents a flow diagram for the various pathways dairy manure may take from excretion to final disposal. Figure 2.16 shows a canonical solid separator

used to separate solid material from moisture prior to composting the solid DB. A device similar to this was used to prepare the LADB used in this experimentation. Additional information about manure collection techniques and preparing manure for thermochemical conversion processes can be found in Heflin and Sweeten (2006) Annamalai et al. (2012).

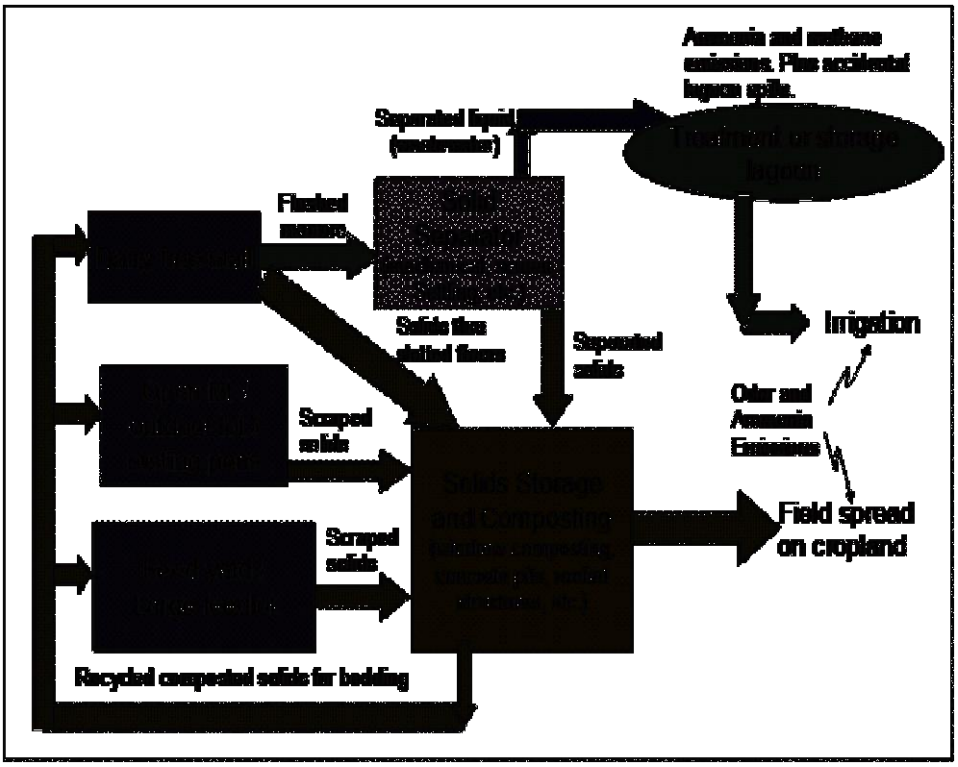

Fig 2.15 Current dairy and feedlot manure disposal. (Adapted from Schmidt et al., 1988.)

Fig 2.16 Screen solid-liquid separator. (Adapted from Annamalai et al., 2012.)

As of 2011, there were 23 states in the United States with more than 1,000 head of dairy cows with California (1,760,000) and Wisconsin (1,266,000) being the only states with more than 1,000,000 dairy cows. At the end of 2011, Texas had 426,000 dairy cows producing an average of 1,945 pounds of milk per cow for a total of 829 million pound of milk. According to the National Agricultural Statistical Services (NASS) in the United States, there were 8,425,000 cows producing an average of 1,872 pounds of milk per cow for a total of 15,773 million pounds of milk. (NASS, 2012). Table 2.4 presents the 2011 numbers of cows, milk produced per cow, and total milk production for the major milk producing states.

Table 2.4 Number of milk cows, milk produced per cow, and total milk production for the major milk producing states. Texas is emphasized (Adapted from NASS, 2012.)

State	Milk Cows (1000)	Milk per Cow (Pounds)	Milk Production (1,000,000 Pounds)
California	1760	2040	3590
Wisconsin	1266	1775	2247
New York	610	1810	1104
Idaho	576	1880	1083
Pennsylvania	543	1710	929
Minnesota	469	1660	779
Texas	***426***	***1945***	***829***
Michigan	364	1985	723
New Mexico	325	2150	699
Ohio	269	1660	447
Washington	254	2025	514
Iowa	209	1825	381
Arizona	187	2180	408
Indiana	172	1795	309
Vermont	135	1635	221
Colorado	125	2015	252
Kansas	122	1830	223
Florida	119	1865	222
Oregon	119	1750	208
Illinois	98	1715	168
Virginia	96	1615	155
Missouri	94	1365	128
Utah	87	1770	154
	Total 8425	**Average 1872**	**Total 15,773**

2.4 Thermochemical Conversion of Biomass

Co-firing coal with CB or using CB as a reburn fuel in existing boiler burners could reduce most of these land application problems when appropriate technology matures. Thus an interdisciplinary, system-oriented research program was initiated to provide environmentally benign, but economically viable, methods to convert low–value inventories of CB (which includes FB and DB), or any other animal waste based

biomass into renewable energy using a suite of energy conversion technologies (Annamalai et al. 2003a). Figure 2.17 presents an overview of emerging energy conversion processes for CB. If these technologies are demonstrated and subsequently commercialized, they will help reduce fossil based CO_2, mitigate the environmental stress posed by the disposal of animal waste, improve environmental sustainability to meet growing energy demands for the operation of CAFOs, and provide profitable avenues through sale of CB for feedlot and dairy operators. A combined heat and power 18 MW CFB power plant in Denmark cofires coal and straw from local agricultural operations with very satisfactory results (Jakobsen, 1998). Damstedt et al. (2007) performed cofiring experiments with coal and straw investigating the importance of air distribution on NO formation. They found that producing an initial fuel rich zone forced volatile nitrogen to be reduced to N_2 and thus overall NO_x formation was reduced. A state-of-the-art review on co-firing by Sami et al. (2001) summarizes biomass fuel properties and combustion behavior of biomass fuels used in co-firing and reburning, together with fundamental concepts related to coal-biomass blend combustion and modeling studies.

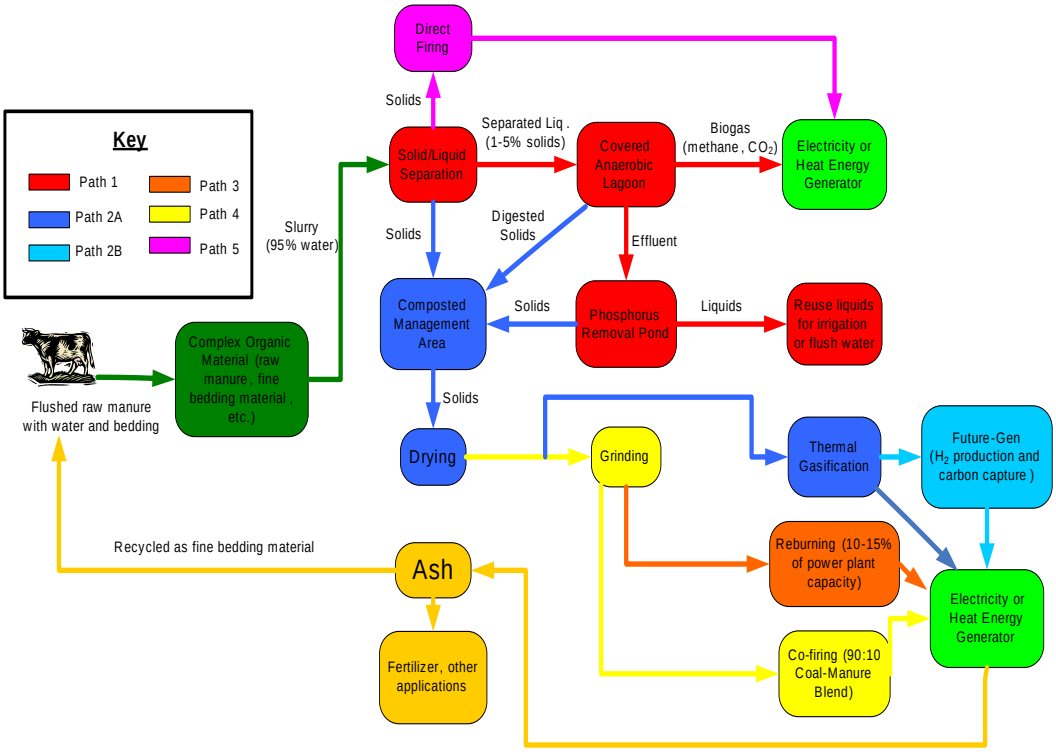

Figure 2.17 CB thermochemical conversion pathways.

One of the most important aspects of thermochemical conversion of CB is the fuel properties. Sweeten et al. (2003 and 2006) determined fuel and feed ration properties which include the HHV of CB. The HHV on a DAF basis remained approximately constant at 19.3-20.5 MJ/kg (8,300-8,800 BTU/lb) for most CB fuels independent of feed ration or composting time (RM, PC, or FC).

Most of the research during the 1980s concentrated on using pure CB in fluidized and circulating bed boilers (Raman et al. 1980, Sweeten et al. 1986, Annamalai et al. 2007). Dahlquist (2013) also has summarized a significant amount of research on the topic of thermochemical conversion of biomass.

Recent research conducted by Texas A&M University, funded by the United States Department of Energy-National Energy Technology Laboratory, USDA, and TCEQ has shown that coal (80% by mass) can be cofired with CB (20% by mass) in power plants (Annamalai et al. 2003b, Arumugam et al. 2005). CB was used as a reburn fuel at a 100,000 BTU/hr Texas A&M facility, which resulted in reduction of NO_x by as much as 95%. This has led to securing a United States patent for the NO_x reduction process using FB. A second United States patent on CB processing and production for reburn is under review by the patent office. From the A&M results, CB reburning can be considered superior to natural gas reburning to reduce NO_x. However, on an economic basis, CB reburning technology must also prove to be an acceptable investment for power plant proprietors. Thus, marketability of CB as a reburn fuel faces an uphill task because most of the units have decommissioned reburn systems and retro-fitted with LNB systems.

Cofiring coal and all forms of biomass is a well-represented technology in literature and a summary of research efforts was provided by Sami et al. (2001). Cofiring of coal and animal waste based biomass is not as readily available, but some investigations are presented here. To investigate the feasibility of cofiring biomass with coal, Whitely et al. (2006) performed TGA-FTIR experiments with PL. This work demonstrated that PL will release ammonia during drying, devolatilzation, and combustion. As a continuation of this work, Li et al. (2008) cofired a bituminous coal with PL in a CFB boiler to study the effect of cofiring on emissions formation. The PL was scraped from the chicken house floor and contained sawdust, wood chips, and fecal

matter. Table 2.5 presents the fuel properties of the coal and PL that was cofired by Li et al. (2008).

Table 2.5 Fuel properties of coal and PL cofired in a CFB by Li et al. (2008)

Parameter	**Coal**	**PL**
Proximate analysis (%)		
Moisture	2.6	11.3
VM	31.6	57.8
FC	56.4	6.1
Ash	9.4	24.8
Ultimate analysis (%,dry)		
Carbon	71.3	28.2
Hydrogen	5.3	5.0
Oxygen	8.8	35.0
Nitrogen	1.4	3.4
Sulfur	3.5	0.9
Ash	9.7	27.5
Heat Content		
HHV (kJ/kg)	30117	11802

As shown in Figure 2.18, Li et al. (2008) demonstrated that NO formation increased with the initial increase of PL in the cofired fuel 0% to 10%. However, further increasing the PL from 25% had minimal impact on NO formation, and then even further increases in PL to 50% worked to decrease NO formation to less than NO formation from pure coal. The authors explain state that the initial increase in NO formation is due strictly to the increase in fuel nitrogen loading from the addition of PL. When the amount of PL is increased, the VM of the cofired fuel also increases which accelerates the combustion reaction and reduces local oxygen concentration. When the VM loading

is sufficiently increased, the combustion reaction is accelerated to the point that a fuel rich environment is rapidly formed near the fuel injection location. Once this fuel rich environment is created, the uncombusted VM from the PL will thermally decompose (pyrolyze) to form large pockets of NH_3, which will reduce the NO that has formed to N_2 and H_2O. These results show the amount of biomass that needs to be cofired with coal for the biomass to act as a NO_x reducing agent.

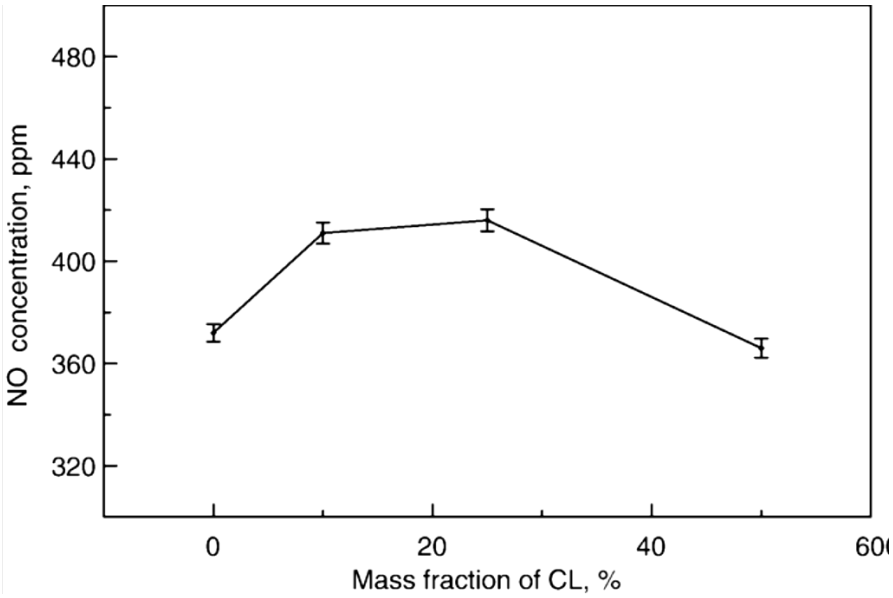

Figure 2.18 Effect of amount of PL in cofired fuel on NO formation. (Adapted from Li et al., 2008.)

Jia and Anthony (2011) expanded the laboratory scale testing of cofiring coal and PL in a CFB to a pilot scale plant in Oklahoma. Table 2.6 presents the fuel properties of the coal and PL Jia and Anthony (2011) cofired. PL was blended into the 0%, 10%, and 40% amounts on a heat basis. Figure 2.19 presents the NO_x concentrations and Fuel

Nitrogen Conversion Efficiencies reported by Jia and Anthony (2011) from their cofiring experiments. They report that adding PL to the cofired fuel increased NO_x emissions but disproportionately less than expected from the increased nitrogen loading. Similarly, they reported fuel nitrogen to NO_x conversion decreased from 9% to 3.8%. They report that fuel handling was not affected by adding PL to the coal. The most significant problem they encountered was the horrible odor produced by the PL. Workers insisted that PL only be handled on weekends when no one else was present in the fuel handling area. In addition, the high phosphorous content of PL can lead to high amounts of phosphoric acid being formed in the stack. Note that the initial increase in PL amount in the fuel increased NO_x emission, but beyond this initial increase further increases lead to a NO_x reduction. This is similar to the behavior that was seen in the laboratory scale experiments (see Figure 2.18).

Table 2.6 Fuel properties reported by Jia and Anthony (2011)

Parameter	**Coal**	**PL**
Proximate analysis (%)		
Moisture	1.12	7.34
VM	17.07	54.34
FC	64.49	13.25
Ash	17.32	25.07
Ultimate analysis (%,dry)		
Carbon	73.62	31.84
Hydrogen	3.21	3.98
Oxygen	2.01	27.5
Nitrogen	1.49	3.52
Sulfur	1.23	0.75
Ash	17.3	25.1
Heat Content		
HHV (kJ/kg)	29270	12770

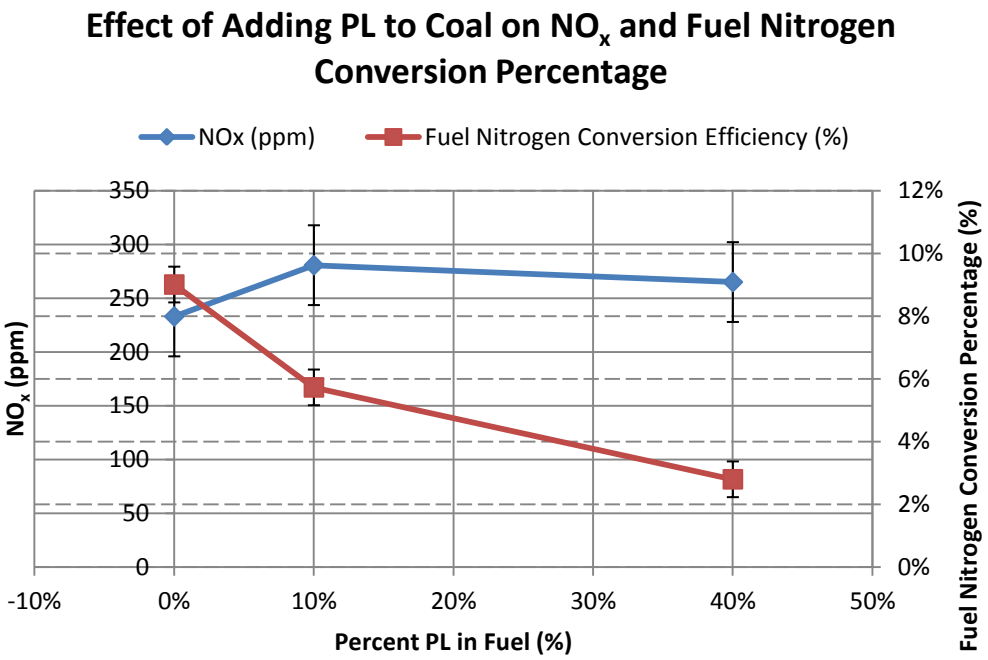

Figure 2.19 NO_x emissions and fuel nitrogen conversion percentage from coal and PL cofiring experiments in a pilot scale CFB, by Jia and Anthony (2011). Note that the NO_x behavior is similar to what is seen in Figure 2.18.

Lundgren and Pettersson (2009) investigated using the waste bedding material (a combination of wood-shavings and horse manure) from Swedish horse stables as a fuel in an on-site furnace for space heating and hot tap water. Current Swedish legislation forbids disposing of animal waste in a landfill, which is more aggressive legislation than the no more than 30% animal waste disposed in a landfill enforced by the European Union. The furnace Lundgren and Pettersson (2009) used resembles a grated fired stoker furnace with the addition of a secondary combustion zone above the grate that is similar to OFA. One of the major technical hurdles they encountered was the increased fuel nitrogen loading of the manure and wood-shavings fuel over the base case wood-chips,

as shown in Table 2.7. Despite the increased fuel nitrogen loading, the fuel nitrogen content remained significantly below the levels experienced in feedlot biomass cofiring experiments at Texas A&M University. Note that some of the values in Table 2.7 do not add perfectly to 100% due to rounding.

Table 2.7 Fuel analyses of fuels used by Lundgren and Pettersson (2009). The cofired fuel of horse manure and wood-shavings had more fuel-bound nitrogen than the base case fuel of wood-chips, but was still less than other biomasses derived from animal waste.

Parameter	Woodchips	Horse manure and wood shavings	Poultry litter	Feedlot manure
Ultimate analysis (%, DAF)				
Carbon	49.5	48.6	46.1	49.7
Hydrogen	6.1	5.8	6.5	5.6
Oxygen	43.5	44.3	40.6	39.1
Nitrogen	0.1	0.9	6.63	4.25
Sulfur	0.0	0.1	0.16	1.36
Heat Contour				
HHV (kJ/kg)	20560	19370	Not Reported	Not Reported

The primary focus of Lundgren and Pettersson's (2009) work was investigating the feasibility of combusting the bedding material. They were also concerned with the ash formed from combustion. Therefore, they did not precisely control total air-fuel ratio or air distribution between primary and secondary air. Nevertheless, preliminary combustion emissions were reported and presented in Figure 2.20. In Figure 2.20, Experiment No. 4 had the second most total air and second smallest percentage of air staging. Therefore, it is understandable that it also had the smallest CO concentration. In going from Experiment No. 3 to Experiment No. 4, the total air was decreased and the

amount of air staging was increased. But doing so, they were able to reduce uncorrected O_2 concentration, as well as corrected CO concentration and corrected NO_x concentration. This is a demonstration of how proper OFA tuning can improve combustion performance.

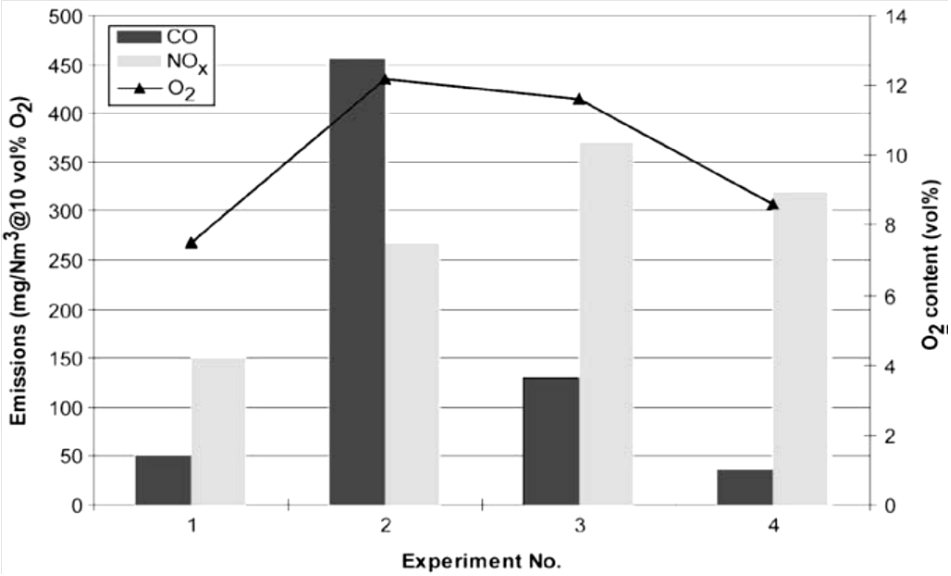

Figure 2.20 Emissions from initial combustion experiments performed by Lundgren and Pettersson (2009). By decreasing the total air supplied and adjusting the OFA percentage, the authors were able to reduce CO and NO_x simultaneously when going from Experiment No. 3 to Experiment No. 4. Note that neither total air nor air-fuel ratio was held constant during experiments.

There is also a considerable amount of research occurring at Texas A&M University investigating cofiring coal with various forms of animal waste. Figure 2.21 shows the NO_x results from Lawrence et al.'s (2009) work cofiring PRB with LADB in a

conventional furnace. Figure 2.22 shows the NO_x results from Thien et al.'s (2012) work cofiring coal and litter biomass in a conventional furnace.

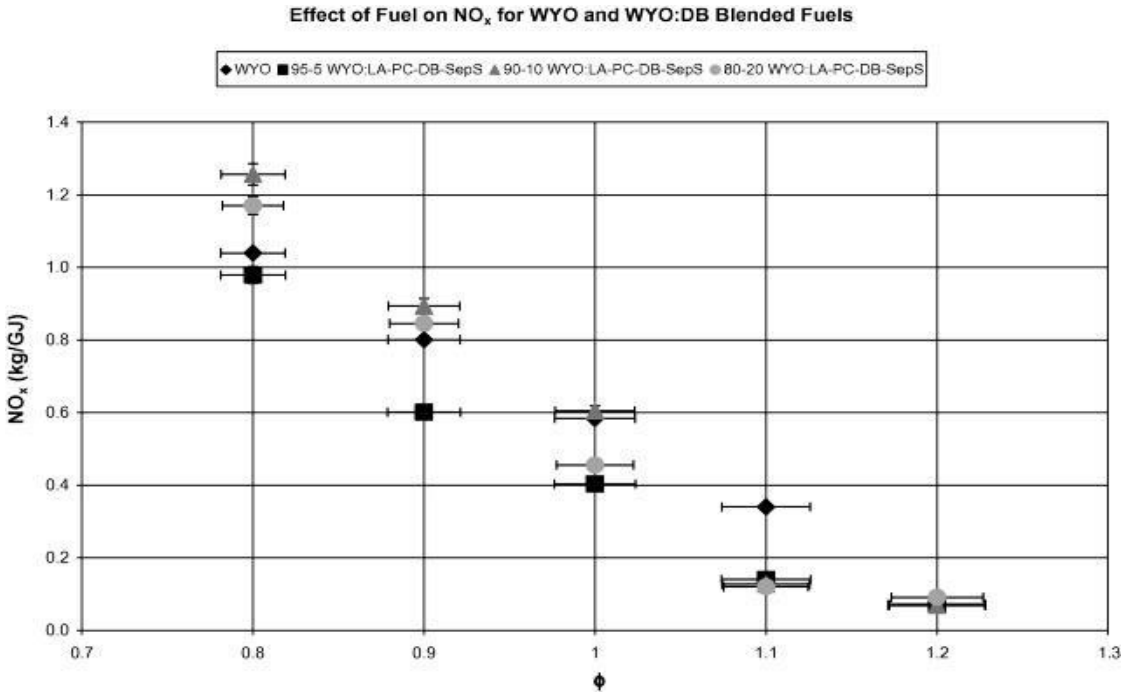

Figure 2.21 NO_x results from cofiring PRB and LADB in a conventional furnace. (Adapted from Lawrence et al., 2009.)

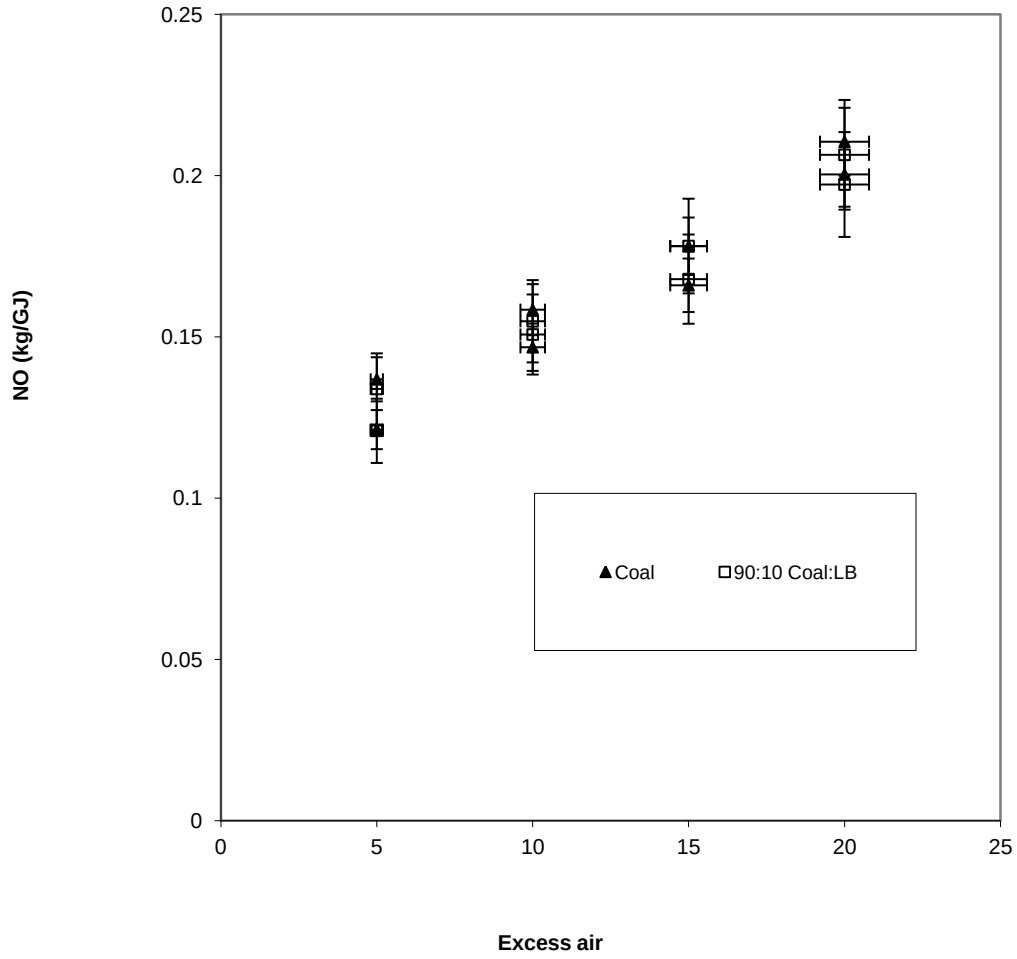

Figure 2.22 NO_x results from cofiring coal and litter biomass in a conventional furnace. (Adapted from Thien et al., 2012).

Considering that cofiring coal and all forms of biomass is readily available in the technical literature, cofiring combined with staged combustion is surprisingly sparse. Laux et al. (2011) present results from cofiring coal and woody biomass in utility LNBs work they did for Foster Wheeler. The authors state that cofiring with high volatile, low nitrogen biomass can work to increase NO_x reduction because the high volatile biofuel in

the center of the flame rapidly consumes the oxygen and results in very low excess air levels that promote NO_x reduction. However, Low NO_x burners have already primary flame conditions with low oxygen levels and care must be taken to provide sufficient oxygen to both biofuel and coal in order not to delay combustion.

Savolainen (2003) cofired coal and sawdust in a 315 MW tangentially fired utility low NO_x burner. Figure 2.23 presents the emissions data from the work with heat basis NO_x on the abscissa and Total Unburnt Carbon in Fly Ash on the ordinate. As can be seen in Figure 2.23, at an unburnt carbon level, adding sawdust to the fuel increased the heat basis NO_x formation and the heat basis NO_x formation increased with increasing sawdust addition. It is important to note that the sawdust had a dry nitrogen content of 0.2%, the Polish coal 1.2%, and the Russian coal 1.9%. Despite the decreased nitrogen content of the cofired fuel, NO_x formation increased. The author states the NO_x increased due to increased particle size from using mills not designed for biomass and the increased moisture content of the sawdust compromising combustion performance. Unfortunately, the author was only concerned with assessing the feasibility of cofiring coal with sawdust. Therefore, no NO_x tuning work was performed for each fuel to determine the optimum air distribution for NO_x reduction. It is apparent from the literature review that there is very limited primary literature on cofiring coal and AnB in low NO_x burners.

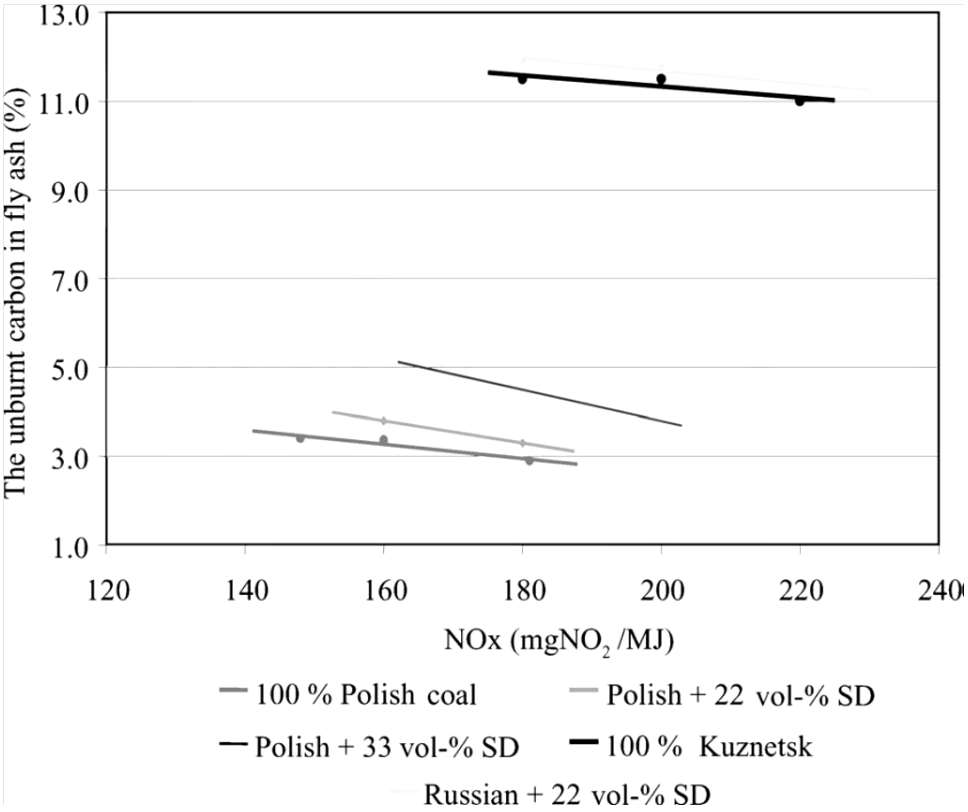

Figure 2.23 NO_x and Unburnt Carbon in Fly Ash concentrations for coal and coal-sawdust cofired fuels in a 315 MW tangentially fired low NO_x utility boiler. (Adapted from Savolainen, 2003).

3. OBJECTIVES

The overall objectives of the current research are to 1) cofire coal and LADB in a low NO_x burner and determine the combustion and emission performance under staged and unstaged conditions, and 2) investigate whether staged combustion and cofiring can work synergistically to achieve greater NO_x reduction than either technology alone. In order to achieve these objectives, the following tasks were performed:

1. Modify the low NO_x furnace to include arm staging to improve combustion staging performance.
2. Grind fuels to pulverization classification and obtain fuel particle size analysis on fuels to verify pulverization.
3. Obtain standard solid fuel analyses (ultimate, proximate, and heat value) of coal and LADB.
4. Perform cofiring experiments with constant heat input for both unstaged and staged combustion and collect combustion and emissions data from cofiring experiments.
5. Conduct gas analysis and evaluate combustion and emission performance in terms of burnt fraction and synergistic NO_x reduction.

4. EXPERIMENTAL FACILITY AND PROCEDURE

4.1 Preexisting Facility

The low NO_x burner facility at Texas A&M University was built by Brandon Martin and Gomez. They used Thien's (2002) conventional burner facility as a model. The facility, shown in Figure 4.1, was used by Gomez for his masters' work (2008). The two primary difficulties Gomez experienced in his experimentation were 1) an inability to control secondary air swirl and 2) an inability to delay tertiary air mixing with the main burner flame. Gomez used swirl helixes welded to the pipes to induce swirl and to inhibit tertiary air mixing. This design was ineffective as secondary and tertiary air would flow around the helixes and mix directly with the primary air at the flame front. In addition to these difficulties, the furnace had significant air in-leakage in the horizontal burn out section, which necessitated Gomez taking emissions readings at the base of the vertical section of the furnace which did not provide sufficient residence time to provide reliable emissions data.

Figure 4.1 Furnace used in Gomez's experiment (2008).

4.2 Modifications

Due to the difficulties described in the previous section, it was necessary to modify the LNB prior to experimentation. The modifications were performed with the assistance of undergraduate student researchers and German exchange students who documented the work.

Figures 4.2 and 4.3 (Brubaker, 2010) show the lip-style air staging coal nozzle that was originally suggested to force tertiary air mixing further downstream. Primary air and pulverized coal come from the center pipe. Secondary air comes through the inside of the pipe with the flared lip welded to it. The sum of this air and the primary air is the initial combustion air seen by the coal and is used in main burner equivalence ratio

calculations. Over-fire air (also called tertiary air) flows through the gap between the sleeve and the outside of the secondary air pipe.

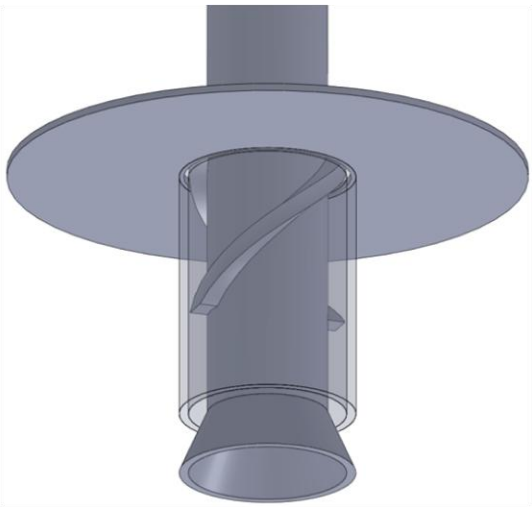

Figure 4.2 Schematic of coal nozzle used for lip-style air staged combustion. Swirl vanes welded to the secondary air pipe swirl the tertiary air and the flared lip at the end of the secondary air pipe diverts the tertiary air away from the initial combustion zone. (Adapted from Brubaker, 2010.)

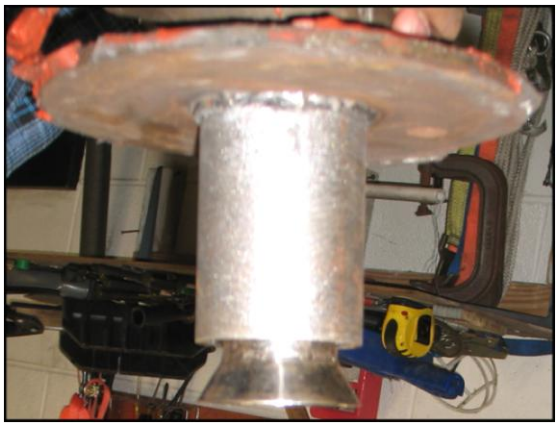

Figure 4.3. Lip-style air staging nozzle. (Adapted from Brubaker, 2010.)

As can be seen in Figure 4.2, the OFA is swirled by swirl vanes welded to the secondary air pipe and the tertiary air is swirled in the same direction as the secondary air. Upon exiting tertiary air sleeve, the OFA is diverted away from the initial combustion zone by the flared lip to delay mixing. Figure 4.4 (Brubaker, 2010) shows a picture of the lip-style air-staging nozzle after being manufactured.

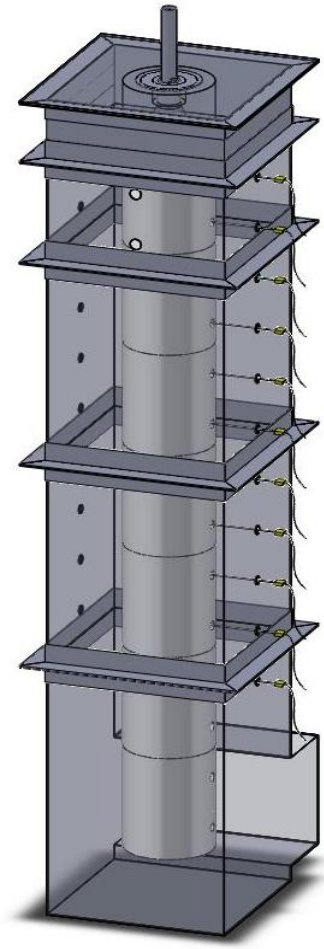

Figure 4.4 Schematic of the vertical portion of the furnace. Thermocouple and sampling ports are visible along the axial length of the furnace and the sight glasses at the top of the furnace. (Adapted from Brubaker, 2009.)

Because air mixing was still not sufficiently delayed, the lip OFA staging technique was not successful in reducing NO_x. A different staging technique was needed. After consulting with the literature to gain a deeper appreciation of the importance of SOFA air staging, the furnace was modified to mimic SOFA staging. This was accomplished by replacing the third thermocouple location with ¼ galvanized steel pipe with the opening flush with the refractory interior wall to both sides of the furnace.

Figures 4.5 and 4.6 (adapted from Barth, 2009) show a side view and top view schematic of the modification, both pre and post modification. This staging technique will henceforth be referred to as Arm Staging. By injecting the tertiary air through a pipe that has been placed physically downstream of the initial combustion zone, the delayed mixing is assured.

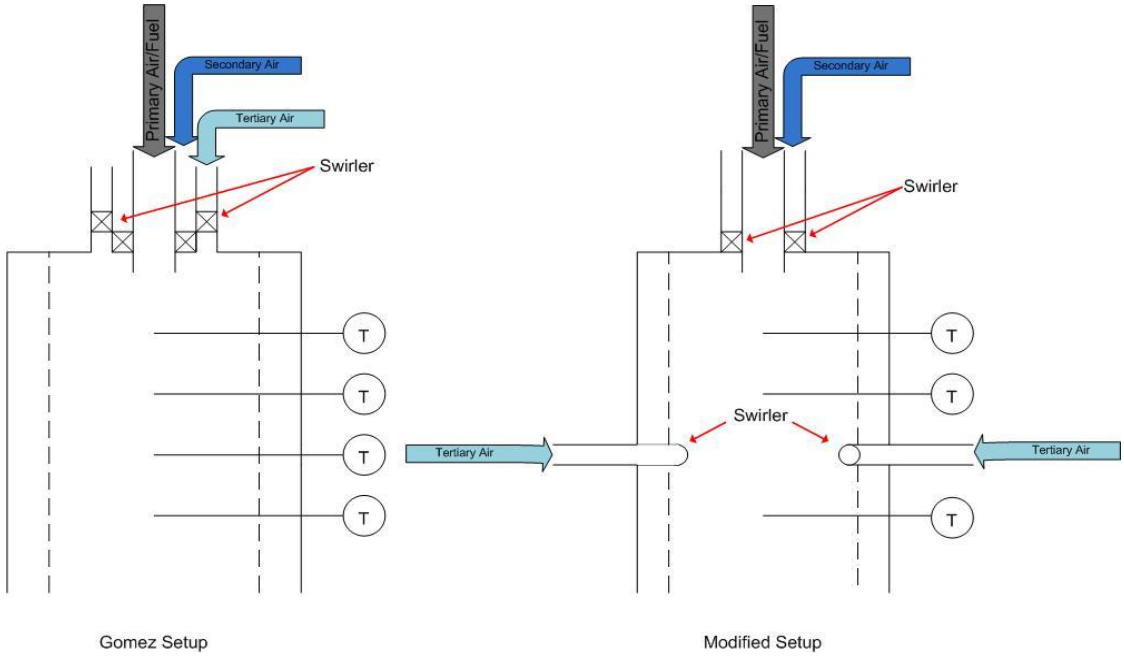

Figure 4.5 Side view schematic of the Arm Staging modification to the furnace. Tertiary air staging was valved out from the lip attachment and directed through the newly installed piping downstream of the initial combustion zone. (Adapted from Barth, 2009.)

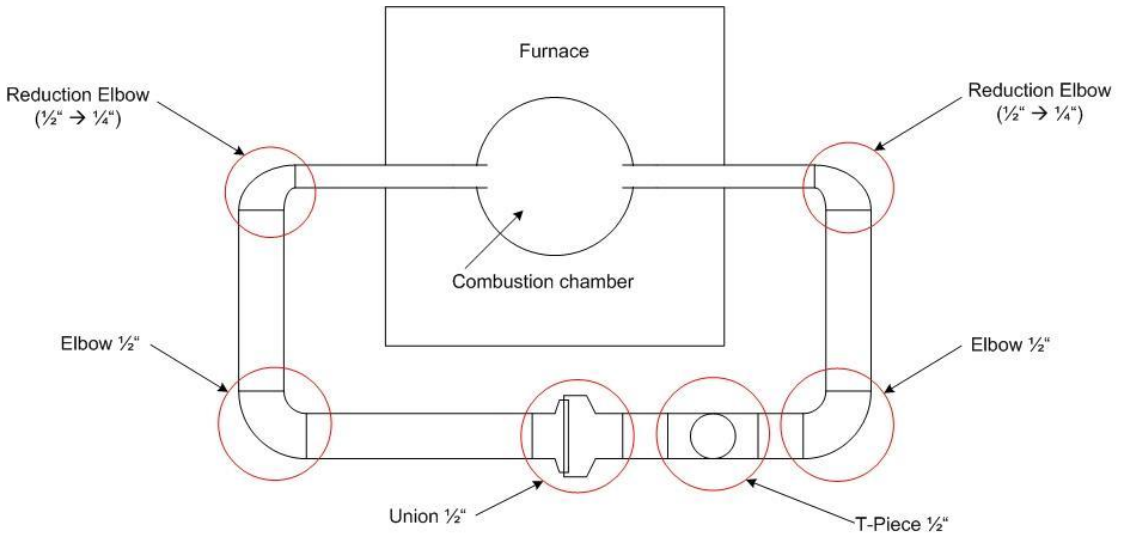

Figure 4.6 Top view schematic of the Arm Staging modification. (Adapted from Barth, 2009.)

Figures 4.7 and 4.8 show pictures of the furnace post modification and the interior of the furnace showing the arm injection points. The air in-leakage difficulty was overcome by applying a heavy coat of silicone sealant to all gaps in the horizontal burnout portion of the furnace.

Figure 4.7 Picture of the furnace after the arm staging modification. (Adapted from Barth, 2009.)

Figure 4.8 Picture of the furnace interior after the arm staging modification. The galvanized steel elbows are visible near the refractory walls. (Adapted from Barth, 2009.)

4.3 Modified Facility Used in Experiments

After completing all modifications, it was possible to perform combustion experiments. The total vertical height of the furnace is 2.61 m (103 in.) with a refractory internal diameter of 0.15 m (6 in). The exterior diameter of the furnace is 0.508 m (20 in) with insulation filling in the space between the refractory and the furnace shell. The primary air/fuel mixture is injected right at the furnace top through a 0.00635 m (0.25 in) pipe. Secondary air is swirled (swirl number = 0.7) immediately before being injected into the furnace through a 0.0508 m (2 in.) pipe concentrically aligned around the primary air/fuel pipe. Over fire air is injected through 2 opposing 0.00635 m (0.25 in)

pipes transverse to the flame path 0.457 m (18 in.) downstream of the primary and secondary air injection location. Tertiary air was staged in 0%, 10%, 20%, and 30% amounts through the arms attachment of the LNB. Propane and natural gas are used to heat the furnace to the operating temperature of 1100 °C (2000 °F). Type K (shielded, ungrounded, radiation compensated) thermocouples are used to measure the temperature along the axial length of the furnace.

Solid fuel was fed at approximately 6.80 kg/hr (15 lb/hr). A solid fuel hopper feeds pulverized coal and coal/biomass blends and disperses the fuel into the primary air stream. The fuel hopper uses a load cell, variable frequency drive, and screw feeder to control coal flow rate. The solid flow metering system was calibrated using playground sand to be accurate to within +/- 1%.

A gas sampling system is used to measure the gas composition at the end of the horizontal burn out portion of the furnace, which is used to pull a small stream of exhaust gases. After being pulled, the gases pass through a series of filters and an ice water cooled condensing coil continuously. They remove particulate matter and condensable liquids. After gas conditioning, the stream flows through an emissions analyzer (http://www.e-inst.com/industrial-gas-analyzers/products-E8500, 2013) that measures O_2, CO_2, CO, NO, NO_2, SO_2, and total hydrocarbons on a dry basis. Prior to venting to ambient, all exhaust gases pass through a water-cooling spray to lower the temperature of the gases significantly.

4.4 Experimental Procedure

The experimental procedure consisted of the following steps:

1. The gate damper at the base of the exhaust duct is fully opened to verify the induced draft fan is pulling a slight vacuum as demonstrated by the furnace manometer indicating a vacuum.
2. The gate damper is slowly closed until the furnace manometer shows very slight furnace vacuum.
3. The secondary airline is opened and ~200 SLPM flow of secondary air through the furnace is established.
4. The propane torch is lit and placed in the furnace in the flow path of natural gas when natural gas is flowing. The propane torch is never placed in the flow path of natural gas if natural gas is already flowing. In the event of previous natural gas flow, the furnace must be purged and verify that the furnace has a vacuum.
5. When good secondary air is flowing and the propane torch is burning stably, begin flowing ~15 SLPM of natural gas.
6. When the furnace temperature profile shows a sharp rise in temperature, indicating natural gas flame, close the primary valve on the propane tank and allow the propane line to purge naturally.
7. Visually verify that the furnace is sealed tight and that a slight vacuum is still present.
8. Over the next 30 minutes, gradually increase the natural gas flow to 40 SLPM and increase the secondary airflow to 400 SLPM. Periodic monitoring of the

exhaust O_2 should indicate ~1.5% O_2 in the exhaust demonstrating that the flame is slightly lean.

9. After heating the furnace for ~3 hours, the near burner furnace temperature should be ~1477 K (2200 °F). At this temperature, the natural gas can be turned off, valved out and coal flow can begin.
10. Open the primary air valve and establish 100 SLPM flow through the primary airline.
11. Increase the secondary airflow to a very lean combustion setting.
12. Turn off the natural gas and shut the natural gas valve. Only after the natural gas valve is closed should coal flow be initiated.
13. Begin flowing coal at the desired heat input rate. The fuel HHV should be used to determine the mass flow necessary to establish 100,000 BTU/hr. Use the sight glass and temperature profile to confirm flame is present.
14. Starting from the very lean setting, begin decreasing secondary air until the desired equivalence ratio is reached.
15. Conduct experiments at all desired equivalence ratios and OFA percentages.
16. When all desired data has been collected, turn off the coal feeder and allow the primary air to purge the coal line.
17. Open the gate damper to full wide open to establish a strong vacuum in the furnace. This will accelerate the cool down process.

18. Wearing thermal protective gloves and being careful to not burn yourself, unscrew the sight glasses and place them in a safe location. This will accelerate the cool down process.
19. Turn off the primary air and close the primary air valve.
20. Reduce the secondary airflow to ~300 SLPM.
21. Continue to monitor the furnace periodically as it cools. Cool down will last ~3 hours.
22. Repeat experiments for PRB and 90-10 PRB-LADB to determine experimental repeatability.

5. RESULTS AND DISCUSSION

5.1 Overview

This chapter presents the results from firing pure PRB and cofiring PRB with LADB. It begins with information on the measured fuel properties, the calculated fuel properties, and the fuel particle size distribution. It is followed by the RQ method of gas analysis and air distribution. Next, the concentrations for O_2, CO_2, CO, and NO_x are presented along with a discussion of trends and results. Only gas concentration data is provided in this chapter. Temperature data can be found in Appendix B. Prior to performing cofiring experiments, a limited number of combustion experiments were performed using natural gas. The purpose of these experiments was to verify that the furnace modifications were successful in addressing the issues encountered by Gomez. Natural gas was fired at a 0.85 equivalence ratio and staged at 0%, 10%, 20%, and 30%. Exhaust concentrations of combustion products were measured and checked for reasonableness. Figure 5.1 presents the NO_x and CO results from these experiments. As Figure 5.1 demonstrates, the facility was appropriately modified to eliminate air in-leakage and enable staging combustion.

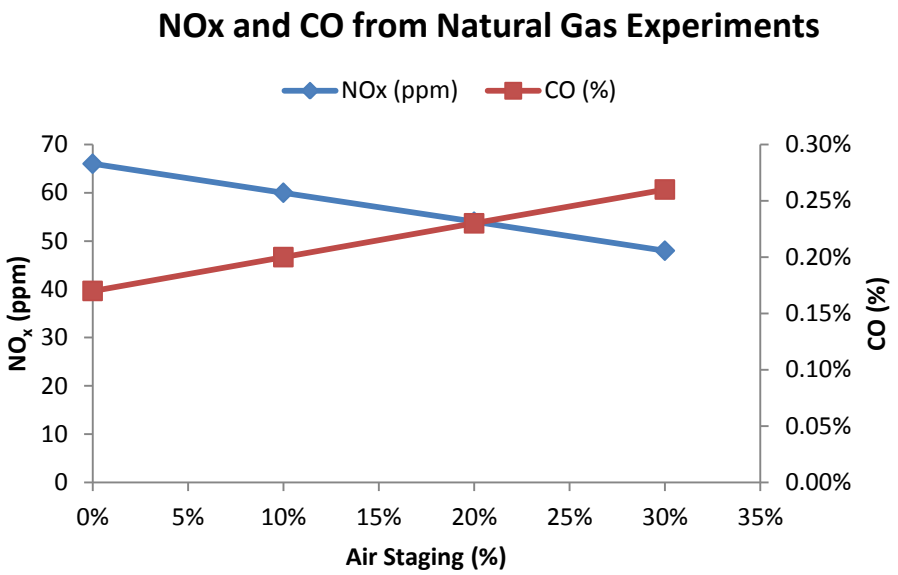

Figure 5.1 NO_x and CO results from natural gas experiments. The experiments demonstrated that the air in-leakage and staging difficulties experienced by Gomez had been resolved.

5.2 Fuel Preparation

The coal studied in this work was PRB coal from the Wyoming Powder River Basin, which is a subbituminous coal. The biomass used for this study came from a dairy outside of Stephenville, Texas. The dairy has concrete floored pens with manure collected by flushing with a hose. The flushed manure is passed through a mechanical separator that separates the solids and the liquids. The separated solids were then composted for 90 days in a decommissioned USDA greenhouse in Amarillo, Texas. Because the dairy pens are concrete floored, dirt (the primary contributor to ash content) did not get collected with the biomass; hence, the biomass is low in ash. The collection and preparation techniques employed for the biomass lead to the fuel name of low ash,

partially composted, separated solids dairy biomass, known as LABD. For additional information about the fuel preparation, see the Literature Review.

Table 5.1 presents the measured fuel properties for the fuels investigated. Note that all the values presented in Table 5.1 are on an as received basis. As can be seen in Table 5.1, the biomass has half the fixed carbon of the coal. This means that most of the carbon in the biomass is contained in the volatile matter. This is confirmed by the biomass having significantly more volatile matter than either coal. Note that even though the biomass ash is low compared to other DB fuels, the DB still has more ash than the coal does.

Table 5.1 Measured fuel properties for fuels investigated

As Received Proximate Analysis		
	PRB	LADB
Moisture	32.88	25.26
Volatile Matter	28.49	46.88
Fixed Carbon	32.99	13.00
Ash	5.64	14.86
As Received Ultimate Analysis		
	PRB	LADB
Carbon	46.52	35.21
Hydrogen	2.73	3.71
Oxygen	11.29	18.60
Nitrogen	0.66	1.93
Sulfer	0.27	0.43
As Received Heat Value		
	PRB	LADB
HHV (kJ/kg)	18193	12844

Table 5.2 Calculated fuel properties for fuels investigated

Calculated Fuel Properties		
	PRB	LADB
Dry HHV (kJ/kg)	27,107	17,186
Dry Ash Free HHV (kJ/kg)	29,593	21,450
As Received HHV (kJ/kg of stoichiometric air)	3,192	2,886
Boie HHV (kJ/kg)	18,348	14,799
As received Air-Fuel Ratio	5.70	4.45
Dry Ash Free Air-Fuel Ratio	9.22	7.44
Dry Ash Free Fixed Carbon (%)	53.7%	21.7%
Dry Ash Free Volatile Matter (%)	46.3%	78.3%
Ash Loading (kg/GJ)	3.10	11.57
Nitrogen Loading(kg/GJ)	0.36	1.50
Sulfer Loading (kg/GJ)	0.33	0.15
Empirical Formula	$C_{3.873}H_{2.709}O_{0.706}N_{0.047}S_{0.008}$	$C_{2.931}H_{3.681}O_{1.163}N_{0.138}S_{0.013}$
Carbon Normalized Empirical Formula	$CH_{0.699}O_{0.182}N_{0.012}S_{0.002}$	$CH_{1.256}O_{0.397}N_{0.047}S_{0.005}$
Respiration Coefficient	0.92	0.94

Listed in Table 5.2 is the stoichiometric air-fuel ratio for PRB and LADB. Due to changes in fuel composition, the stoichiometric air-fuel ratio changes for the fuels and also for the blended fuels. During experimentation, the operating air-fuel ratio was adjusted accordingly to account for the changes in stoichiometric air-fuel ratio to maintain the nominal value for equivalence ratio. Table 5.2 lists the respiration coefficients for PRB and for LADB. Details of the calculation of the respiration coefficient are available in the Appendixes. As indicated in the Literature Review, the respiration coefficient is a measure of the amount of carbon dioxide the fuel with release through oxidation. Because the heat content of a solid fuel per unit of stoichiometric oxygen is constant for most fuels, fuels with a larger RQ will produce more carbon dioxide per unit of heat input to a power plant. For additional information on the

respiration coefficient, see Hall (2012), Richardson (1929), Morinaka et al. (2012), and the Appendixes.

According to Babcock and Wilcox (1978) solid fuels with less than 69% FC and a HHV less than 11,000 BTU/lb need to be ground to 60% less than ASTM mesh 200 (75 microns). This requirement applies to coal for use in a pulverized coal fired, water tube boilers. Coarser ground fuels can be fired in stokers and cyclone furnaces. Fuels were ground separately in a Sweco grinding mill. Fuels were ground to improve fuel fineness, which accelerates combustion due to increased surface area to volume ratio for fuel particles. All fuels were sieved in a CE Tyler Roto-Tap model B. The Rossin-Ramler distribution is a weighted probability distribution that has been approved by ASTM (2006) standard C136-06 for coal, clay, gypsum, and coarse aggregate. The Rossin-Ramler distribution is a form of the generalized Weibull distribution modified to be appropriate for solid fuel particle sizing. This standard was followed for shaking the fuels. Table 5.3 presents the scale factor and shape factor of the Weibull distributions that describe the particle distributions for PRB and LADB as well as Sauter Mean Diameter for PRB and LADB (Lawrence, 2007; www.filtration-and-separation.com, 2013).

Table 5.3 Fuel particle size distribution for PRB and LADB. Note that the fuels have been ground to a nominal value of 70% passing through a 75 μm mesh indicating that the fuels are pulverized

Fuel Particle Size Distribution		
	PRB	**LADB**
Shape Factor	1.43	0.781
Scale Factor	114	61.8
% Smaller than 75 μm	71.1%	69.9%
Sauter Mean Diameter (μm)	57.6	35.3

5.3. Air Distribution

The primary objective of staged combustion is to properly distribute air into the furnace to inhibit NO_x formation while still providing sufficient residence time to oxidize carbon fully to carbon dioxide. As such, the air distribution in the furnace is one of the most important parameters. It is important to present the air distribution as a magnitude (m^3/min) to demonstrate air:fuel ratio as well as presenting air distribution as a percentage to demonstrate the tertiary air percentage was properly controlled. Primary air is presented first.

5.3.1 Primary Air. LADB was blended in with the PRB in 0%, 5%, 10%, and 15% amounts by mass. The fuels were fired at overall equivalence ratios 0.85, 0.90, 0.95, 1.00, and 1.05. Tertiary air was staged into the flame in 0%, 10%, 20%, and 30% of the total air stream. Tertiary air was staged either through the arm attachment downstream of the main burner. Air distribution results will be discussed in this chapter.

Figure 5.2 presents the results for primary air as a magnitude and Figure 5.3 presents the results for primary air as a percentage. Figure 5.2 is important to demonstrate that primary air was maintained at a nominal value of 0.1 m^3/min tin order to comply with manufacturer instructions for feeding coal. Figure 5.3 demonstrates that as equivalence ratio increased, total air decreased which caused primary air as a percentage to increase. The uncertainty in primary air measurements has also been included in Figure 5.4. In addition to primary air uncertainty measurements, Figures 5.5, 5.6, and 5.7 present uncertainty measurements for the independent variables: equivalence ratio, percent LADB in the fuel, and percent air staging. The uncertainty in

the independent variables presented in Figures 5.5-5.7 is applicable to all experimental results. All uncertainty analysis was performed using the algorithm laid out by Kegel [1996] based upon the methodology developed by Kline and McClintock [1953].

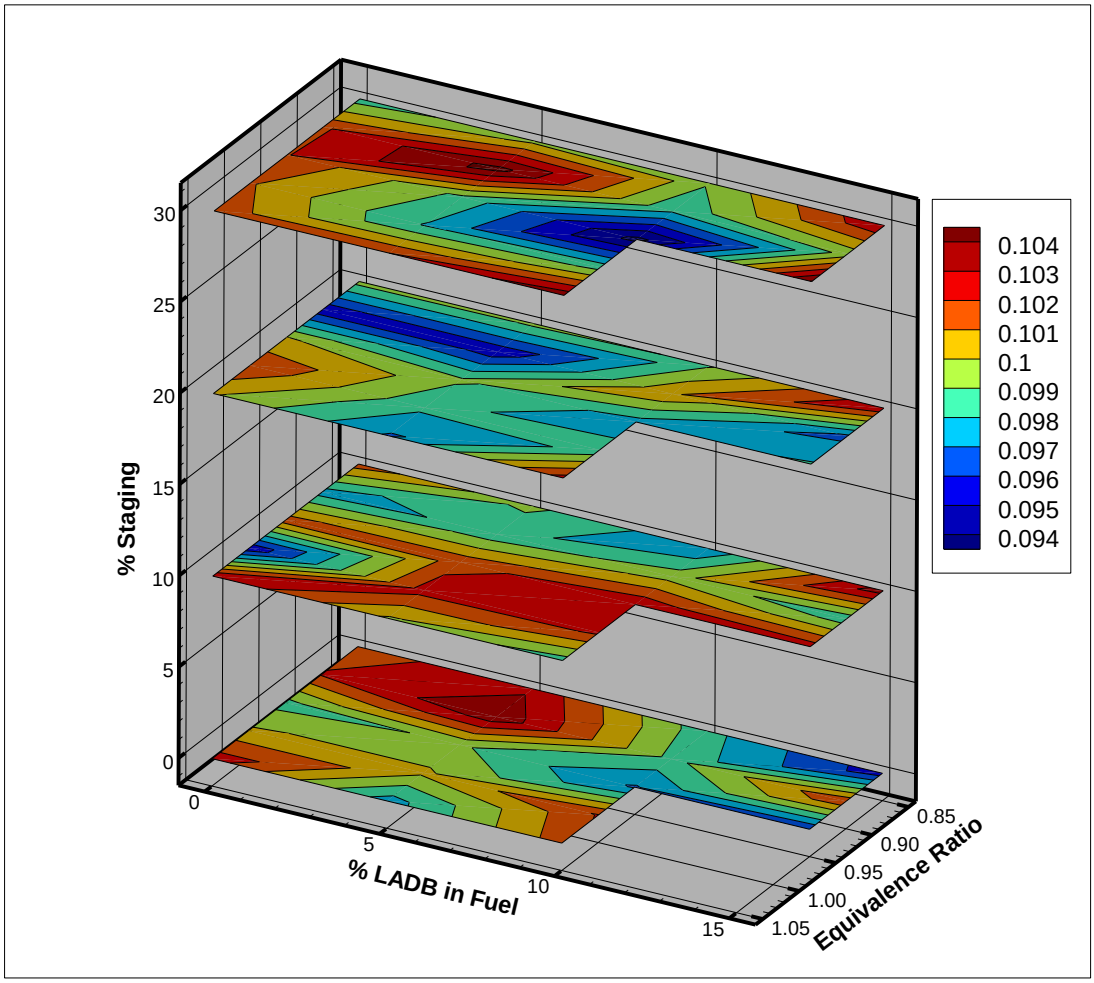

Figure 5.2 Primary air in m^3/min. The scale on the figure ranges from 0.094 to 0.104 m^3/min, which is within the precision of the primary airflow meter. The fuel feeder requires 0.1 m^3/min of primary air for proper operation.

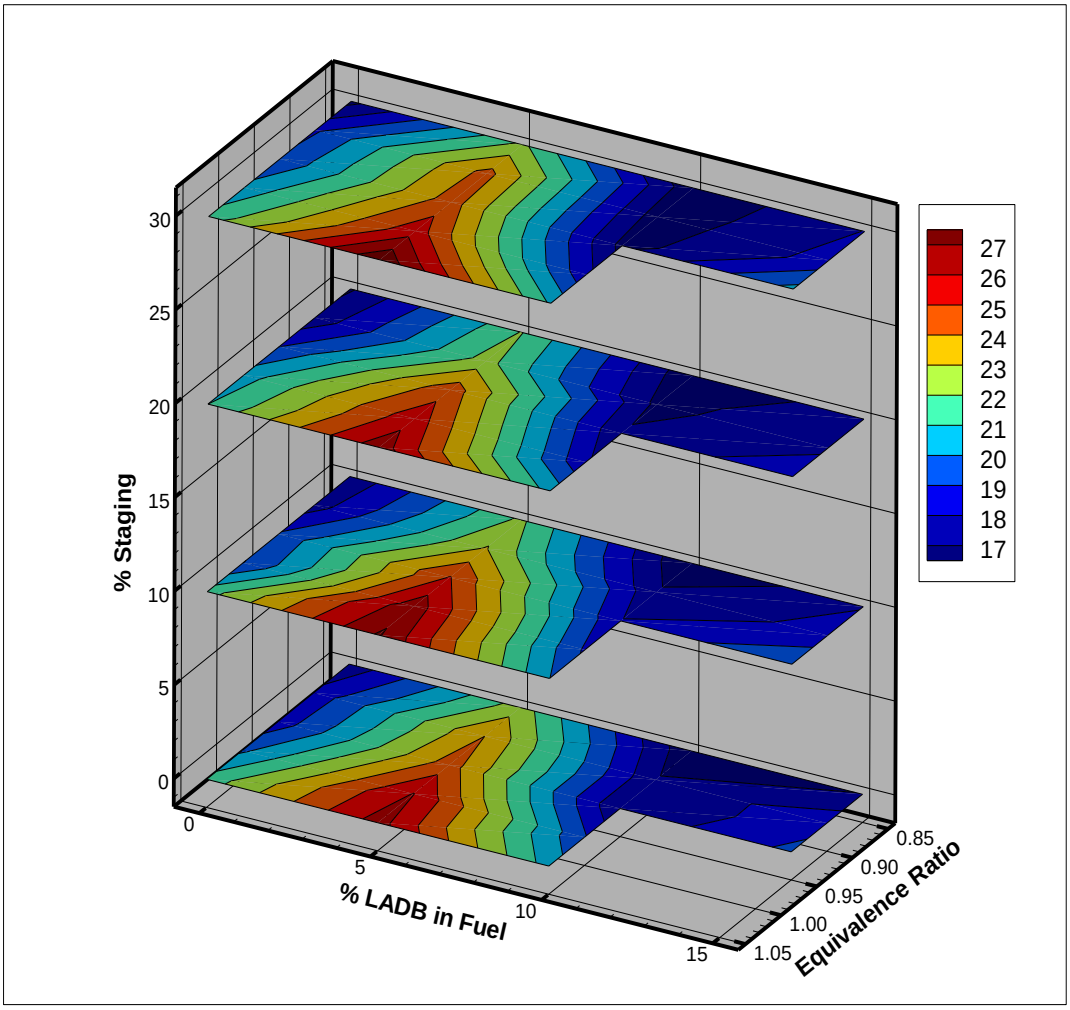

Figure 5.3 Primary air as a percentage. Because primary air was kept at a constant nominal value of 0.1 m^3/min in order to ensure proper transportation of fuel, the amount of primary air as a percentage increased with increasing equivalence ratio due to decreased secondary and tertiary airflows. The scale on the figure ranges from 17% to 27%.

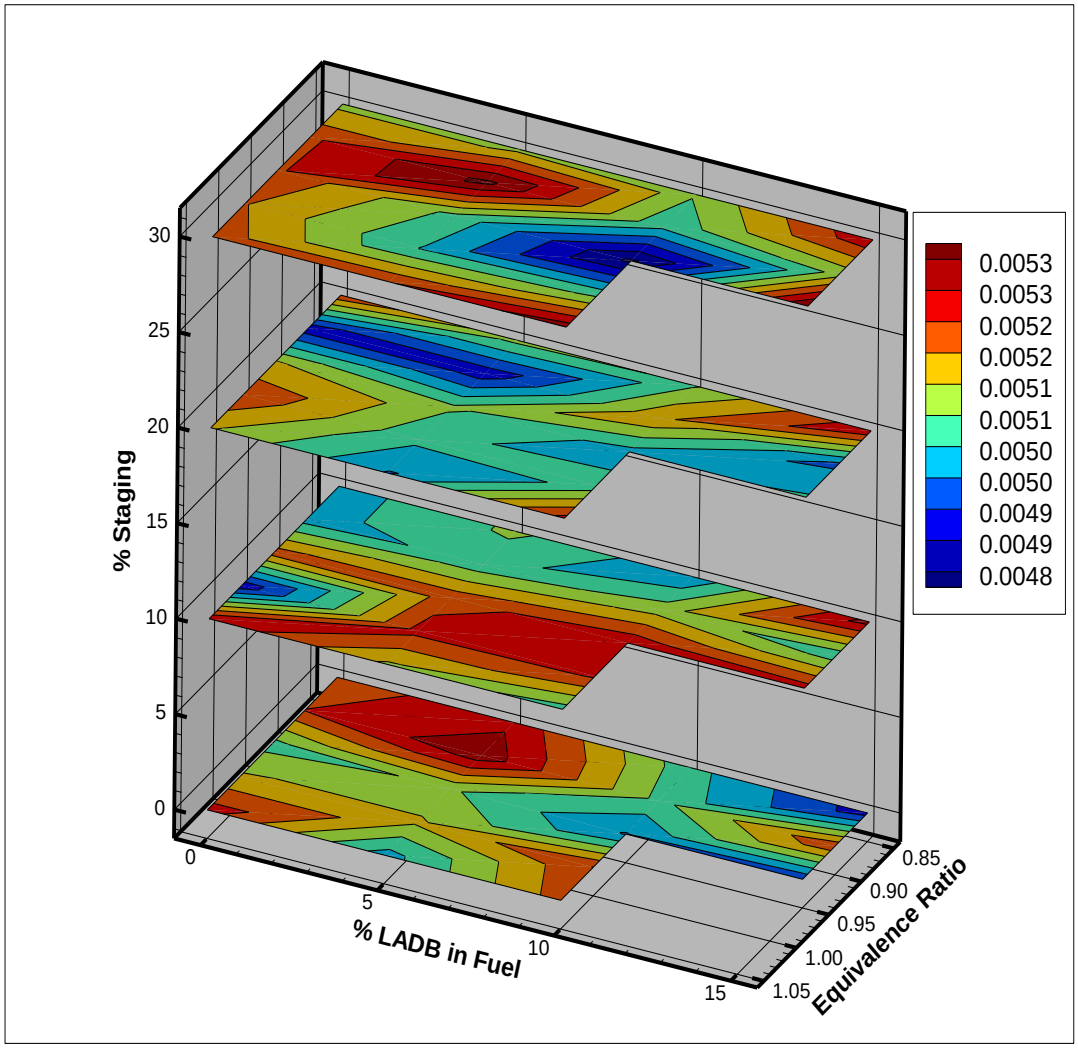

Figure 5.4 Primary air uncertainty analysis.

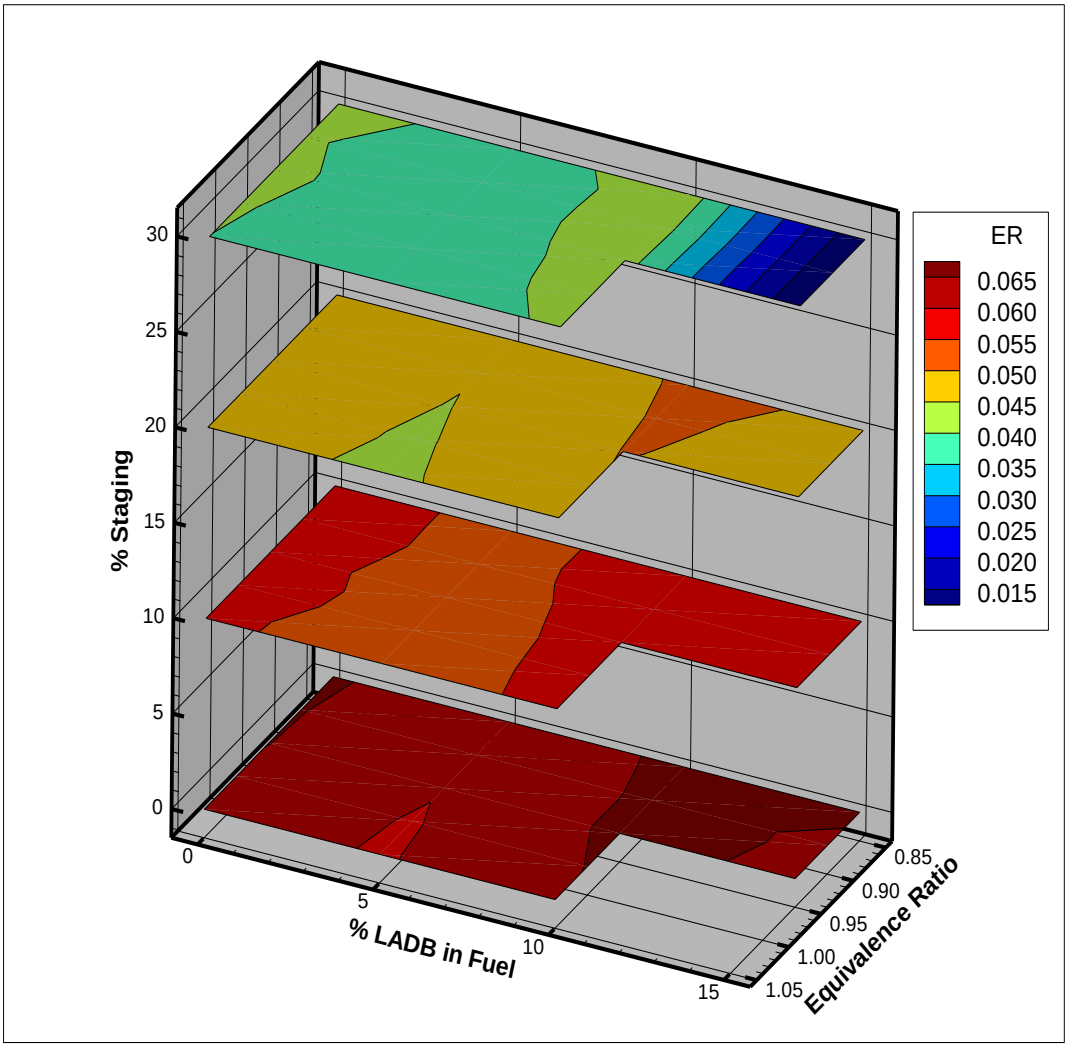

Figure 5.5 Equivalence ratio uncertainty analysis.

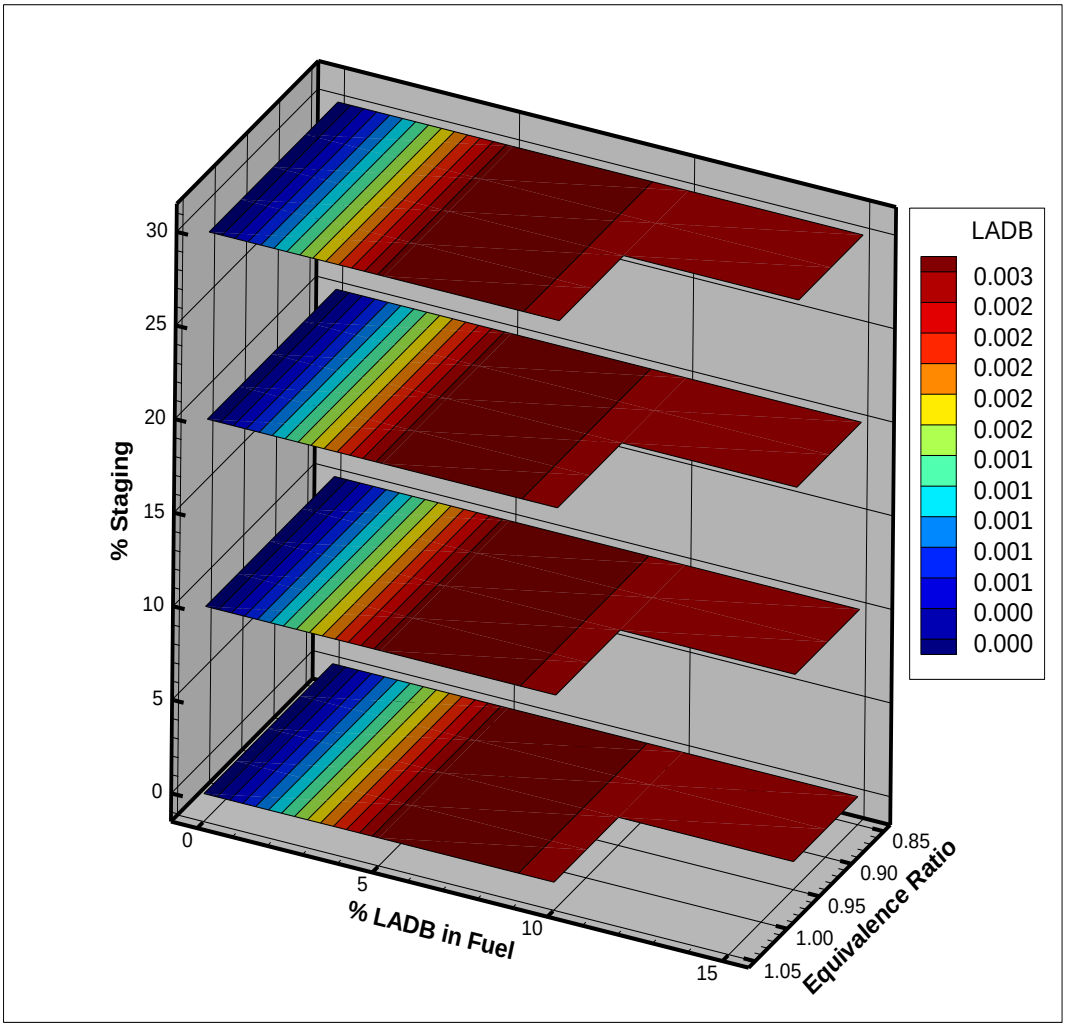

Figure 5.6. Percent LADB in fuel uncertainty analysis.

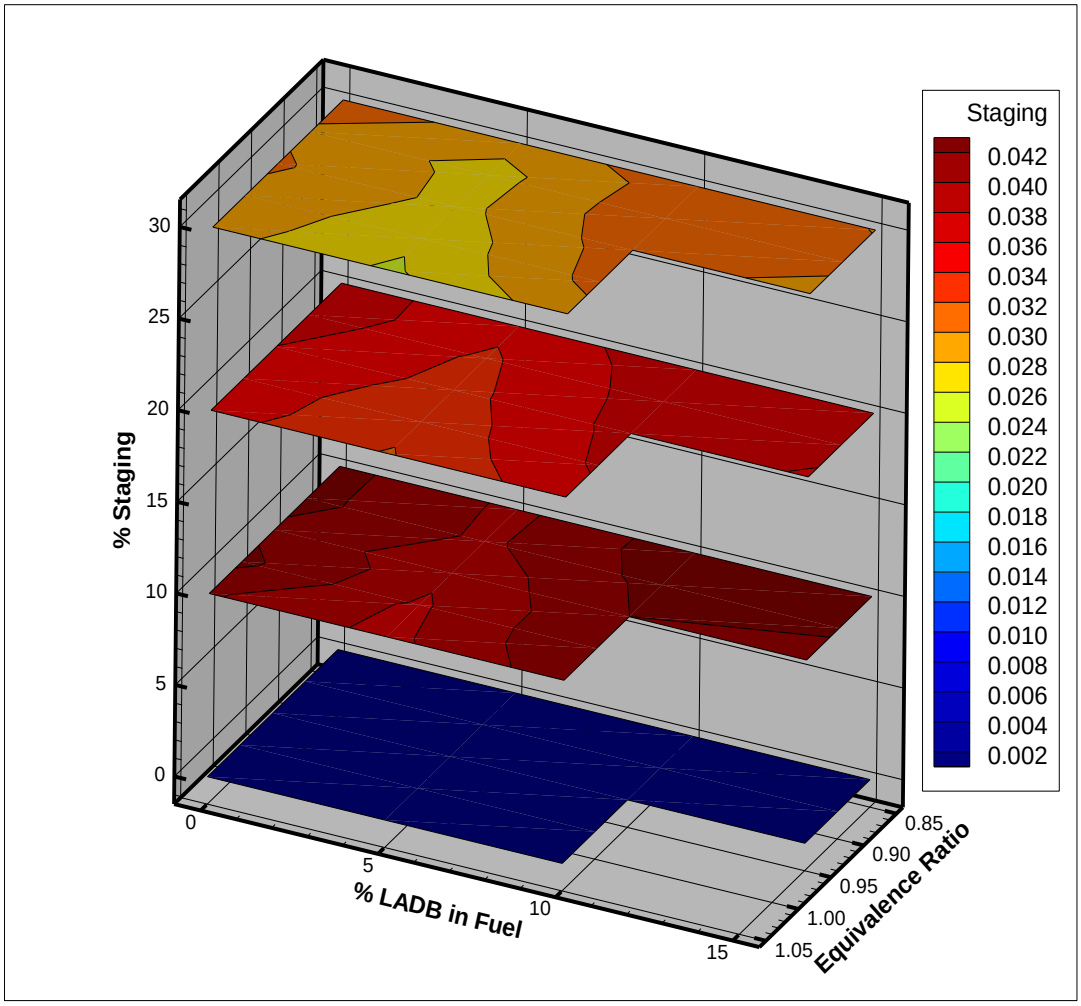

Figure 5.7 Percent staging uncertainty analysis. It should be noted that the stoichiometric air-fuel ratio for PRB and for LADB are different and therefore the stoichiometric air-fuel ratio for the blended fuel changes as the amount of LADB in the blended fuel is increased. The stoichiometric airflow was adjusted to obtain the desired equivalence ratio.

5.3.2. Secondary Air. Figure 5.8 presents secondary air as a magnitude and Figure 5.9 presents secondary air as a percentage. To increase the intensity of the air staging, tertiary air was increased at the expense of secondary air and thus the amount of secondary air both as a magnitude and as a percentage decreased with the amount of

staging for the combustion. This is demonstrated especially vividly in Figure 5.9 where the colors ranges from bright red for the unstaged combustion to deep blue for 30% staged combustion. At a fixed non-swirling primary airflow, the reduction in secondary air with increasing equivalence ratio increases the ratio of angular momentum to linear momentum. This may result in reduced recirculation zone gases, which will affect the combustion emissions. Figure 5.10 presents the secondary air uncertainty analysis.

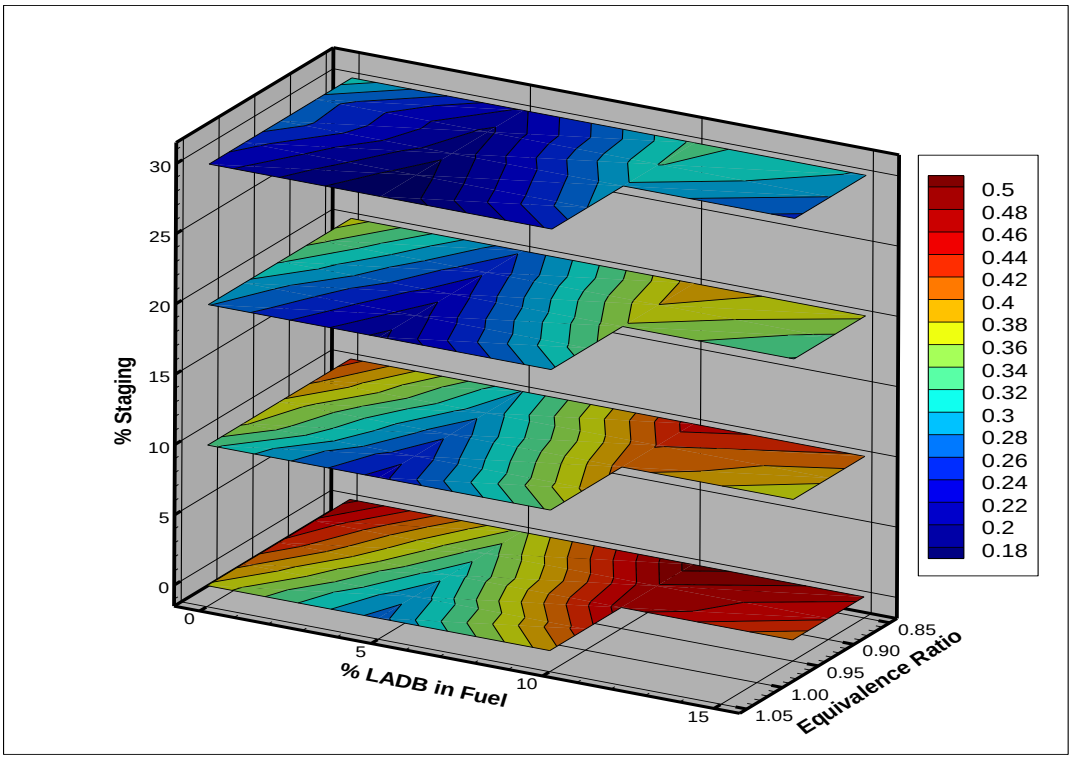

Figure 5.8 Secondary air in m^3/min. The scale on Figure 5.8 ranges from 0.18 to 0.5 m^3/min. Tertiary air was taken from secondary air and diverted to the tertiary air ports. Thus, when the amount of staging increased, the amount of secondary air decreased. Increasing equivalence ratio decreased the total air decreased and with primary air fixed, secondary air must decrease.

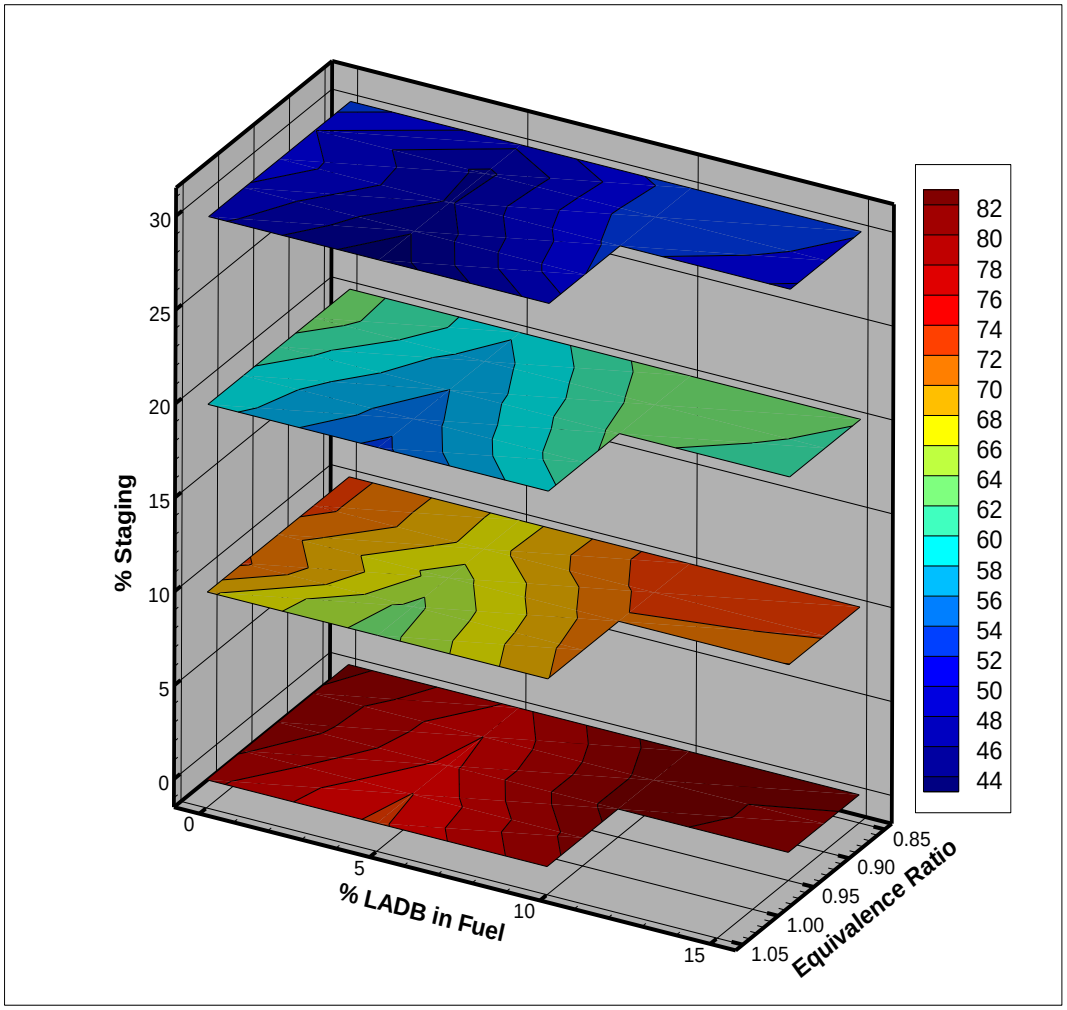

Figure 5.9 Secondary air as a percentage. The scale on Figure 5.9 ranges from 44% to 82%. Increasing tertiary air and reducing secondary air to maintain a fixed total airflow had a profound impact on secondary air when presented as a percentage. Secondary air as a percentage of total air ranged from 82% for unstaged combustion to 44% for 30% staged combustion.

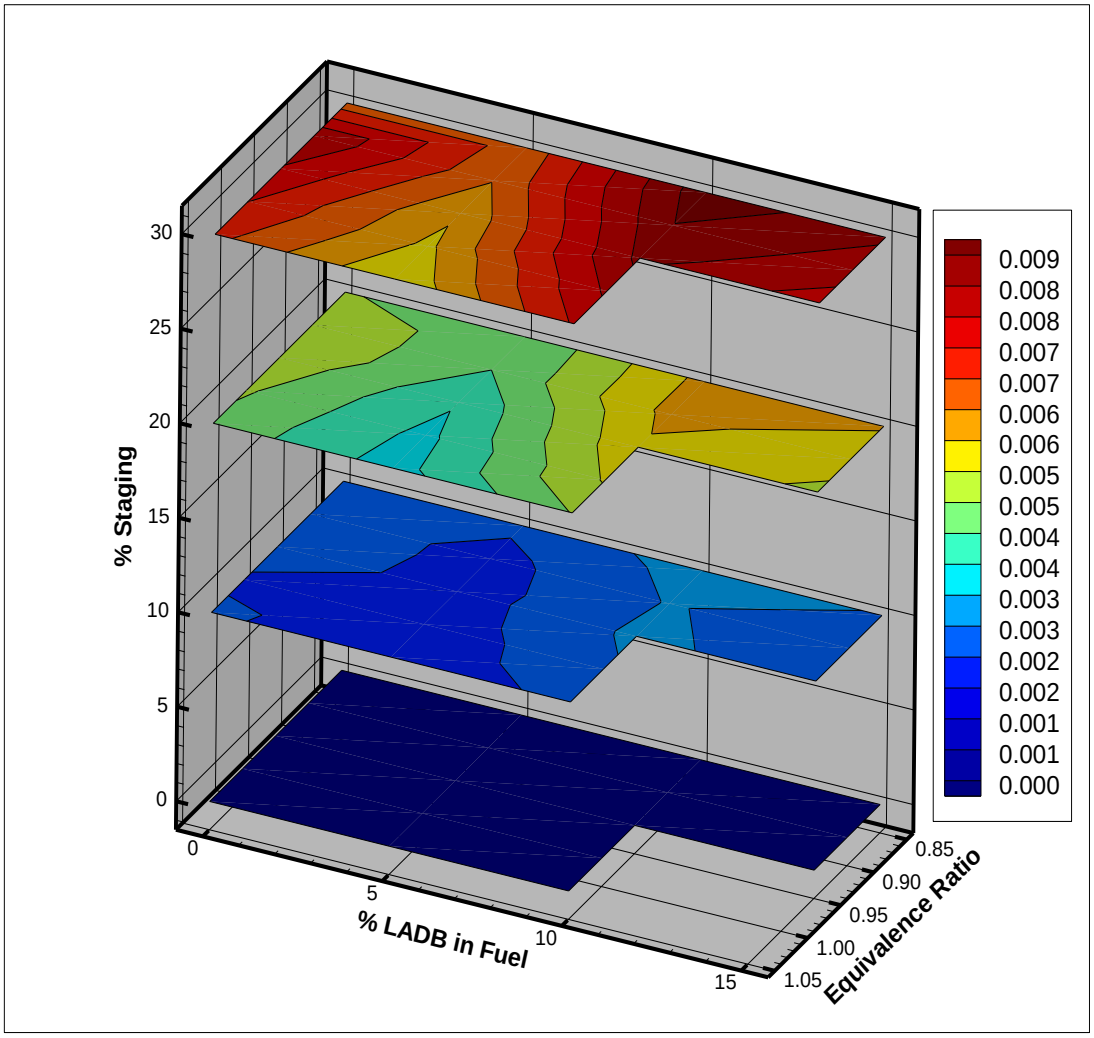

Figure 5.10 Secondary air uncertainty analysis. It should be noted that as the staging intensity is increased, the swirled momentum of the secondary air decreases and the swirled momentum of the tertiary air increases. These changes also changed the total swirled momentum and the structure of the internal recirculation zone of the flame.

5.3.3. Tertiary Air. Figure 5.11 presents the amount of tertiary air as a magnitude and Figure 5.12 presents the amount of tertiary air as a percentage. Tertiary air was staged 0%, 10%, 20%, and 30% which is representative of normal values used in utility boilers (~20%). As expected, as the amount of air staging is increased, the amount

of tertiary air also increases. As the name implies, 0% air staging was accompanied by 0 m^3/min of tertiary air. Figure 5.12 shows particularly clearly that the nominal values for percent of air staging were maintained. Also at a fixed equivalence ratio, increasing swirled tertiary air also reduces mixing of tertiary air with the gases and fuel which will affect the rate of heating of particles thus affecting combustion and emissions performance. Figure 5.13 presents the tertiary air uncertainty analysis.

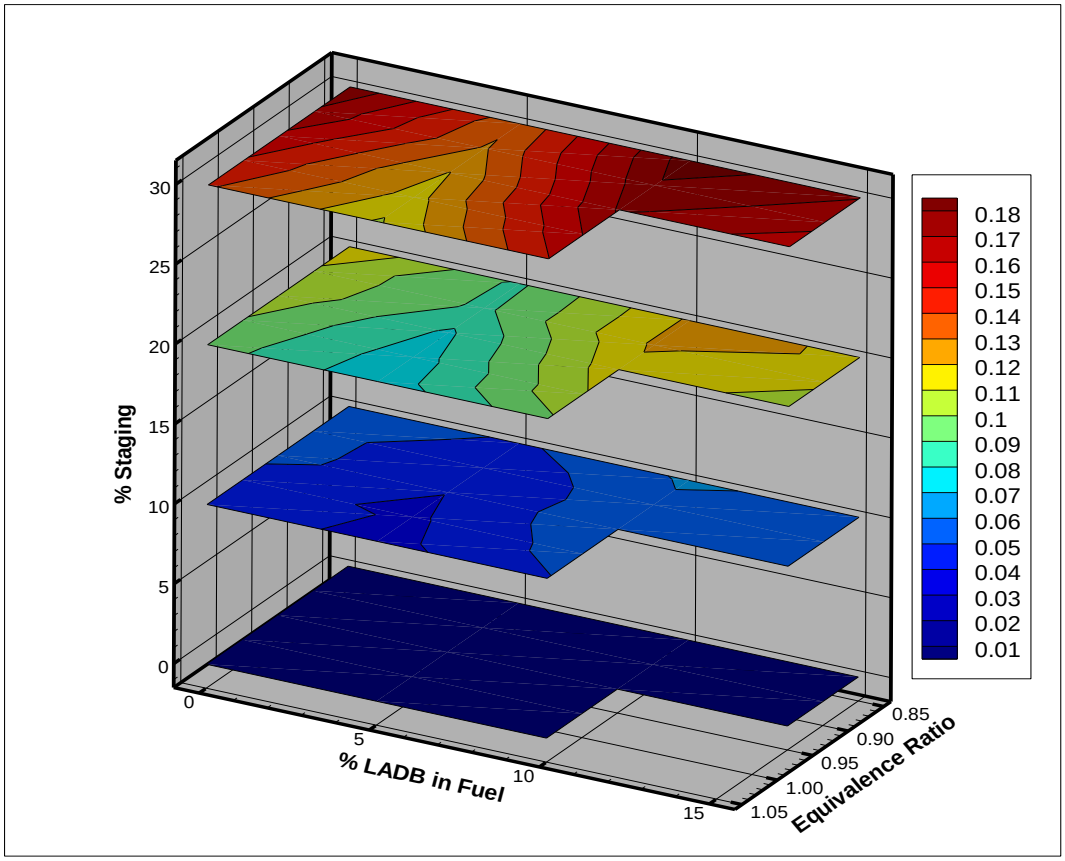

Figure 5.11 Tertiary air in m^3/min. The scale on the figure ranges from 0.01 to 0.18 m^3/min. As expected, as the amount of air staging increased, the magnitude of tertiary air also increased. Tertiary air is not swirled and thus increasing tertiary air at a fixed equivalence ratio requires reducing secondary air. The reduced angular momentum of the secondary air will decrease the effective swirl number, which will reduce the recirculated gas flow back towards the main burner.

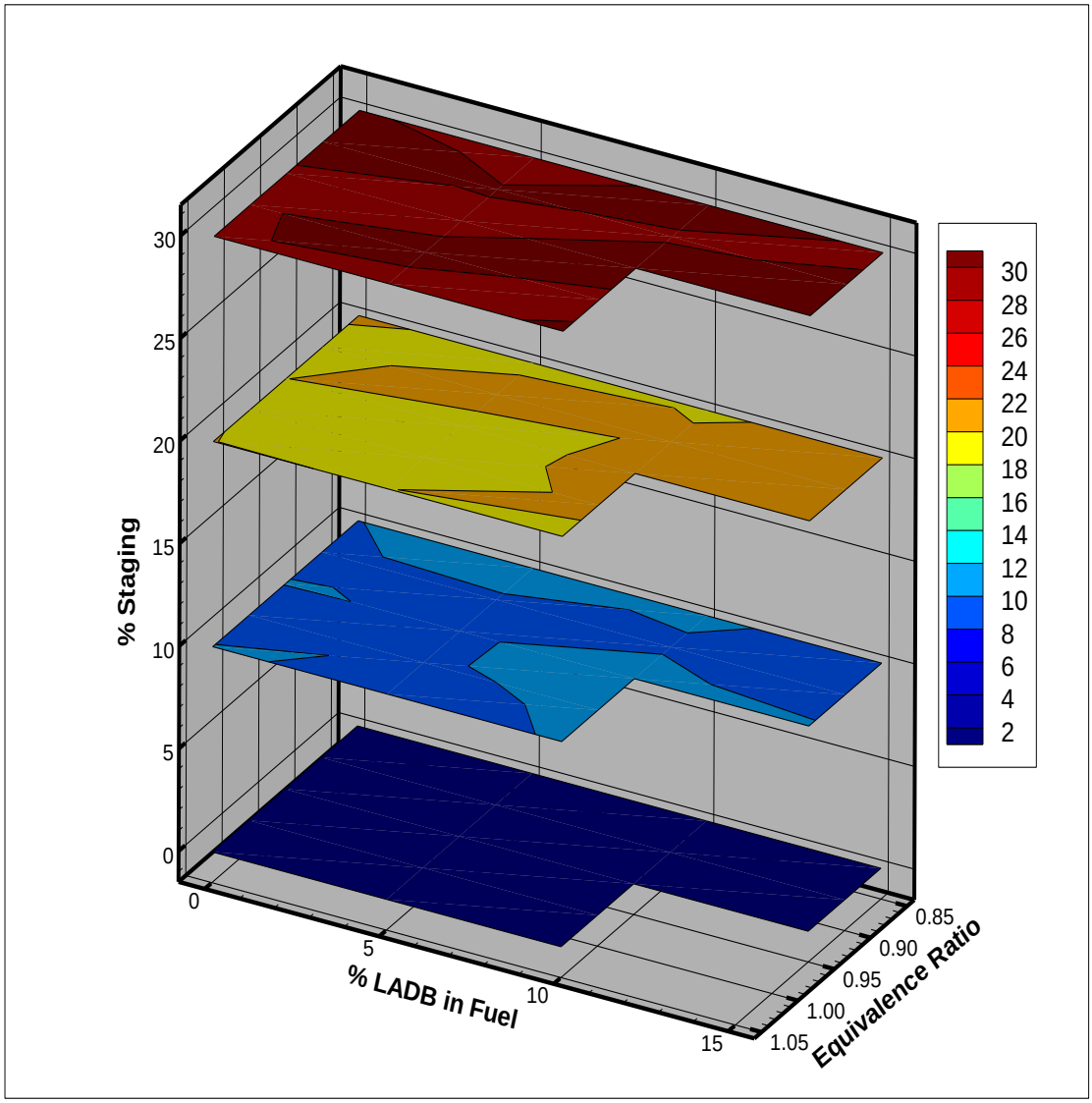

Figure 5.12 Tertiary air as a percentage. The scale on the figure ranges from 2% to 30%. Each percentage level of staging is one color, demonstrating that the nominal percent of air staging was maintained.

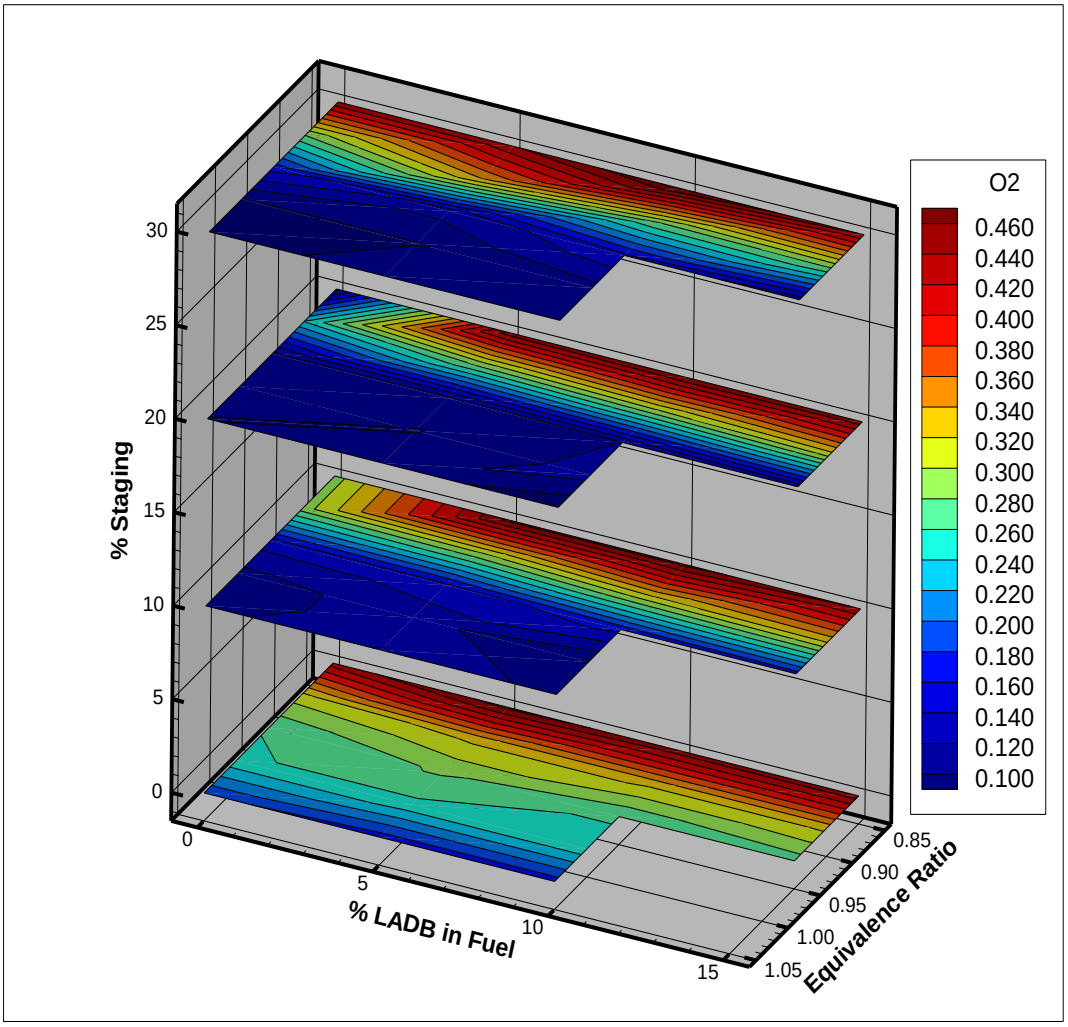

Figure 5.13 Tertiary air uncertainty analysis.

Figure 5.14 presents the main burner zone equivalence ratio, which is a measure of the sum of primary air and secondary air relative to the total stoichiometric air.

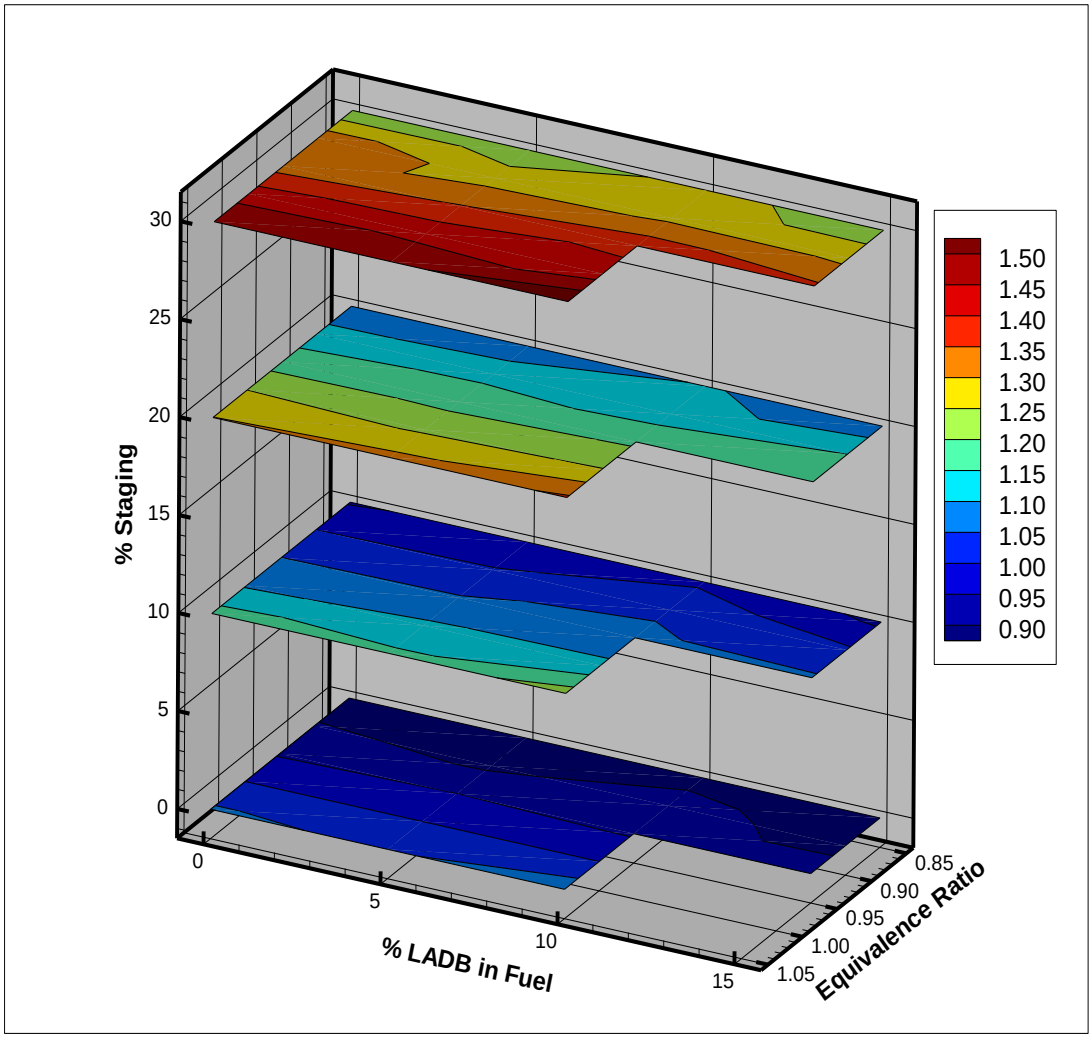

Figure 5.14 Main burner zone equivalence ratio. As the intensity of the staging increased, the main burner zone equivalence ratio also increased due to air being removed from secondary air and moved to tertiary air.

5.4. Oxygen

Oxygen concentration plays an important role in oxidation of carbon, hydrogen, nitrogen, and sulfur compounds. Thus, oxygen is the first indicator of combustion efficiency. Decreased oxygen concentration indicates a raised equivalence ratio and decreased combustion efficiency. For lean combustion, there should be excess oxygen in

the exhaust stream. If there is no oxygen in the exhaust stream, operators immediately know there is a problem in the process that needs to be addressed prior to addressing any other issue. Simply put, oxygen concentration is the first and most important indicator of combustion status.

Figure 5.15 presents the oxygen concentrations for all test cases investigated and Figure 5.16 presents the oxygen concentrations uncertainty analysis. Moving from the 0.85 equivalence ratio data points to the 1.05 equivalence ratio data points, the oxygen concentrations are characterized by straight ribbons of color beginning with red and ending with deep blue. This demonstrates that for each type of fuel and for each amount of air staging, the measured oxygen concentration was consistent for a fixed equivalence ratio. This is to be expected because oxygen concentration is most heavily a function of equivalence ratio. Further, although LADB has been blended into the fuel, the amount of LADB is a small relative to the amount of PRB. Therefore, there should not be significant changes in oxygen concentration as the amount of LADB in the fuel is increased provided thermal output is maintained constant. Note that the LADB mass percentage input is not the same and the heat input percentage due to differences in heat value. It is interesting to observe that as amount of tertiary air is increased at the same equivalence ratio, the oxygen concentration decreased indicating more oxygen is consumed in the main burn zone. When air staging is increased at a constant equivalence ratio, the main burner equivalence ratio decreases so the recirculation zone temperature increases which accelerates combustion. Further, there is rapid mixing of the burnt gases in the main burner zone. This turbulent mixing enhances combustion and oxygen

consumption. It will be seen later that the reduced oxygen concentration will have a significant effect on the NO_x concentrations because oxygen concentration inhibits NO_x formation.

When equivalence ratio increased (reduced airflow at a fixed fuel flow rate), the emitted oxygen concentration decreased. The explanation for this trend is as follows. For a given fuel, to maintain the constant heat input of 100,000 BTU/hr, a constant fuel mass flow rate is necessary. The stoichiometric air-fuel ratio is a fuel property and is constant. Thus, the only parameter that can be adjusted to change equivalence ratio is supplied airflow rate. In order to increase the equivalence ratio, the supplied airflow rate (mostly secondary air) had to be decreased. This decrease in supplied air causes a decrease in oxygen in the exhaust gas stream. A 0-D model of the LNB furnace has also be formulated and used to verify the experimental results. The results from this modeling work are being prepared for publication.

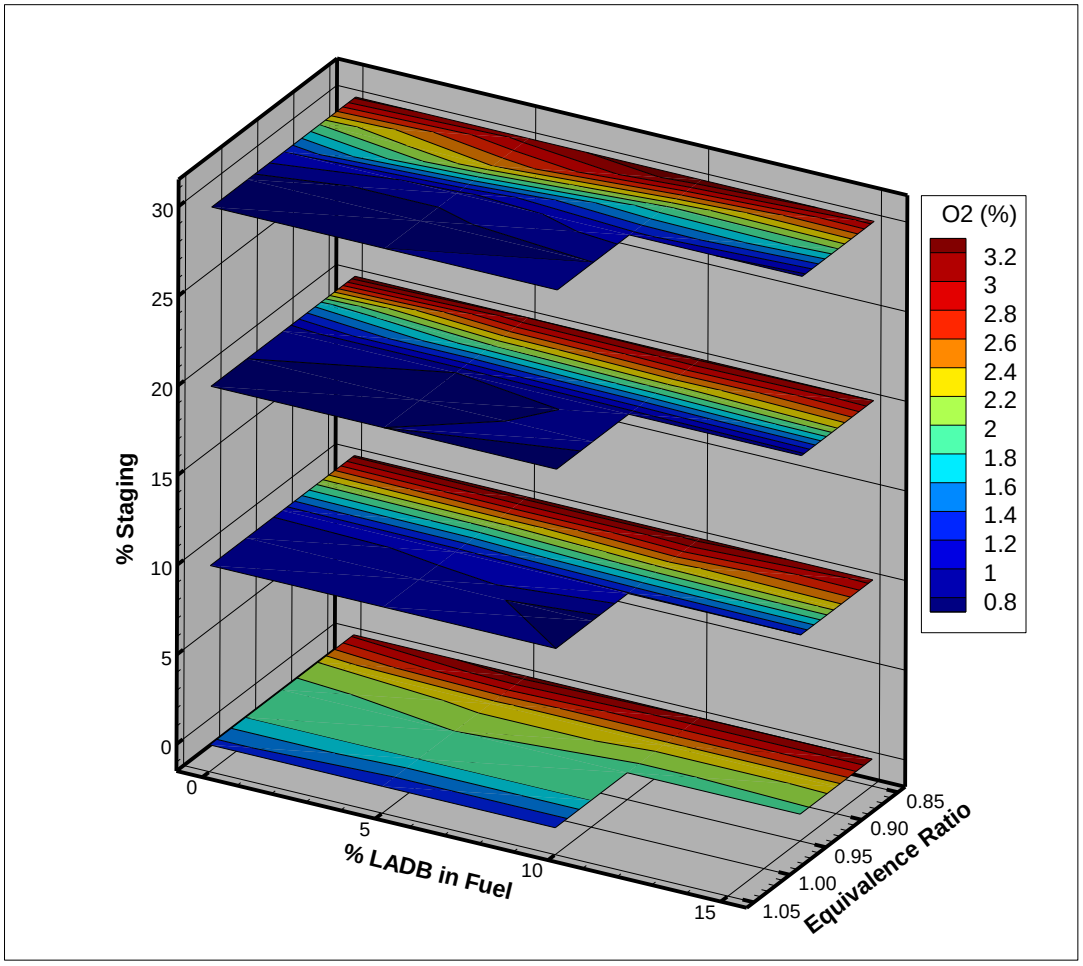

Figure 5.15 Exhaust oxygen concentration for all experimental cases investigated. Exhaust oxygen concentration was most heavily influenced by equivalence ratio. This is expected because equivalence ratio has the greatest influence on total amount of combustion air, which in turn influences oxygen consumed by combustion.

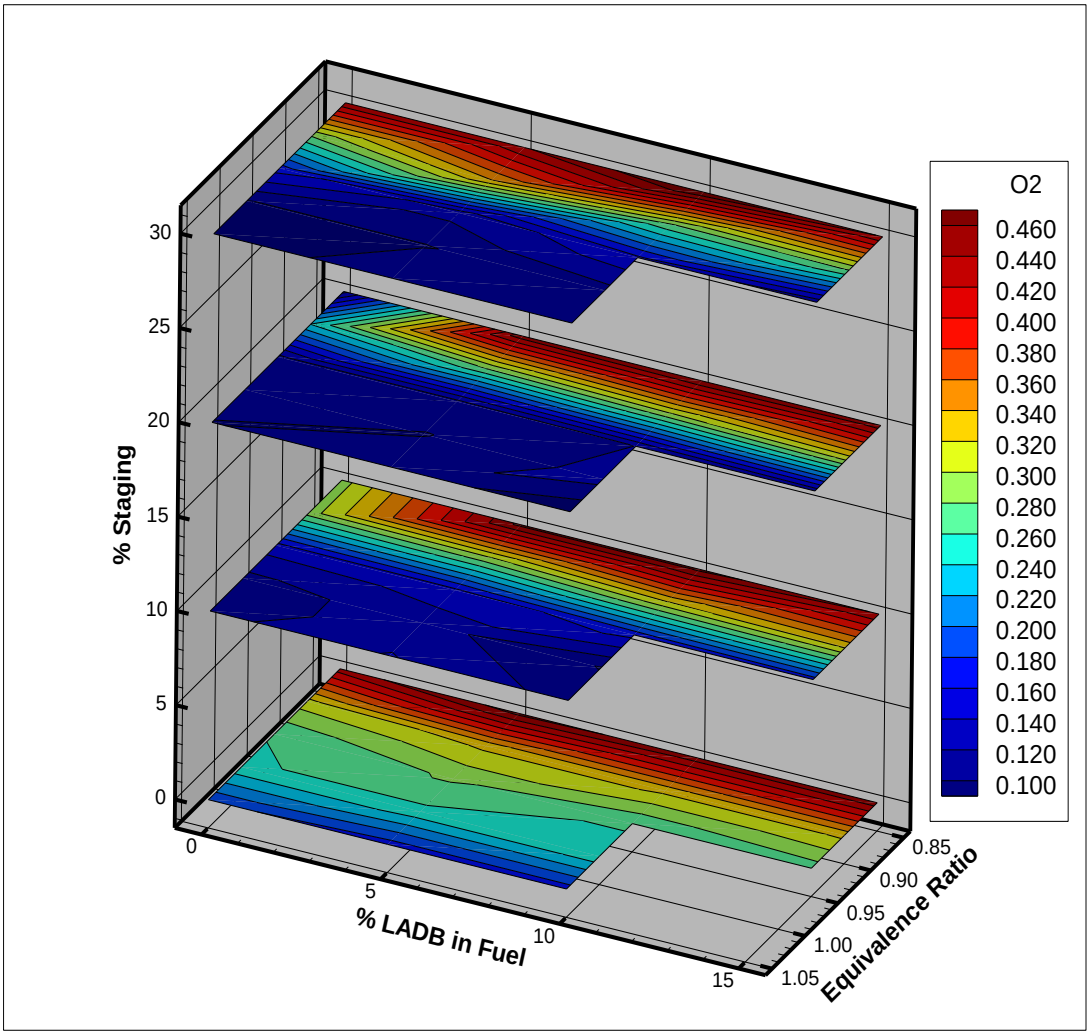

Figure 5.16 Oxygen concentration uncertainty analysis.

5.5. Carbon Dioxide

Excluding nitrogen, which is treated as semi-inert (only a small fraction of a percentage of atmospheric nitrogen is oxidized in solid fuel combustion), carbon dioxide is the primary product of combustion. This is true of all forms of combustion: gaseous, liquid, and solid. Predominantly comprised of carbon, coal combustion is one of the largest producers of carbon dioxide. Although lower in carbon than coal, biomass is still

a major producer of carbon dioxide. The reduced carbon in biomass is replaced predominantly by oxygen, which lowers the heat content of biomass. Therefore, more biomass must be consumed to provide an equivalent amount of heat. Thus, both coal and biomass have comparable RQ values (~0.93). Carbon dioxide is important because in addition to carbon monoxide, it is one of the major indicators of complete combustion. For any fuel, there are theoretical maximum amounts of carbon dioxide that could be formed under complete combustion at a fixed equivalence ratio. Carbon dioxide levels less than the theoretical maximum indicate poor performance (burnt fraction less than 1.0) and present an opportunity for improved combustion.

Figure 5.17 presents the carbon dioxide concentrations for all the experimental cases investigated and Figure 5.18 presents the carbon dioxide concentration uncertainty analysis. Carbon dioxide was minimized for both very lean (0.85 equivalence ratio) and very rich combustion (1.05 equivalence ratio). For lean combustion, both the oxygen and inert nitrogen flow work to dilute carbon dioxide in the product gas mixture. It is reduced for rich combustion because there is not enough oxygen to oxidize all fuel-bound carbon fully to carbon dioxide. Carbon dioxide was maximized under complete combustion and under stoichiometric combustion (1.0 equivalence ratio), which fits with combustion theory. The air-staged experiments produced more carbon dioxide than the unstaged experiments. In addition, the LADB blended fuels generally produced more carbon dioxide than the pure PRB at the same equivalence ratio, indicating better combustion. This is due to the greater amount of volatile matter in LADB, which burns rapidly. The volatile combustion also raised the flame temperature, which assists in

burning low volatile matter coal. Typically, volatile combustion occurs much more quickly than fixed carbon combustion. The large amount of LADB volatile matter resulted in more combustible volatile content near the main burner and increased gas temperature, which produced more carbon dioxide.

As shown in Figure 5.17, the maximum amount of CO_2 is formed at or near stoichiometric combustion. This is true whether the fuel is PRB or PRB-LADB cofired fuel. In lean combustion, there is excess O_2 in the exhaust. This acts to dilute the CO_2 concentration. In rich combustion, there is not enough O_2 to oxidize all of the fuel-bound carbon fully. Thus, the full CO_2 potential will not be met. This explains why the maximum amount of CO_2 is formed in stoichiometric combustion.

The RQ method based upon gas analysis suggests that the RQ value is a fuel property and thus will not change with equivalence ratio due to CO2 formation and O2 consumption changing proportionally when equivalence ratio is changed. Oxygen and carbon dioxide emissions from these experiments support this hypothesis. When the equivalence ratio was 0.85, PRB had a measured RQ of 0.93 and had a measured RQ of 0.90 when equivalence ratio was 0.95.

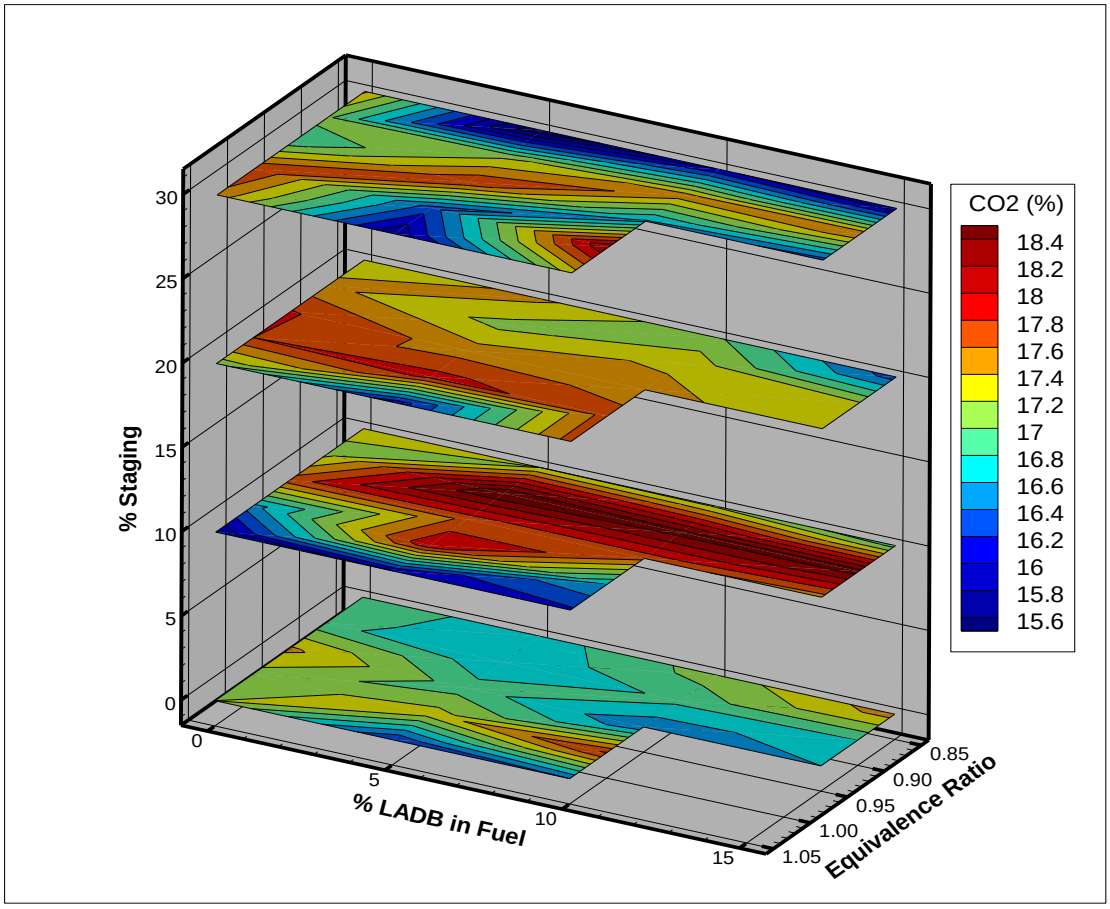

Figure 5.17 Exhaust carbon dioxide concentration for all experimental cases investigated. Carbon dioxide production was maximized with the addition of LADB due to the increased volatile matter, staged combustion promoting turbulent mixing, and at or near stoichiometric combustion.

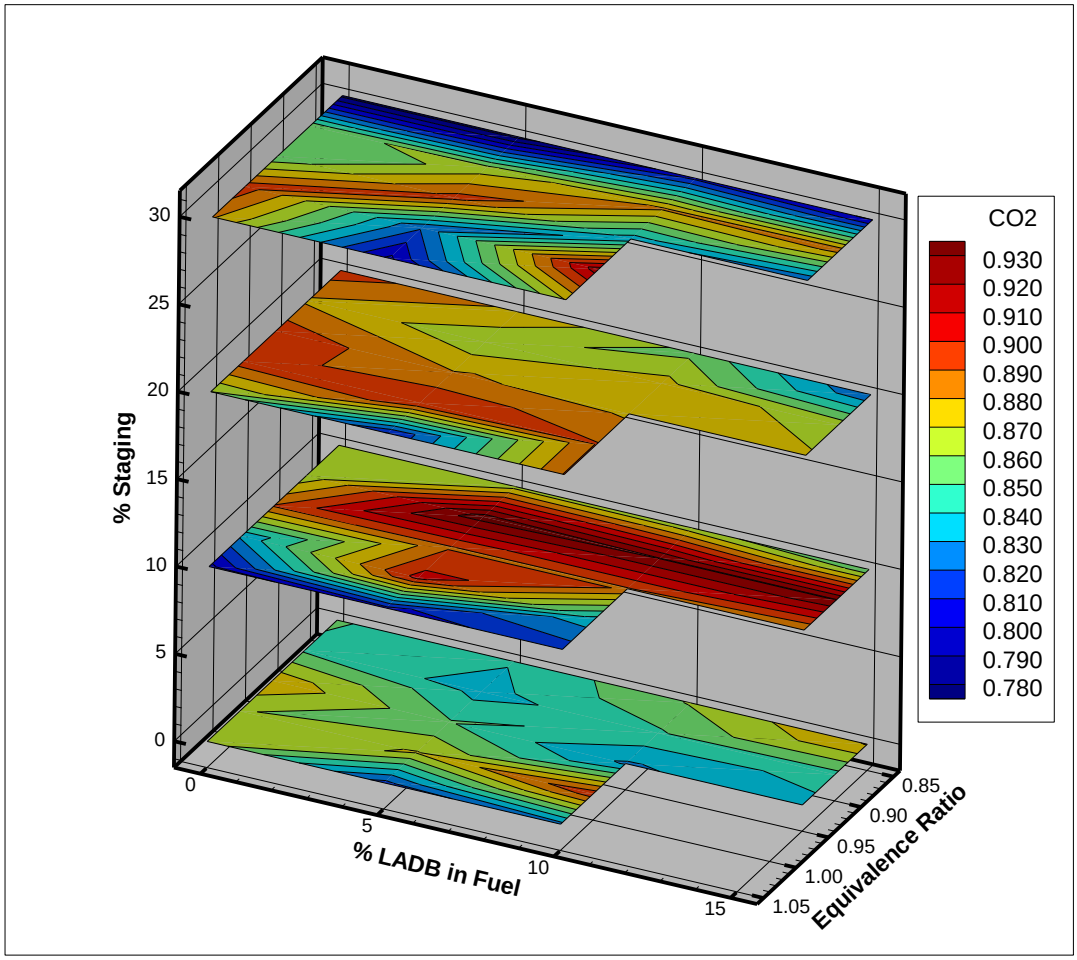

Figure 5.18 Analysis of carbon dioxide concentration uncertainty.

5.6. Carbon Monoxide

Typical solid fuel combustion theory assumes that coal releases volatile matter, which rapidly oxidizes to CO followed by CO oxidation. Next, char oxidizes to CO before it oxidizes to carbon dioxide downstream of the main burner. At reduced oxygen levels and lowered flame temperatures, the rate of CO oxidation is reduced. If there is insufficient oxygen to oxidize carbon fully or if kinetics, residence time, and mixing limit the full oxidation of carbon, then high amounts of carbon monoxide will be

produced. As shown in Figure 5.19, when equivalence ratio increases (less air being provided for combustion), carbon monoxide concentration also increases and oxygen concentration decreases. This indicates incomplete combustion. Not only does carbon monoxide indicate that the fuel is not being completely burned, which is wasteful, but carbon monoxide is also a concern because it is a health hazard and a pollutant. This section discusses carbon monoxide results from firing pure PRB and cofiring PRB with LADB.

Figure 5.19 presents the carbon monoxide concentration for all experimental cases investigated and Figure 5.20 presents the carbon monoxide concentration uncertainty analysis. In general, carbon monoxide generation was minimal. For the unstaged combustion, there was hardly any carbon monoxide formed for any of the operating conditions. When the amount of air staging was increased, there was some increase in carbon monoxide generation. The variable that most heavily influenced carbon monoxide generation was equivalence ratio, which fits with combustion theory. The same overall equivalence ratio that increases staging intensity causes the main burner equivalence ratio to increase. This causes a reduction of oxygen in the main burner zone, which leads to more carbon monoxide formation. The amount of LADB in the fuel did appear to have some influence on carbon monoxide formation as increasing the amount of LADB increased the amount of carbon monoxide formed. This is due to the increased oxygen within the LADB promoting carbon monoxide formation during volatile matter release. The carbon monoxide increased slightly from $\phi = 0.85$ to $\phi = 0.90$, then increased markedly when the equivalence ratio increased to 0.95. Further

increasing the equivalence ratio does increase carbon monoxide, but not as much as the jump from 0.90 to 0.95. This is important because the tradeoff between NO_x destruction and CO production is one of the primary constraints on LNB technology. Figure 5.19 suggests that operators should attempt to keep ϕ below 0.95 while still obtaining good NO_x performance. One other item worth noting from Figure 5.19 is that for pure PRB and 90-10 PRB-LADB, the pure PRB produces more CO at every equivalence ratio. LADB has almost half the fixed carbon content of coal. Further, due to the higher volatile content of the LADB leads to better combustion and encouraging the combustion reaction to proceed to completion. As can be seen in Figure 5.19, there is no real trend to how tertiary air affected CO production. In some cases increasing the amount of tertiary air increased CO production and in some cases it decreased CO production.

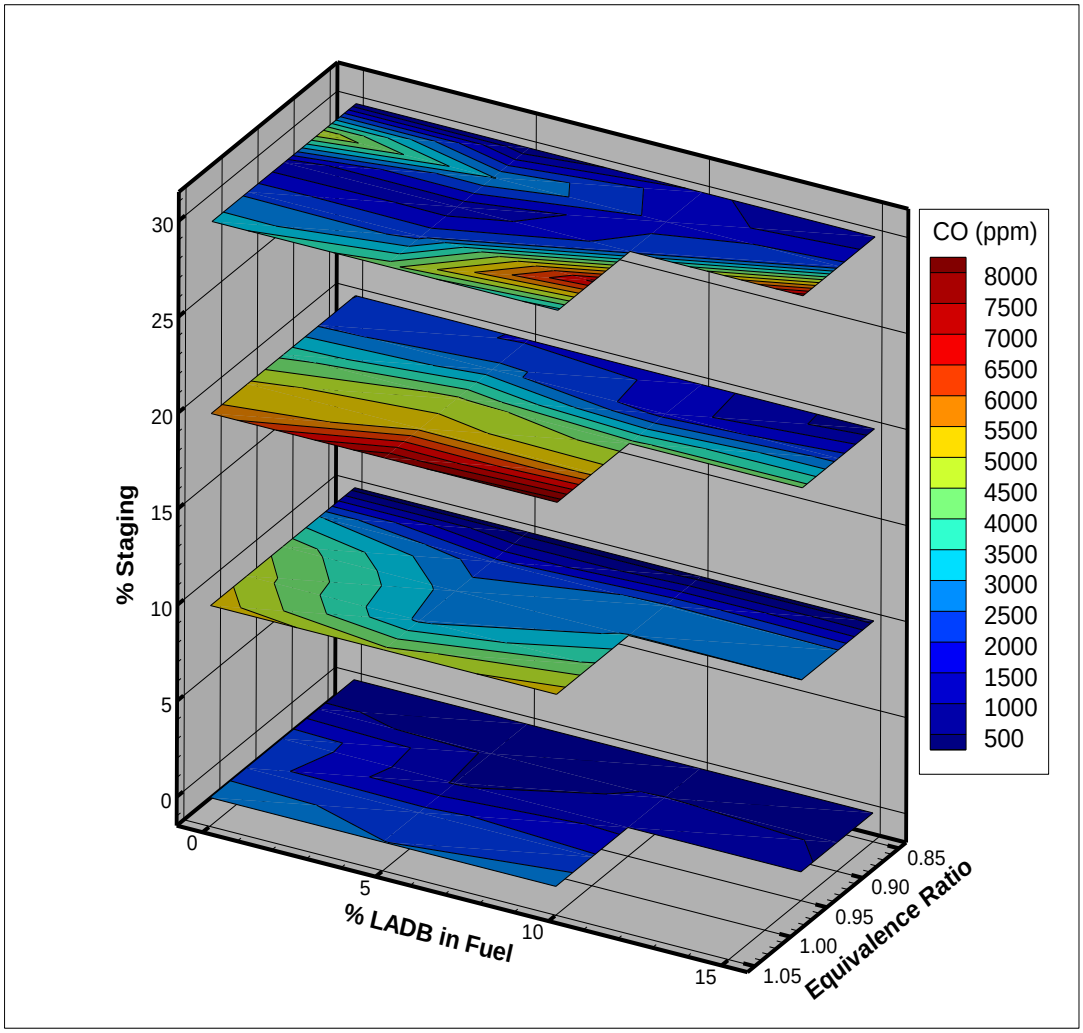

Figure 5.19 Exhaust carbon monoxide concentration for all experimental cases investigated. The equivalence ratio most heavily influenced carbon monoxide formation with rich combustion forming the most carbon monoxide. The amount of air staging and amount of LADB in the fuel also had a minor influence on carbon monoxide formation with increasing either also increasing carbon monoxide.

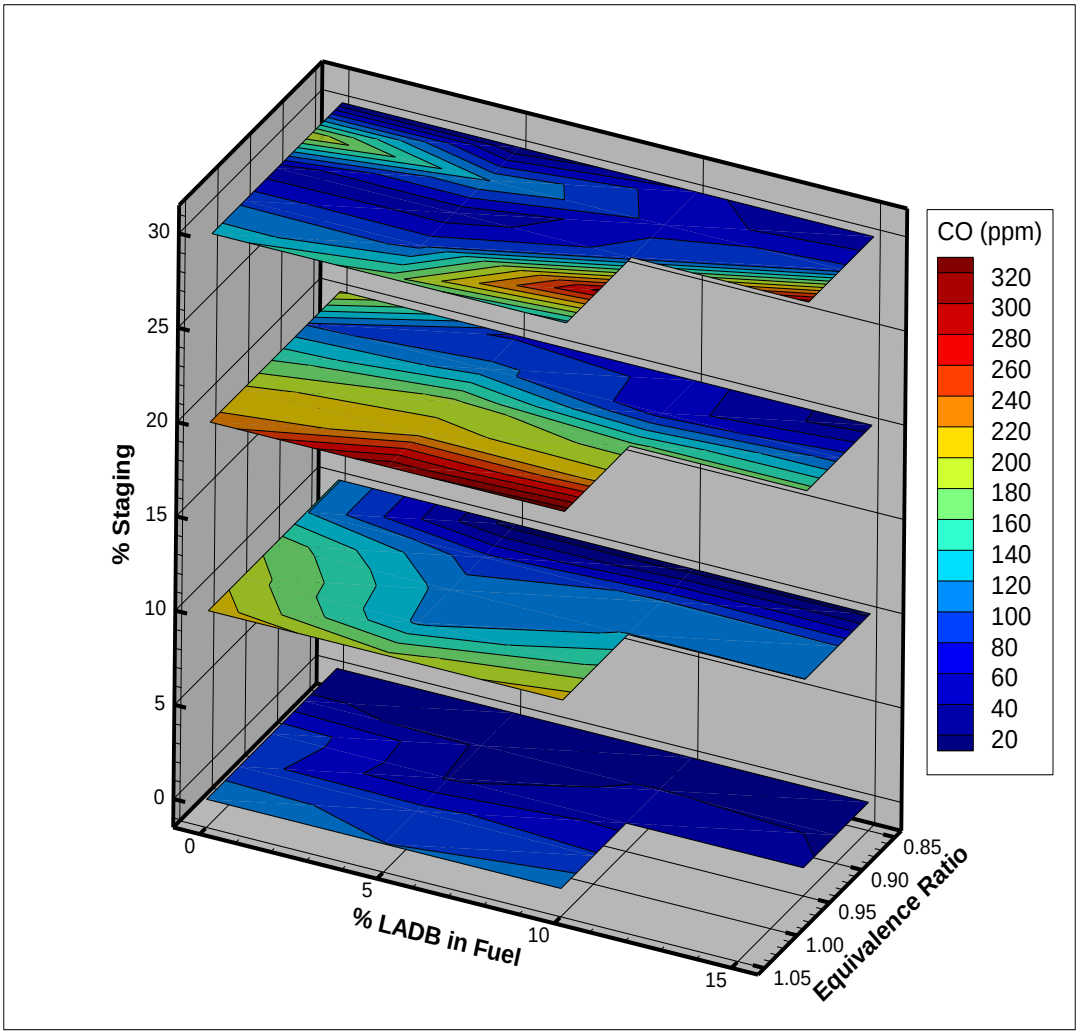

Figure 5.20 Carbon monoxide concentration uncertainty analysis.

5.7. Burnt Fraction Analysis

Burnt fraction is the last indicator of the completeness of combustion that will be discussed. For detailed quantification of the burnt fraction, carbon content in the ash is necessary. Given the limitations of the laboratory scale furnace, such an analysis is impractical. To remedy this difficulty, Thien (2002) derived the following approximation, which was later used by Lawrence et al. (2009):

$$BF \approx \frac{1}{\Phi} * \left(1 - \frac{X_{O_2}}{X_{O_{2,A}}}\right) \quad (1)$$

As can be seen in Equation (1) as oxygen is consumed to oxidize carbon (either to carbon monoxide or carbon dioxide) the burnt fraction will increase. If all the fuel is burned and the equivalence ratio is known, it is possible to estimate oxygen mole fraction in the exhaust under complete combustion conditions. However, if the measured oxygen mole fraction is larger than what is estimated under complete combustion, then not all of the fuel has been burned for the measured equivalence ratio. Therefore, it is a ratio of the equivalence ratio computed from exhaust oxygen concentration to the actual equivalence ratio based upon air and fuel flow rates. For burnt fraction to increase, fuel bound carbon must be at least gasified to carbon monoxide. For this reason, burnt fraction is sometimes referred to as gasification fraction. It is important to note that Equation (1) is an approximation and does have limitations. The most significant limitation is that it can be greater than one (100%) for very lean combustion (ϕ = 0.85 or 0.90), which indicates more than 100% of the combustible material is combusted. This is due to experimental uncertainty in oxygen measurements and fluctuations in atmospheric oxygen concentration due to relative humidity. It is also important to note that the experimental uncertainty of burnt fraction is in the range of 5%. Thus, values greater than 100% have an experimental uncertainty that could put them back below 100%. This limitation will be demonstrated in the figure in this section. Nevertheless, Equation (1) is a very useful tool for quickly quantifying the completeness of combustion and comparing the reactivity of various fuels.

Figure 5.21 presents the burnt fractions for all the experimental cases investigated and Figure 5.22 presents the burnt fraction uncertainty analysis. As expected, the parameter that had the strongest influence on burnt fraction was the equivalence ratio. Due to insufficient combustion air, particularly rich conditions had a detrimental impact on burnt fraction, sometimes as low as 90%. Even near stoichiometric lean combustion (0.95 equivalence ratio) had a burnt fraction around 96%. Thus, there appears to be approximately 4% loss through fine particulates in the exhaust and bottom ash. Losses are minimal at near stoichiometric because higher temperatures lead to faster reactions. For industrial purposes, a burnt fraction of 96% is very good and the conditions necessary for a 100% burnt fraction are not practical. The amount of LADB in the fuel and the amount of air staging did not influence burnt fraction based on exhaust oxygen analyses.

Equivalence ratio and exhaust oxygen are the parameterized variables that have the greatest impact on BF. As Figure 5.21 demonstrates, the 90-10 PRB-LADB burned more completely than the pure PRB, especially at higher equivalence ratios. This can be explained by the higher VM in the LADB initiating the combustion reaction earlier and sustaining it longer. The 90-10 PRB-LADB has a greater BF at $\phi = 0.95$ than pure PRB has at $\phi = 0.90$. This suggests that the cofired fuel can be burned closer to stoichiometric and still be assured that the combustion reaction will go to completion.

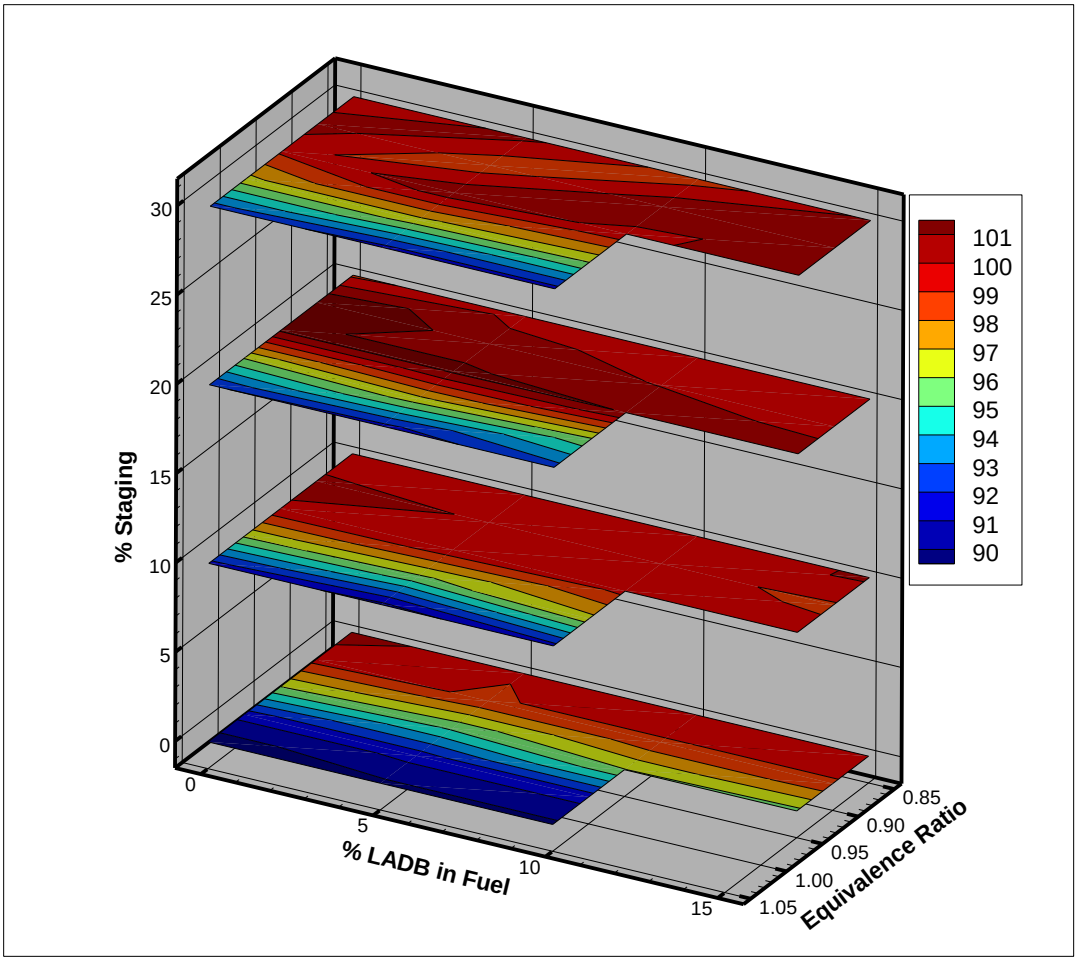

Figure 5.21 Burnt fraction for all experimental conditions investigated. The equivalence ratio strongly influenced burnt fraction with rich combustion significantly inhibiting fuel consumption. The amount of LADB and air staging did not influence burnt fraction, which agrees with the exhaust oxygen concentration results.

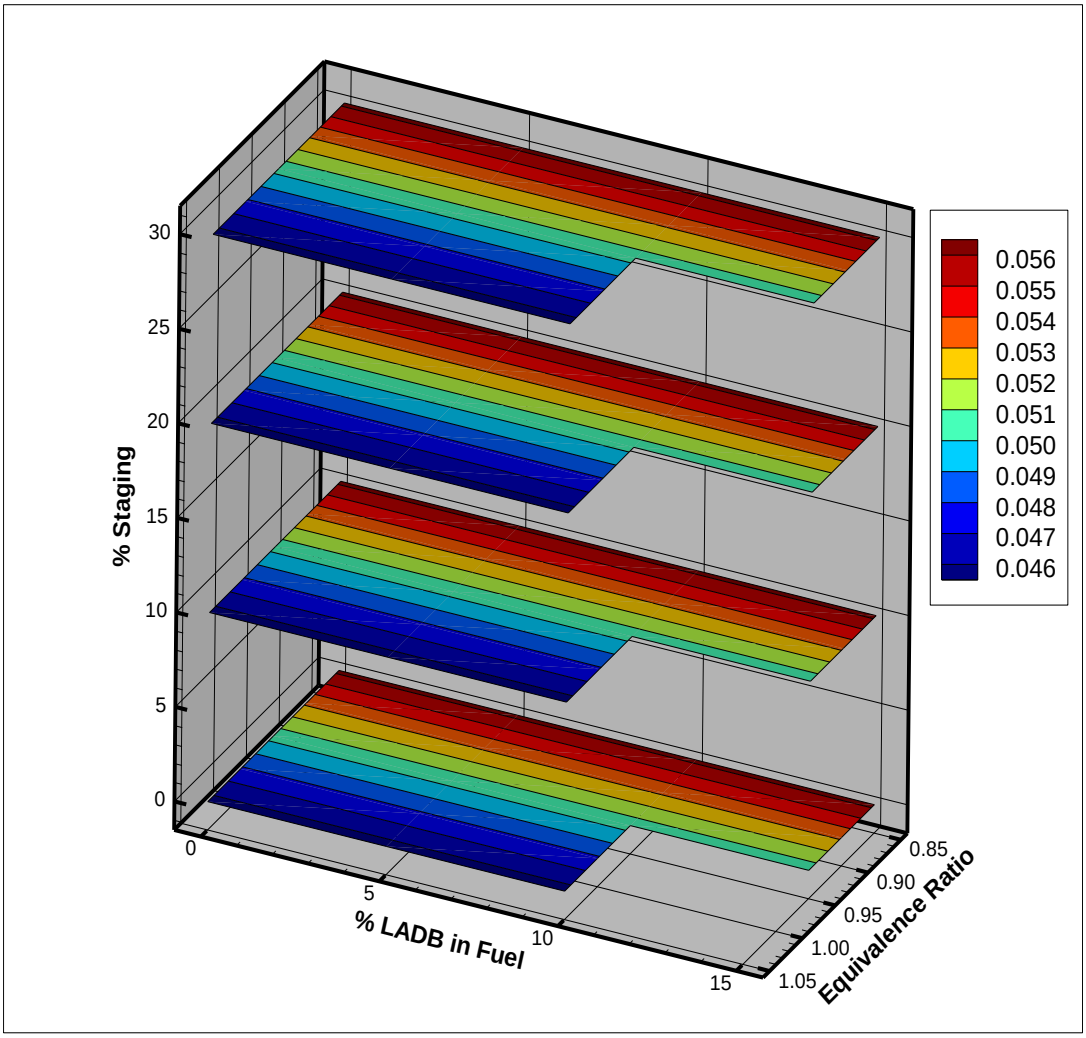

Figure 5.22 Burnt fraction uncertainty analysis.

5.8. NO_x

This section discusses the effect of cofiring coal with LADB and the effect of staging combustion on NO_x emissions. Unlike the previously discussed emissions, NO_x is not very useful in evaluating the quality of combustion occurring, but is important from an emissions perspective. NO_x is produced in minor (ppm) concentrations, but only a small amount is needed to bring about significant health and environmental impacts.

This section presents the results from cofiring PRB with LADB, as well as the results from using OFA to stage combustion for both pure PRB and for PRB-LADB cofired fuels. Figure 5.23 presents the ppm NO_x concentrations for all the experimental cases investigated and Figure 5.24 presents the ppm NO_x uncertainty analysis.

Note that LADB has a much greater nitrogen loading. Looking at Figure 5.23, the 90-10 PRB-LADB curve shows the best data. For this data set, the initial increase in equivalence ratio from 0.85 to 0.90 causes NO_x emissions to increase. This is due to a decrease in excess air, which increases gas temperature, reduces product gas flow, and increases nitrogen oxidation from both PRB and LADB. At such a high excess air ratio as $\phi = 0.85$, the unreacted nitrogen and oxygen in the air dilute the NO_x emission, which is only a trace concentration. Decreasing the amount of excess air decreases this dilution effect. Subsequent increases in equivalence ratio act to decrease NO_x emission because there is now less excess oxygen available to bond with nitrogen and form NO_x. Furthermore, NO_x can be reduced to nitrogen under very oxygen deficient combustion. The NO_x concentration for $\phi = 0.95$ and $\phi = 1.00$ are virtually indistinguishable. As expected, NO_x is highest for very lean (0.85 equivalence ratio) combustion. As the equivalence ratio increases, oxygen in the products decreases and reduces NO_x concentration because the reaction rate of hydrogen cyanide and ammonia to NO_x is proportional to oxygen concentration. Increasing the amount of LADB in the fuel increased the NO_x formation. This is due to the increased nitrogen loading associated with increasing amount of LADB, especially for lean mixtures. For very lean (0.85 equivalence ratio) unstaged cofiring with 15% LADB, NO_x could get as high as 900 ppm

which is significantly more than rich (1.05 equivalence ratio) unstaged combustion of pure PRB which produced 475 ppm of NO_x. Previous research (Lawrence et al. 2009) has established that cofiring PRB with LADB in unstaged combustion has the potential to increase NO_x formation. The novelty of this research is the addition of staged combustion. Figure 5.23 demonstrates that staging the combustion was effective in inhibiting NO_x formation. As the staging intensity increased, the NO_x concentration decreased. Rich combustion of pure PRB with 30% air staging produced virtually no NO_x. By staging combustion to 30% staging, it was possible to cofire 10% PRB with LADB at 0.85 equivalence ratio and produce similar NO_x concentrations as unstaged pure PRB at 0.95 equivalence ratio.

From a NO_x reduction standpoint, operating closer to stoichiometric is desired to obtain minimum NO_x. It is noted that thermal NO_x will increase as the flame chemistry approaches stoichiometric, but thermal NO_x is insignificant compared to fuel NO_x. Even if a cofired fuel produces more NO_x at the same equivalence ratio (see section 5.8), cofiring can reduce NO_x by moving operating conditions closer to stoichiometric without adversely affecting BF. Adding LADB to PRB should increase the burnt fraction due to the increased volatility of LADB, as shown in Figure 5.21. It is well known that a major limitation to staged combustion is increasing staged air, which decreases combustion efficiency and BF due to the main burner operating in rich conditions. It is desirable for OFA not to affect BF, and thus the curves appear as horizontal lines in Figure 5.21.

One of the major topics investigated in this research was the effect of blending LADB into PRB on NO_x emissions. The high fuel-bound nitrogen content of LADB is a

cause for concern because increased fuel NO_x production is expected. Conversely, the high volatility of the LADB could rapidly consume local oxygen and act to starve the flame of oxygen and decrease the NO_x production. As seen in Figure 5.23, the effect of adding LADB to PRB is difficult to summarize and almost impossible to predict. There are some instances where adding LADB increased NO_x and some instances where NO_x decreased. The discouraging information shown in Figure 5.23 is for every equivalence ratio; the 90-10 PRB-LADB fuel produced more NO_x than the pure PRB. Staged combustion technology was developed with the specific intent of reducing NO_x emissions. One of the primary areas of interest in this research was successfully constructing a LNB that would stage combustion and effectively reduce NO_x. For most of the equivalence ratios, staging combustion did decrease NO_x. The one exception to this is the stoichiometric combustion curve, which is probably incorrect. In addition, Figure 5.23 shows that the amount of staging needed to see a NO_x reduction decreases with increasing equivalence ratio. This fits with intuition. For a very lean flame (ϕ = 0.85) removing some initial air and staging it in the OFA is not sufficient to make the initial flame rich. However, for lean flames closer to stoichiometric (ϕ = 0.90 and 0.95), removing some initial air causes the initial flame to go to rich and reduce NO_x. One explanation for why staged combustion and cofiring did not work together to enhance NO_x reduction can be found by examining the mechanisms the two techniques employ to reduce NO_x. Staged combustion reduces NO_x by starving the main burner zone of oxygen. This forces the fuel bound nitrogen to reform as N_2. PRB nitrogen is not

reactive in the tertiary air region of the flame. However, under lean conditions, there is sufficient oxygen in the initial burner zone for oxidation of nitrogen to NO_x.

This is not the case with LADB nitrogen. There are two effects present. The first is that LADB nitrogen loading is greater than PRB nitrogen loading. The second is the rapid reduction in oxygen concentration due to increased volatile matter compared to coal as shown in the fuel properties table. The increased nitrogen loading causes more NO_x while decreased oxygen concentration will reduce NO_x. So, under very lean conditions, the nitrogen loading dominates and as the flame approaches stoichiometric, the reduced oxygen effect dominates.

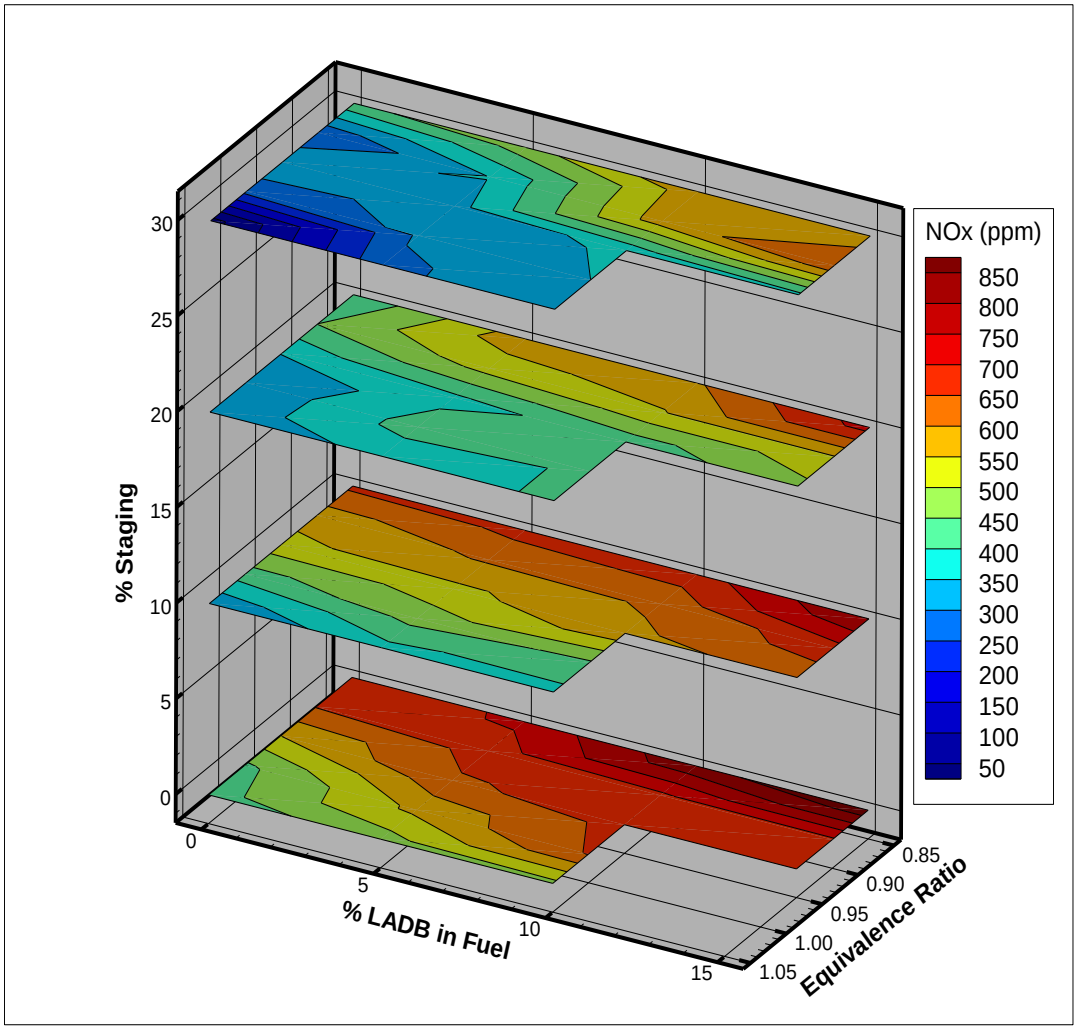

Figure 5.23 Exhaust NO_x concentration for all experimental cases investigated. NO_x production increased with decreasing equivalence ratio and increasing LADB in the cofired fuel. Increasing the staging intensity decreased NO_x production. Air staging allowed cofired fuels to produce similar NO_x levels as unstaged pure PRB.

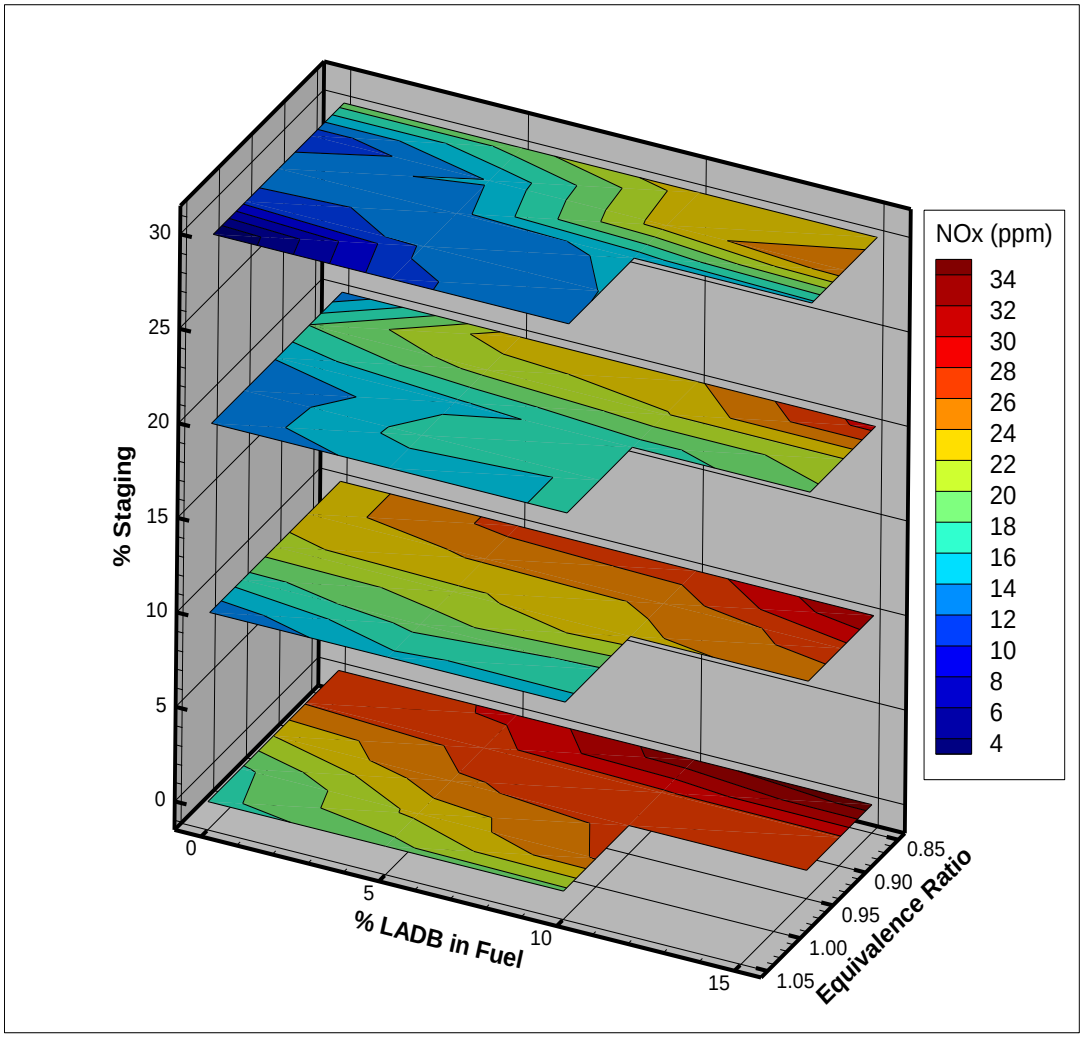

Figure 5.24 NO_x concentration uncertainty analysis.

Figure 5.25 presents the percentage NO_x change relative to the base case of unstaged PRB at 0.85 equivalence ratio. As can be seen in Figure 5.25, the general trend was that increasing LADB in the fuel increased NO_x and increasing equivalence ratio and increasing staging intensity decreased NO_x. What can also be observed in Figure 5.25 is that increasing equivalence ratio and increasing staging intensity decreased NO_x faster than increasing LADB in the fuel increased NO_x. As an example of this generality,

observe that 90-10 PRB-LADB, 0.95 equivalence ratio, 20% staging shows a ~30% NO_x reduction from the base case. Figure 5.26 presents the percentage NO_x change due to staging which is a measure of how much NO_x could be reduced holding all other experimental cases constant. As an example of what the data in Figure 5.26 presents, Figure 5.26 shows that when combustion was 20% staged 90-10 PRB-LADB, 0.95 equivalence ratio, NOx was reduced ~25% from unstaged combustion of 0.95 equivalence ratio 90-10 PRB-LADB.

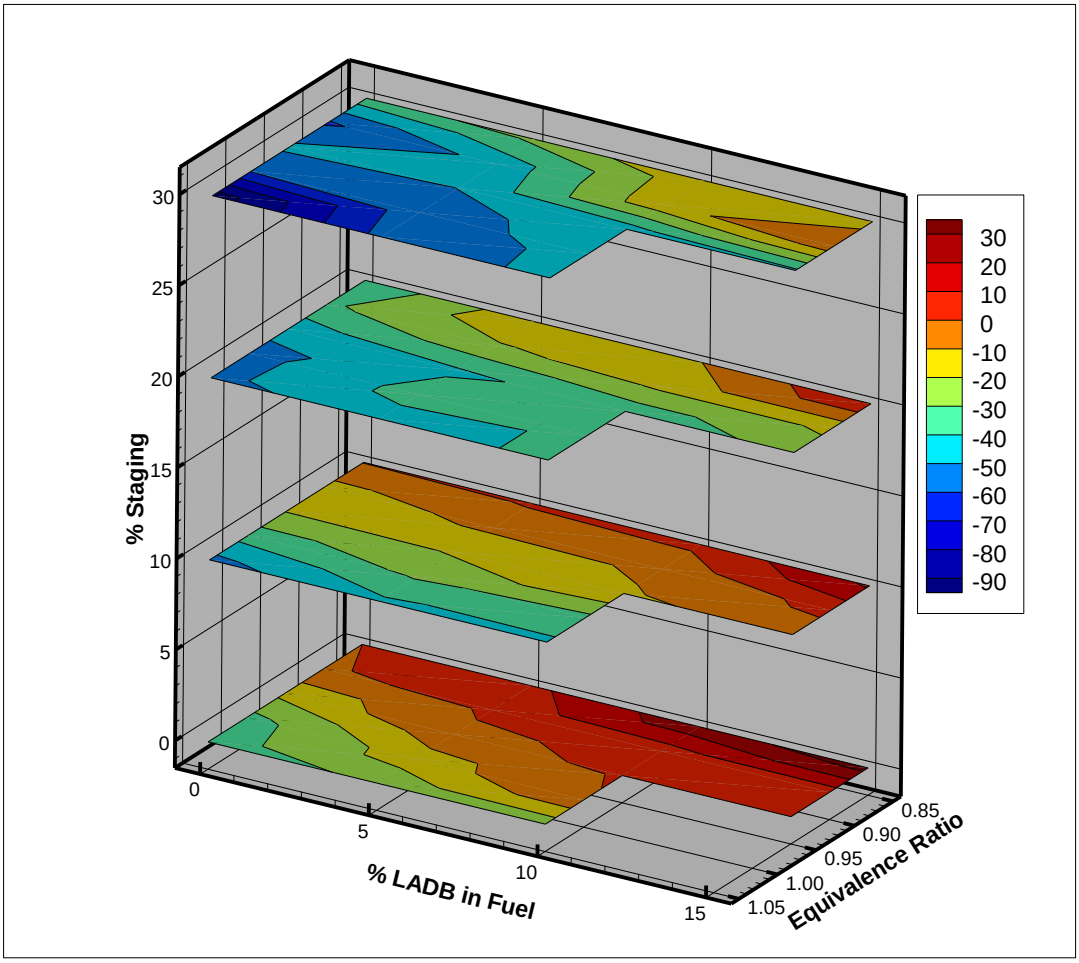

Figure 5.25 Percent NO_x change from base case.

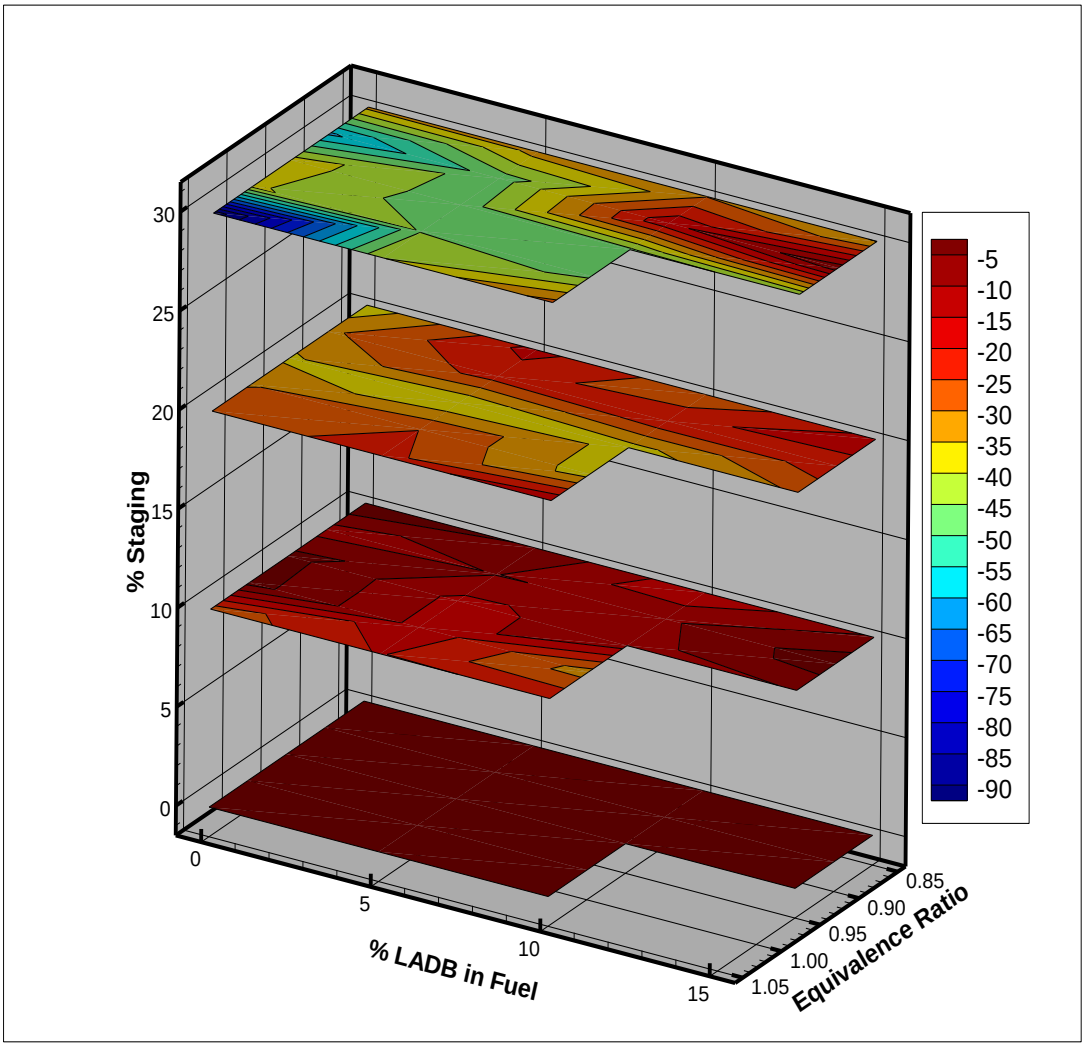

Figure 5.26 Percent NO_x change due to staging.

5.9. Heat Basis NO_x

Section 5.8 presented the emissions of NO_x on a ppm basis. This information is useful because all emissions are measured on a concentration basis. However, from a regulating perspective, reporting NO_x on a ppm basis has its limitations. Most notably,

because it is a concentration, the emission can be artificially diluted by flooding the exhaust steam with a dilutant such as nitrogen or air. Air is the most common dilutant. One method employed to circumvent this is reporting emissions on a standard O_2 concentration with 3% being the most common for coal fired boilers and 6% being the most common for gas turbines (Annamalai and Puri, 2005). The more commonly used method is to report NO_x on a heat basis with the numerator being a unit of mass (normally pounds) and the denominator being a unit of energy (normally mmBTU). Because this is a scientific report, g/GJ will be used here, but converting between lb/mmBTU and g/GJ can be performed by using a unit conversion. Reporting emissions on a lb/mmBTU basis is attractive especially to boiler operators because they have an annual generation target, which will be in MW-hrs and an annual NO_x emission target which will be in tons. With these two targets established, the utility can know what its average emission must be by dividing the generation target by the emission target and performing a unit conversion.

This section reports the NO_x emissions from cofiring experiments on a g/GJ basis. As stated previously, equivalence ratio is the parameter that has the most significant impact on combustion in general and NO_x formation in particular. During lean combustion, significant amounts of NO_x should be formed due to excess oxygen being available to bond with fuel-bound nitrogen radicals. In addition to this, some air borne N_2 molecules will fracture into N radicals, which will then bond with oxygen to form thermal NO_x. Although fuel NO_x is the dominant manifestation of NO_x, thermal NO_x does also need to be considered particularly when total NO_x is low. As has

consistently been the case, the 90-10 PRB-LADB cofiring experiments continue to behave the closest to expected behavior. Increasing the equivalence ratio from 0.85 to 0.90 did not have a significant impact on NO_x, then increasing to 0.95 lead to a dramatic decrease in NO_x, and subsequent increases in equivalence ratio did not have a further impact.

Figure 5.27 presents the heat basis NO_x emissions for all the experimental cases investigated and Figure 5.28 presents the heat basis NO_x uncertainty analysis. The trends presented in Figure 5.27 are similar to the trends presented in Figure 5.23. This is because the addition of LADB to the cofired fuel did not dramatically alter the HHV of the cofired fuel per unit of stoichiometric oxygen. The NO_x for 30% staged, 10% LADB cofired fuel at 0.85 equivalence ratio had less heat basis NO_x than unstaged pure PRB at the same equivalence ratio. This is an exciting result because it demonstrates that air staging will allow cofiring and not negatively affect NO_x performance relative to unstaged coal combustion. Thus, it is recommended that staged combustion be adopted when dealing with high nitrogen fuels. As shown by Figure 5.23, the lowest NO_x concentration was achieved with a 1.05 equivalence ratio and 30% staged combustion of pure PRB. This is the condition that minimizes fuel nitrogen loading and excess available oxygen, as well as inhibiting NO_x formation kinetics. The high nitrogen content of LADB is of concern because fuel NO_x is related directly to fuel nitrogen content and is the most significant manifestation of NO_x from solid fuel combustion. Changing the amount of LADB in the fuel did affect the heat basis NO_x, with increased LADB increasing NO_x, but its impact was not as pronounced as equivalence ratio. Figure 5.27

shows that for lean combustion, staging reduced NO_x emissions, which is desired. Even more encouraging is the fact that a moderate amount of staging had the most significant NO_x reduction.

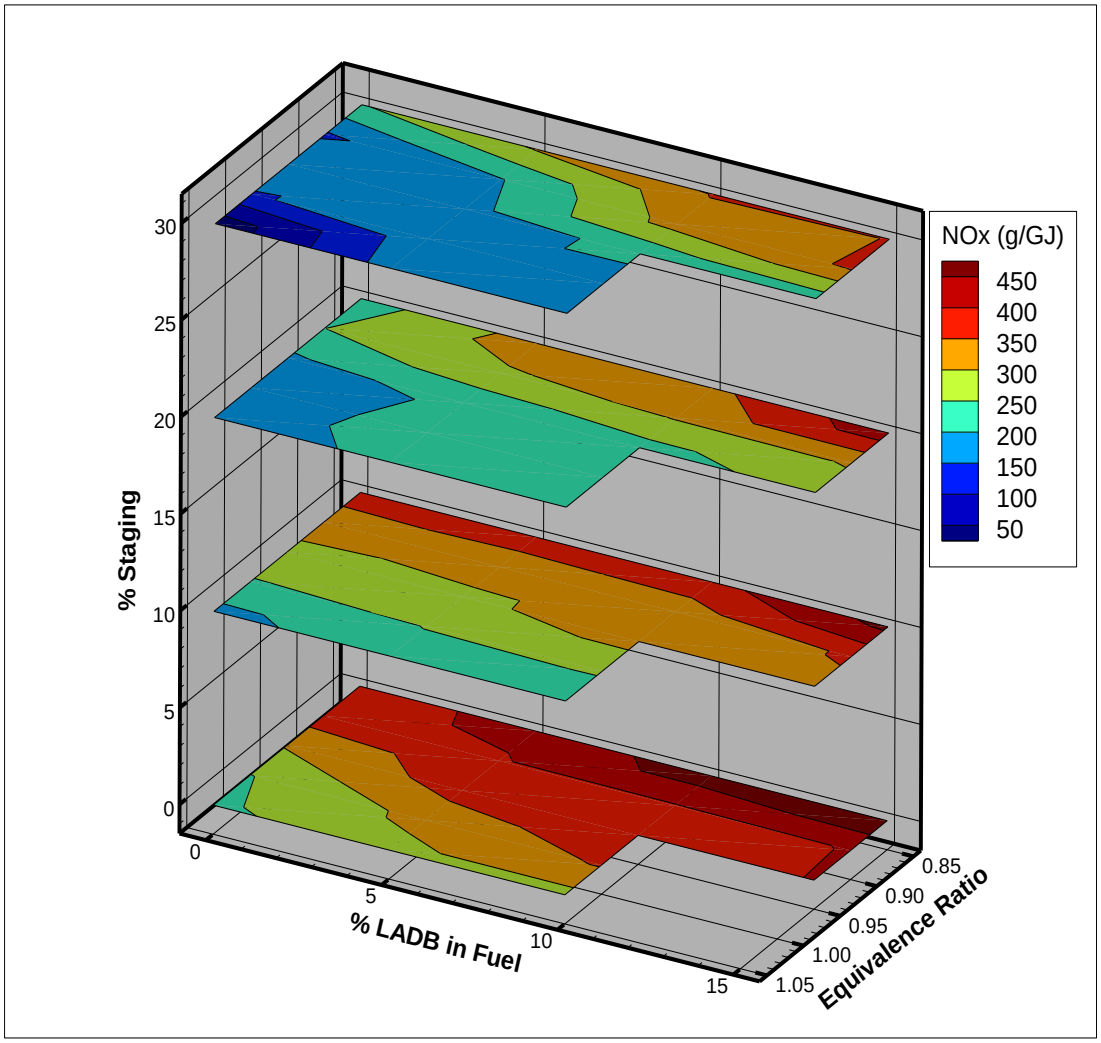

Figure 5.27 Heat basis NO_x emissions for all experimental cases investigated. Cofiring 10% LADB with PRB at 0.85 equivalence ratio and 30% staging produce similar heat basis NO_x concentrations as unstaged, pure PRB at the same equivalence ratio. Heat basis NO_x was minimized when pure PRB was fired at a 1.05 equivalence ratio with 30% staging.

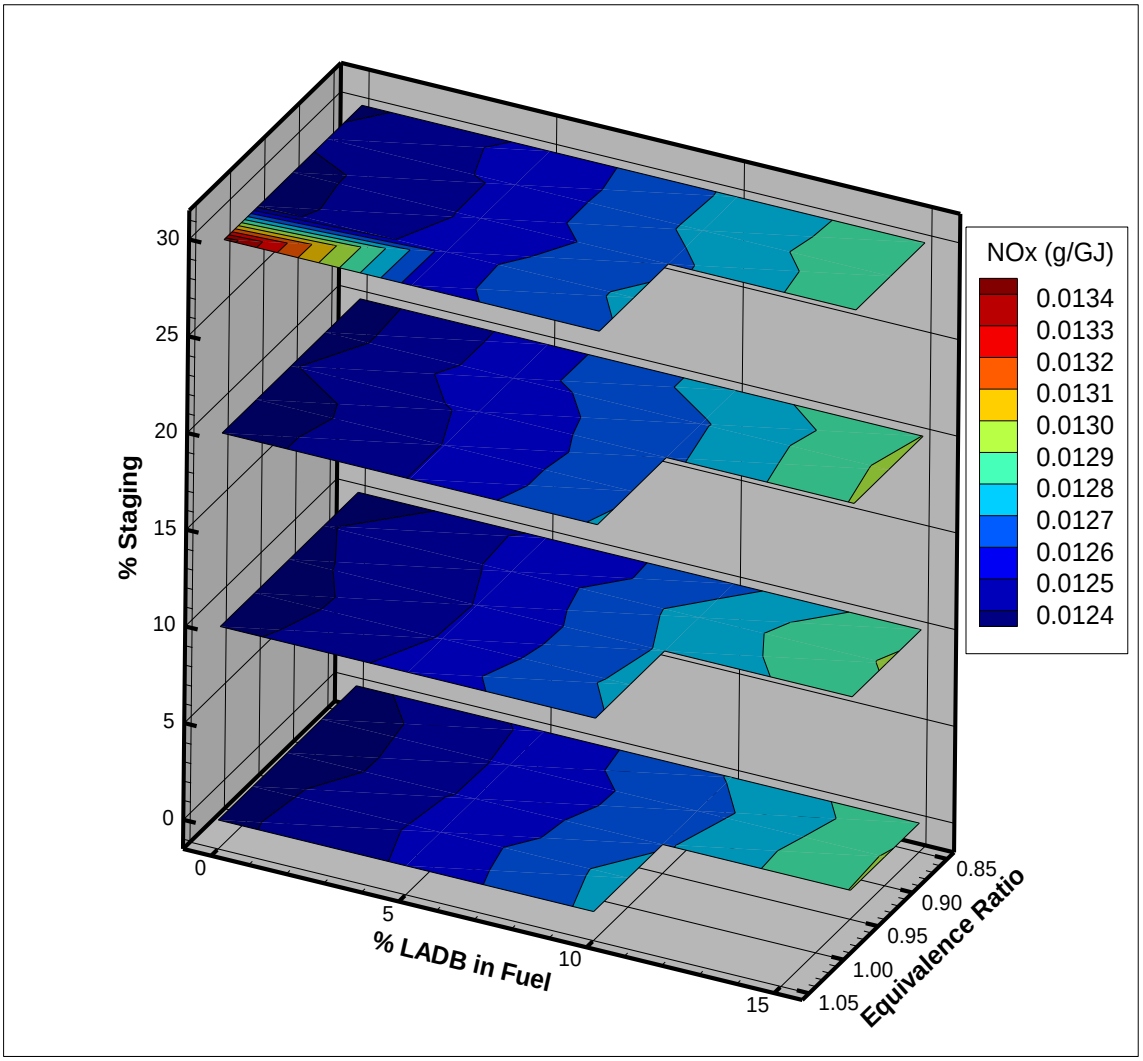

Figure 5.28 Heat basis NO_x uncertainty analysis.

5.10. Fuel Nitrogen Conversion Percentage

One other calculated parameter that needs to be discussed is fuel nitrogen conversion percentage, which is a measure of the amount of fuel-bound nitrogen converted to NO_x during the combustion process. During combustion, fuel-bound nitrogen and fuel-bound carbon compete for oxygen to advance the oxidation reactions.

Thus, it stands to reason that ultimate analysis carbon and nitrogen concentrations need to appear in the equation for fuel nitrogen conversion percentage, which is presented in Equation (2), from Annamalai and Puri (2007).

$$N_{CONV} = \frac{\left(\frac{C}{N}\right) * X_{NO_x}}{X_{CO_2} + X_{CO}} \quad (2)$$

Note that the equation assumes that all NO_x comes from fuel nitrogen. It is known that a portion of NO_x comes from atmospheric nitrogen, so fuel nitrogen conversion percentage is known to be an overestimation, but it is still a reasonable calculation because a majority of NO_x from solid fuel combustion comes from fuel NO_x (see section 4.2). As can be seen in Equation (3), in order to decrease the amount NO_x formed, the concentration of fuel-bound carbon should decrease. Note that the ratio of carbon to the sum of carbon dioxide and carbon monoxide is typically constant. In contrast with the conventional idea of efficiency, smaller numbers approaching 0% are desired with fuel nitrogen conversion percentage. Because equivalence ratio has an impact on NO_x formation and the fractionation of carbon oxides between CO_2 and CO, it makes sense that it also affects fuel nitrogen conversion percentage, which is discussed in this section.

Figure 5.29 presents the fuel nitrogen conversion percentage for all experimental cases investigated and Figure 5.30 presents the fuel nitrogen conversion percentage uncertainty analysis. Looking at Figure 5.29, the data series for 90-10 PRB-LADB is the best presented. As the equivalence ratio increases, the fuel nitrogen conversion percentage decreases, which implies that less of the fuel-bound nitrogen oxidizes to NO_x. This is expected because oxygen concentration decreases with increasing equivalence ratio. Figure 5.29 presents the fuel nitrogen conversion percentage for all experimental

cases investigated. Figure 5.31 presents work from Bowman (1991) calculating fuel nitrogen conversion percentage for a wide range of fuels. The values of fuel nitrogen conversion efficiency presented in Figure 5.31 match closely with the values presented in Figure 5.29 which helps validate the experimental results. Previous research referred to this calculation as fuel nitrogen conversion percentage. It has been decided to replace efficiency with percentage because increased efficiency implies improved performance. Concerning nitrogen conversion to NO_x, decreased percentage indicates improved performance. Looking at Figure 5.29, the amount of LADB in the fuel did not influence fuel nitrogen conversion percentage as much as equivalence ratio and amount of staging did. It is important to note that even though LADB has a fuel nitrogen loading four times that of PRB, adding LADB to the PRB does not increase nitrogen loading by a factor of four because only a small percentage of LADB was blended into the PRB. It makes sense that equivalence ratio would strongly influence fuel nitrogen conversion percentage because equivalence ratio strongly influences NO_x formation. The same reasoning can be applied to why the amount of air staging strongly influences fuel nitrogen conversion percentage.

The 10% staging plane clearly demonstrates the weak influence that LADB has on fuel nitrogen conversion percentage. Going across the percentage LADB axis, the color bands are approximately parallel. This demonstrates that the same amount of fuel-bound nitrogen will be converted to NO_x regardless of the amount of fuel-bound nitrogen present. This shows that the increased NO_x formation associated with increasing the amount of LADB in the fuel can be attributed exclusively to the increase in nitrogen

loading. A biomass fuel with equivalent nitrogen loading to coal would produce a concentration of NO_x equivalent to pure coal.

This section will discuss how the percent of LADB in the cofired fuel affects fuel nitrogen conversion percentage. Increasing the amount of LADB in the cofired fuel increases the amount of nitrogen in the cofired fuel (i.e. increased loading), which increases the NO_x formation potential. However, because the ratio of carbon to nitrogen appears in the equation for fuel nitrogen conversion percentage, this parameter is fuel nitrogen neutral. As shown in Figure 5.29, there is no real pattern to how adding LADB to PRB affected fuel nitrogen conversion percentage. There were some instances where it increased due to increased LADB and some instances where it decreased due to increased LADB.

Because staged combustion was invented with the intention of reducing NO_x from pulverized coal combustion, it is worth investigating how staging affects fuel nitrogen conversion percentage. As can be seen in Figure 5.29, staging worked to improve Fuel Nitrogen Conversion Percentage for lean combustion (ϕ = 0.85, 0.90, and 0.95).

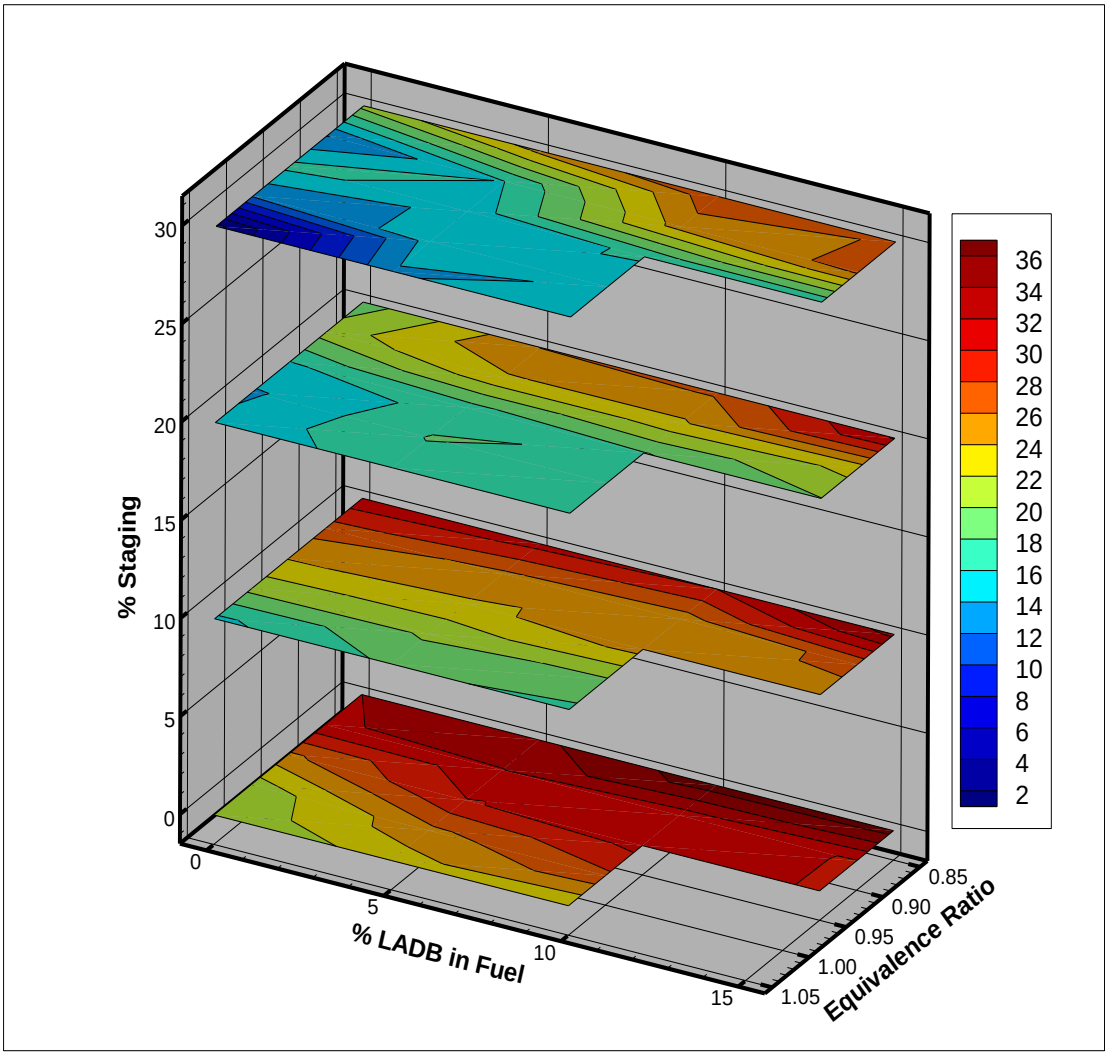

Figure 5.29 Fuel nitrogen conversion percentage for all experimental cases investigated. Going across the % LADB axis the color bands are roughly parallel for the 10% staged plane. This demonstrates that the increased NO_x formed with higher amount of LADB is due to the increased nitrogen loading.

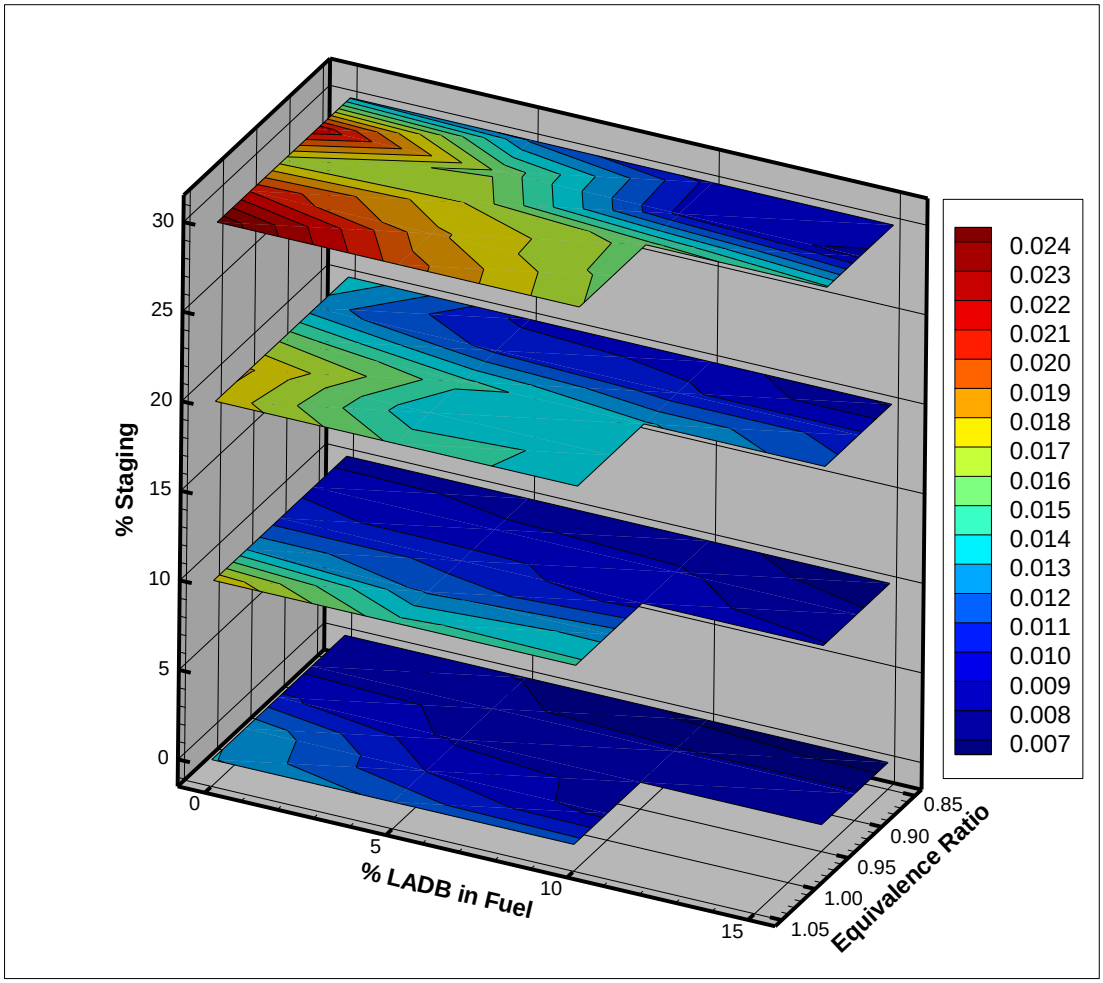

Figure 5.30 Fuel nitrogen conversion percentage uncertainty analysis.

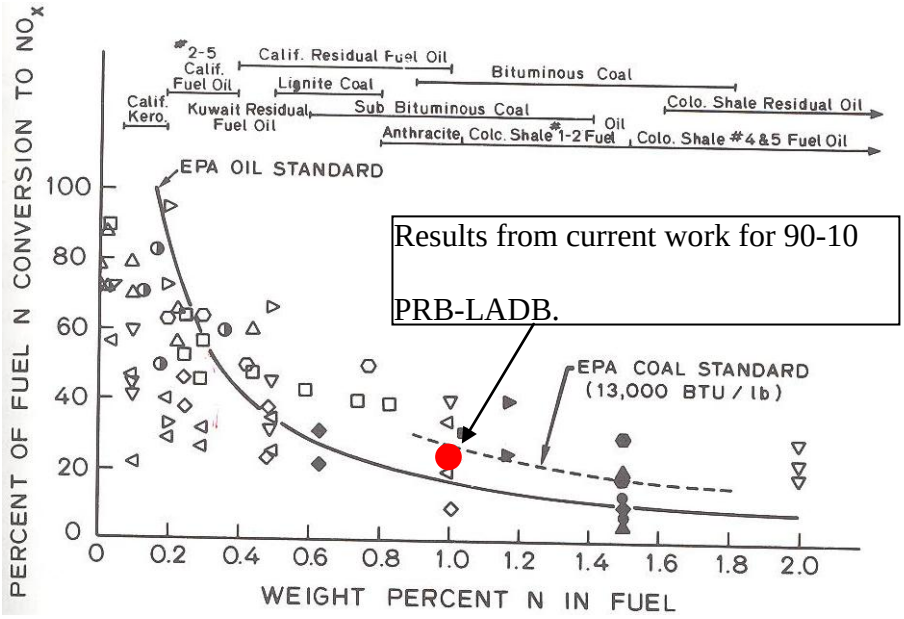

Figure 5.31 Fuel nitrogen conversion percentage for multiple fuels. Note that these results match closely with the results presented in Figure 5.29.

5.11 ANOVA of Experimental Results

An ANOVA was performed on the repeated experimental results for the measured emissions. ANOVA is the preferred statistical tool to determine if results are due to real physical phenomena or due to experimental noise. ANOVA looks at the average and the standard deviation of the measured results and determines the confidence that the differences are due real physical differences between the independent variables. The most common confidence interval used for ANOVA is 95%. Results of ANOVA are reported as a P-value that represents the likelihood on a 95% confidence interval that differences might not be statistically significant. A P-value of zero represents a 0% likelihood that differences are due to random effects. As differences become increasingly less random, the P-value asymptotically approaches zero. The most

common practice is a P-value less than 0.05 represents a statistically significant difference. Table 5.4 presents the results from the ANOVA. Because P-value can take on a value that ranges several orders of magnitude, P-value is presented in scientific notation. As an example of how to interpret P-value, look at the P-values associated with oxygen. The between equivalence ratio P-value for oxygen is 4.02E-06 for 0% staging and 3.74E-07 for 30% staging. Because these P-values are less than 0.05, the differences between equivalence ratios are statistically significant. By contrast, the percentages between LADB P-values for oxygen are 1.82E-01 for 0% staging and 1.00E00 for 30% staging. Because these P-values are greater than 0.05, the differences are not statistically significant and are as likely due to experimental noise as they are due to real differences. This statistical analysis for oxygen fits with intuition. It is expected that changing equivalence ratio will change oxygen concentration and it is expected that changing fuels will not affect oxygen concentration for a given equivalence ratio. As Table 5.4 demonstrates, the NO_x differences are statistically significant for both equivalence ratio and for fuel at both 0% and 30% staging.

Table 5.4 ANOVA of repeated experiments

Emission	Percent Staging (%)	Between Equivalence Ratio P-value	Between % LADB P-value
O_2 (%)	0%	4.02E-06	1.82E-01
O_2 (%)	30%	3.74E-07	1.00E+00
CO_2 (%)	0%	1.94E-01	7.99E-01
CO_2 (%)	30%	7.01E-01	4.80E-01
CO (ppm)	0%	2.30E-04	8.91E-05
CO (ppm)	30%	1.33E-03	1.50E-04
NO_x (ppm)	0%	2.30E-04	8.91E-05
NO_x (ppm)	30%	2.94E-02	2.41E-02

6. SUMMARY AND CONCLUSION

The conclusions from this research are as follows:

- The LADB has a lower heat value compared to pure coal but higher VM compare to coal. However, the ash loading is a concern. LADB had an ash loading of 11.57 kg/GJ, which is more than 3 times the 3.10 kg/GJ ash loading of PRB.
- The respiration coefficient for PRB is 0.92, which is virtually the same as the 0.94 for LADB. This demonstrates that the two fuels will produce approximately the same amount of CO2 per GJ of heat release. The gas analyses from cofiring experiments confirmed the RQ values to be almost same.
- The TGA analyses suggest lower temperatures for pyrolysis compared to coal, which aids in earlier production of VM and hence, a better flame stability if moisture and ash contents are similar.
- The staging introduces a fuel rich main burner zone and lean combustion zone after tertiary air.
- Carbon monoxide production increased with increasing equivalence ratio due to decreasing amount of combustion oxygen to oxidize carbon fully to carbon dioxide. Carbon monoxide production also increased with increasing staging intensity due to the staged air having less residence time in the furnace and richer main burner zone.

- LADB had fuel-bound nitrogen loading of 1.50 kg/GJ, which is more than four times the PRB loading of 0.36 kg/GJ. This increased nitrogen loading caused NO_x production to increase when cofiring PRB with LADB, especially at leaner mixture conditions.
- Staging combustion will bring the cofiring NO_x levels down to acceptable values. At a 0.90 equivalence ratio, cofiring 10% LADB with PRB and staging 20% of air as tertiary air will produce the same amount of NO_x (g/GJ) as unstaged pure PRB at the same equivalence ratio.
- Analysis of Variance demonstrated that differences in NO_x production between equivalence ratios were statistically significant as well as differences in NO_x between pure PRB and PRB:LADB blends.
- The 90:10 blend of PRB and LADB can be cofired into a furnace as a method of disposing of LADB. Boiler combustion performance will not be compromised. Even when paired with staged combustion, fuel burnt fraction is acceptable.

7. FUTURE WORK

Following the completion of this research, several suggestions can be recommended for future work:

- Investigate initial equivalence ratio and its impact on NO_x reduction in more detail. In particular, investigate if the initial equivalence ratio transitions from lean to rich correspond to the point of most significant NO_x reduction.
- Investigate other agricultural waste fuel sources such as forage sorghum and crop residues. If difficulties grinding agricultural wastes cannot be overcome, first torrify the agricultural wastes to increase the Hargrove Grindability Index before pulverizing the torrified products.
- Investigate char produced from LADB gasification as a cofiring fuel source. The gasification process should assist in overcoming the grinding difficulties and the nitrogen loading difficulties, producing a higher quality fuel for cofiring with LADB applications.
- Investigate using unbalanced OFA loads through the arms. This research would determine if the increased turbulence created by unbalanced OFA loading enhance combustion and/or NO_x reduction.
- Develop a more detailed model for a LNB, adopting the commercial combustion codes.
- Experiments measuring mercury emissions from coal combustion were not successful due to inability to obtain reliable, repeatable mercury emissions

measurements. Future EPA regulations are going to require mercury emissions from coal power plants be controlled. Thus, performing mercury experiments is suggested as future work. The high chlorine content of LADB makes it an attractive fuel additive as a mercury control device.

REFERENCES

Annamalai, K., and Puri, I. K. 2005. *Combustion Science and Engineering*. CRC Press. Taylor and Francis Group, LLC., Boca Raton, FL.

ASTM International. 2006. *ASTM Standard C136-06*. ASTM International, Baltimore, MD.

Babcock and Wilcox Company. 1978. *Steam: Its Generation and Use*. Babcock and Wilcox. New York.

Barth, R. 2009, May. *Modification of a Low NO_x Burner for Arm Staging.* MEEN 491 Report. Texas A&M University, College Station, TX.

Baxter, L. 2004. Biomass cofiring overview. Presented at the Second World Conference on Biomass for Energy, Industry, and World Climate Protection, May 10-14, Rome, Italy.

Bowman, C. T. 2001. Chapter 3. *Fossil Fuel Combustion*. John Wiley & Sons Inc., New York. Bartok, W., Sarofim, A. F. Eds.

Brubaker, D. 2009, May. *Effects of Cofiring Coal and Dairy Biomass and Staging Air on Combustion Gas Emissions.* MEEN 491 Report. Texas A&M University, College Station, TX.

Dahlquist, E. (ed.). 2013. *Technologies for Converting Biomass to Useful Energy*. *Vol. 4: Combustion, Gasification, Pyrolysis, Torrefication, and Fermentation.* CRC Press. Taylor and Francis Group. Boca Raton, FL.

Damstedt, B., Pederson, J., Hansen, D., Knighton, T., Jones, J., Christensen, C., Tree, D., and Baxter. L. 2007, January. Biomass cofiring impacts on flame structure and emission. *Proceedings of the Combustion Institute*. **31**(2), 2813-2820.

Duo, W., Dam-Johansen, K., and K. Ostergaard, K. 1992. Kinetics of the gas-phase reaction between nitric oxide, ammonia, and oxygen. *Can. J. Chem. Eng.*, **70**(5), 1014-1020.

Duxbury, J., and Welford, G. B. 1989. The effect of particle size on NO_x emissions during the firing of pulverized coal in a shell boiler. *J. Inst. Energy.* **452**, 147-151.

E Instruments International, LLC. 2013. *Industrial gas analyzers.* Available at http://www.e-inst.com/industrial-gas-analyzers/products-E8500

Filtration and Separation.com. 2013. Available at www.filtration-and-separation.com.

Gomez, P. 2008. Development of a low NO_x burner system for coal fired power plants using coal and biomass. Master thesis. Texas A&M University, College Station, TX.

Goughnour, P. 2006. NO_x reduction with the use of feedlot biomass as a reburn fuel. Master thesis. Texas A&M University, College Station, TX.

Hall, W. S. 2012. *Physiology.* Ulan Press. Philadelphia, PA.

Hao, X., and Jin, J. 2010. The influence of pulverized coal size on nitrogen oxides emission performance from pulverized coal combustion. Presented at the Power and Energy Engineering Conference: 2010 Asia-Pacific. March 28-31, Chengdu.

Heflin, K. and Sweeten, J. 2006. Preliminary interpretation of data from proximate, ultimate, and ash analysis. Results of June 7, 2006 samples taken from feedlot and dairy biomass biofuel feedstocks at TAES/USDA-ARS, Bushland, TX. Texas Agricultural Experiment Station. Texas A&M Agricultural Research and Extension Center Amarillo/Bushland/Etter, TX.

Jakobsen, H. H. 1998. *The analysis report of Plant No. 1: Cofiring of biomass-evaluation of fuel procurement and handling in selected existing plants and exchange of information (cofiring)-Part 2.* Teknik Energy and Environment, Denmark.

Jia, L., and Anthony, E. J. 2011. Combustion of poultry-derived fuel in a coal-fired pilot-scale circulating fluidized bed combustor. *Fuel Proc.Tech.*, **92**, 2138-2144.

Jiang, X., Wei, L. Huang, X., and Zhang, C. 2008. Experimental investigation on emission characteristics of NO_x during micro-pulverized coal oxidation. *Environ. Sci.*, **29**. 583-586.

Kegel, T., 1996. Basic measurement uncertainty. Presented at the 71st International School of Hydrocarbon Measurement. April 9-11, Oklahoma City, OK.

Kline, S. J., and McClintock.,F. A. 1953. Describing uncertainties in single-sample experiments. *Mech. Eng.*, **75**, 3-8.

Laux, S., Grusha, J., and Tillman, D. 2000. Co-firing of biomass and opportunity fuels in low NO_x burners. Presented at the 25th International Technical Conference on Coal Utilization and Fuel Systems, March 6-9, Clearwater, FL.

Lawrence, B. 2007. Cofiring of coal and dairy biomass in a 100,000 btu/hr furnace. Master thesis. Texas A&M University, College Station, TX.

Lawrence, B., Annamalai, K., Sweeten, J. M., and Heflin, K. 2009. Cofiring coal and dairy biomass in a 29 kWt furnace. *Applied Energy*, **86**(11), 2359-2372.

Lawrence, B., Annamalai, K., Sweeten, J. M., and Heflin, K. 2012. Effect of cofiring coal with low ash dairy biomass on NO_x in a 100,000 BTU/hr low NO_x burner. Presented at the Spring Technical Meeting of the Central States Section of the Combustion Institute, April 22-24, Dayton, OH.

Li, S., Wu, A., Deng, S., and Pan, W. 2008. Effect of co-combustion of chicken litter and coal on emissions in a laboratory-scale fluidized bed combustor. *Fuel Proc. Tech.*, **89**, 7-12.

Li, S., Xu, T., Hui, S., and Wei, X.. 2009. NO_x emission and thermal efficiency of a 300 MWe utility boiler retrofitted by air staging. *Applied Energy,* **86,** 1797-1803.

Lundgren, J., and Pettersson, E. 2009. Combustion of horse manure for heat production. *Bioresource Tech.*, **100**, 3121-3126.

Maier, H., H. Spliethoff, A. Kicherer, A. Fingerle, K. R. and G. Hein. 1994. Effect of coal blending and particle size on NO_x emission and burnout. *Fuel*, **73**. 1447-1452.

Moore, J. A., and Hart, J. M. 1997. Manure management system design strategies: How and why. *J. of Dairy Sci.*, **80**. 2655-2658.

Morinaka, T. M Wozniewicz, J. Jeszka, J. Bajerska, P. N. Limtrakul, L. Makonkawkeyoon, N. Hirota, S. Kumagai, and Y. Sone. 2012, May. Comparison

of seasonal variation in the fasting respiratory quotient of young Japanese, Polish, and Thai Women in relation to seasonal changes in their percent body fat. *J. Physiol. Anthrop.,* **31**, 10.

National Agricultural Statistical Services (NASS). 2012. Milk production. Available at http://usda01.library.cornell.edu/usda/current/MilkProd/MilkProd-04-19-2012.pdf.

Partlow, B., Marz, P. ,Kaltenback, R., and Grusha, J. 2011. TMPA Cuts NO_x below 0.11 lb/MBtu with state-of-the-art combustion and controls technology. Available at http://fwc.com/publications/tech_papers/files/TP_FIRSYS_03-04.pdf

Raman, K. P., Walawender ,W., and Fan, L. T. 1980. Gasification of feedlot manure in a fluidized bed reactor: The effect of temperature. *Indust. & Engg Chem. Process Design and Develop.,* **19**(4), 623-629.

Richardson, H. B. 1929. The respiratory quotient. *Physiol.Rev.,* **9**(1), 61-125.

Sami, M., Annamalai, K., and Wooldridge, M. 2001. Co-firing of coal and biomass fuel blends. *Prog. Energy Combust. Sci.*, **27**(2), 171-214.

Savolainen, K. 2003. Co-firing of biomass in coal-fired utility boilers. *Applied Energy,* **4**, 369-381.

Schmidt, J., Seiler, W., Conrad, R. 1988. Emission of nitrous oxide from temperate forest soils into the atmosphere. *J. Atmospheric Chem.,* **6**, 95-115.

Shen, J., Jiang, X., Liu, J., Huang, X., and Zhang, H. 2011. Investigation of NO_x emissions for superfine pulverized coal in air-staging combustion. *Energy Fuels*, **25**(11), 4999-5006, dx.doi.org/10.1021/ef201023g

Spear, A. In preparation. NH_3 and HCN partitioning of solid fuel bound volatile nitrogen during rapid pyrolysis, Master thesis. Texas A&M University. College Station, TX.

Sweeten, J. M., Korenberg, J., LePori, W. A., Annamalai, K., and Parnell, C. B. 1986. Combustion of cattle feedlot manure for energy production. *Energy in Agri.,* **5**(1), 55-72.

Sweeten, J.M. 1979. *Texas Agricultural Extension Service Publication L-1094.* Texas Agricultural Extension Service, Texas A&M University, College Station, TX.

Thien, B. F., Lawrence, B. D., Sweeten, J. M., and Annamalai, K. 2012. Co-firing coal: poultry litter biomass blends in a laboratory-scale boiler-burner. *Transact. ASABE*, **55**(2), 681-688.

Thien, B. 2002. Cofiring with coal-feedlot biomass blends. Ph.D. dissertation, Texas A&M University, College Station, TX.

Tillman, D. A. 2000. Biomass cofiring: The technology, the experience, the combustion consequence. *Biomass and Bioenergy*. **19**(6), 365-384.

U.S. Department of Energy. 2012, April. *Renewable Energy and Environmental Sustainability Using Biomass from Dairy and Beef Animal Production Final Report. Vol. 1: Thermo-Chemical Conversion and Direct Combustion Methods.* Washington, DC: USDOE Office of Scientific and Technical Information, Available at http://www.osti.gov/bridge/servlets/purl/1039414/1039414.pdf

Whitely, N., Ozao, R., Artiaga, R., Cao, Y., and Pan, W. 2006.Multi-utilization of chicken litter as biomass source. Part I. *Combusti. Energy Fuels.* **20**,2660-2665.

Wilder, L. I. 1932. *Little House on the Prairie.* Harper Collins. New York.

APPENDIX A

HIGHER HEATING VALUE PER UNIT STOICHIOMETRIC OXYGEN, CO_2/O_2 RATIO, AND FLUE GAS ANALYSES

A.1 Higher Heating Value Per Unit Stoichiometric Oxygen

HHV_{O2} is defined as the heat value of the fuel divided by the amount of oxygen required to combust the fuel stoichiometrically. This value is generally constant for most fuels. The Boie Equation (Annamalai and Puri, 2005), an empirical calculation of higher heating value based upon ultimate analysis, provides proof for this statement:

$$HHV\ \left(\frac{kJ}{kg}\right) = 422{,}272 * C + 117{,}387 * H - 155{,}371 * O + 100{,}480 * N + 335{,}508 * S \quad \text{(A1)}$$

Equation (A2) can be rearranged by factoring out C to obtain:

$$HHV\ \left(\frac{kJ}{kg}\right) = C\left(422{,}272 + 117{,}387 * \frac{H}{C} - 155{,}371 * \frac{O}{C} + 100{,}480 * \frac{N}{C} + 335{,}508 * \frac{S}{C}\right) \quad \text{(A2)}$$

However, to obtain the Boie Equation in a form that is useful in conjunction with Ultimate Analysis, it is necessary to have the coefficients in terms of mass fractions as reported in Ultimate Analysis:

$$HHV\ \left(\frac{kJ}{kg}\right) = \left(\frac{Y_C}{12.01}\right)\left(422{,}272 + 117{,}387 * \frac{H}{C} - 155{,}371 * \frac{O}{C} + 100{,}480 * \frac{N}{O} + 335{,}508 * \frac{S}{O}\right) \quad \text{(A3)}$$

The hydrogen to carbon ratio can also be replaced in terms of mass fractions:

$$\frac{H}{C} = \frac{12.01Y_H}{1.01Y_C} \quad \text{(A4)}$$

Similar substitutions can be made with the other variables in the Boie Equation. The stoichiometric amount of oxygen needed to combust a fuel can be found using:

$$\nu_{O_2} = 32\left(C + \frac{H}{4} - \frac{O}{2} + S\right) = 32C\left(1 + \frac{H}{4C} - \frac{O}{2C} + \frac{S}{C}\right) \quad \text{(A5)}$$

Equations (A2) and (A5) can now be combined to determine the higher heating value per unit of stoichiometric oxygen:

$$HHV\ \left(\frac{kJ}{kg}\right) = \frac{422{,}272 + 117{,}387 * \frac{H}{C} - 155{,}371 * \frac{O}{C} + 100{,}480 * \frac{N}{C} + 335{,}508 * \frac{S}{C}}{32\left(1 + \frac{H}{4C} - \frac{O}{2C} + \frac{S}{C}\right)} \quad \text{(A6)}$$

Because nitrogen and sulfur exist is solid fuels in trace amounts, it is acceptable to ignore their contributions and treat the fuel as if it was exclusively C-H-O. Making this assumption, plots of Equation (A6) are approximately constant and have a value of 14,250 kJ/kg of stoichiometric oxygen, or 18.6 kJ/standard L of oxygen. Considering that air is 20.9% oxygen, this can also be calculated to give 3,280 kJ/kg of stoichiometric air or 3.9 kJ/standard L of stoichiometric air. As an example, the literature states that HHV per unit of stoichiometric oxygen of methane is 13,550 kJ/kg (17.7 kJ/standard L of oxygen) and the Boie Equation yields 13,934 kJ/kg. For n-octane, the literature value is 13,640 kJ/kg (17.82 kJ/standard L) and the Boie Equation yields 13,730 kJ/kg.

A.2 CO_2/O_2 Ratio

Interesting results are obtained for burnt gases when using the ratio of the number of moles of CO_2 produced per mole of stoichiometric oxygen. This ratio is most commonly encountered in biology. With the introduction of the respiratory ratio, the number of moles of CO2 produced per kmole of fuel can be calculated by:

$$\frac{N_{CO_2}}{N_{fuel}}\left(\frac{mol}{kmol}\right) = q * \nu_{O_2} \quad \text{(A7)}$$

Table A-1 presents the value and range of 1 for several different fuels. For most biomass fuels, q ranges from 0.94-0.97 and for coals it ranges from 0.92-0.93. Animal wastes typically fall in the range 0.92-0.95. Thus, most solid fuels will be somewhere in the range 0.92-0.97. For comparative purposes, most liquid or gaseous fuels are in the range 0.50-0.80. Figure A-1 shows the variation of q with H/C and O/C based upon the Boie Equation.

Table A-1 Values and range of respiratory ratio for various fuels

Fuels	q	Range of q	Remarks
Paraffins, C_nH_{2n+2}	$q=\frac{1}{\left\{1+\left(\frac{1}{2}+\frac{1}{2n}\right)\right\}}$	½<q<(2/3)	q increases slightly with n; q=1/2 for CH_4 and q→(2/3) as n→∞
Olefins, Napthenes or Cycloparafin, C_nH_{2n}	$q=\frac{2}{3}$	$q=\frac{2}{3}$	q constant
Diolefins, C_nH_{2n-2}	$q=\frac{1}{\left\{1+\left(\frac{1}{2}-\frac{1}{2n}\right)\right\}}, \quad n\geq 2$	4/5<q<(2/3)	q decreases slightly with n
Aromatics, C_nH_{2n-6}	$q=\frac{1}{\left\{\left(\frac{3}{2}-\frac{3}{2n}\right)\right\}}, \quad n\geq 6$	4/5<q<(2/3)	q decreases slightly with n
Alcohols, C_nH_{2n+1} O	$q=\frac{2}{3}$	$q=\frac{2}{3}$	q constant
Glucose $C_6H_{12}O_6$	1	1	
Palmitic Acid $C_{16}H_{32}O_2$	0.68	0.68	
Proteien $CH_2O_{0.5}$	0.8	0.8	
Mesquite, $CH_{1.3582}O_{0.5779}N_{0.0122}S_{0.0003}$	0.95	0.95	
Juniper $CH_{1.3708}O_{0.5637}N_{0.0049}S_{0.0001}$	0.94	0.94	
Rice Straw, $CH_{1.414}N_{0.0147}O_{0.638}S_{0.0004}$	0.97	0.97	
PRB $CH_{0.71}N_{0.014}O_{0.18}S_{0.0014}$	0.92	0.92	
Texas Lignite $CH_{0.678}N_{0.0157}O_{0.0.194}S_{0.00615}$	0.93	0.93	
Feedlot Biomass $CH_{1.287}N_{0.04991}O_{0.532}S_{0.0057}$	0.95	0.95	
Dairy Biomass $CH_{1.06}N_{0.047}O_{0.41}S_{0.0045}$	0.94	0.94	
Litter Biomass $CH_{1.55}O_{0.60}$	0.92	0.92	

A.3 Flue Gas Analyses

Consider any fuel which requires ν_{O2} for complete combustion. If the fuel is fired with EA, then the amount of air supplied can be determined from:

$$\nu_{O_{2,supplied}} = \nu_{O_{2,stoichiometric}} * \left(1 + \frac{EA}{100}\right) \quad \text{(A8)}$$

It would be nice to incorporate equivalence ratio into Equation (A8). When this is performed, the resulting equation is:

$$\phi = \frac{\nu_{O_{2,stoichiometric}}}{\nu_{O_{2,supplied}}} = \frac{1}{1+\frac{EA}{100}} \quad \text{(A9)}$$

Considering that the most common oxidant used in combustion is air and air contains 20.9% oxygen, the ratio of nitrogen to oxygen in air is r = 3.76. Ignoring NO_x and SO_2 formed in combustion, the theoretical amount of oxygen in the exhaust is:

$$X_{O_2} = \frac{EA*\nu_{O_{2,stoichiometric}}}{0.01*EA*\nu_{O_{2,stoichiometric}}+q*\nu_{O_{2,stoichiometric}}+r*\nu_{O_{2,stoichiometric}}(1+0.01*EA)} \quad \text{(A10)}$$

Noticing that $\nu_{O2,stoichiometric}$ can be factored out of Equation A.3.3, this can be simplified to:

$$X_{O_2} = \frac{EA}{0.01*EA+q+r*(1+0.01*EA)} \quad \text{(A11)}$$

Additional simplification can be made with the assumption that q is much smaller than r. With this simplification applied, exhaust O_2 concentration is insensitive to q even though q values range as wide as 0.5 to 1.00, as demonstrated by Figure A-1. Thus, with a fixed excess air percentage, most fuels will have the same percentage of O_2 in the exhaust.

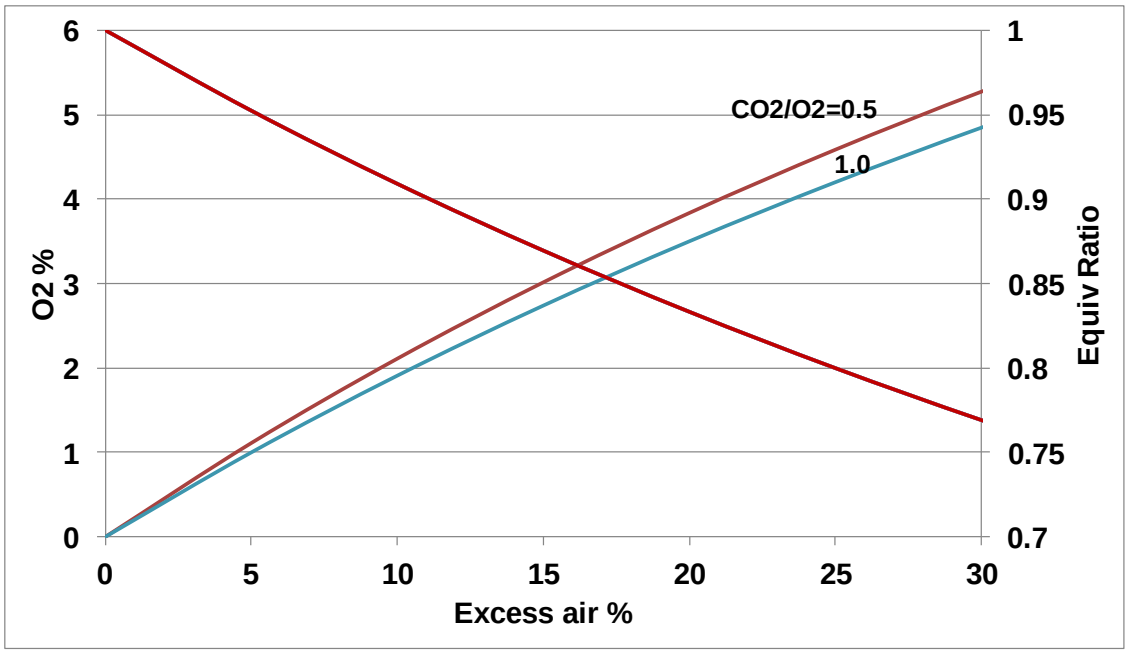

Figure A-1 Exhaust O_2 concentration and equivalence ratio when excess air percentage is varied for q = 0.5 and q = 1.0.

The number of dry moles of product per kmole of supplied air is given by:

$$\frac{N_{dry}}{N_{air}}\left(\frac{mol}{kmol}\right) = CO_2(mol) + O_2(mol) + N_2(mol) = q * \nu_{O_{2,stoichiometric}} + \nu_{O_{2,stoichiometric}} * \left(\frac{EA}{100}\right) + \nu_{O_{2,stoichiometric}} * r * \left(1 + \frac{EA}{100}\right) \quad \text{(A12)}$$

The number of moles of air per kmole of fuel can be found by:

$$\frac{N_{air}}{N_{fuel}}\left(\frac{mol}{kmol}\right) = \nu_{O_{2,stoichiometric}} * \left(1 + \frac{EA}{100}\right) + \nu_{O_{2,stoichiometric}} * r * \left(1 + \frac{EA}{100}\right) = \nu_{O_{2,stoichiometric}} * (1 + r)\left(1 + \frac{EA}{100}\right) \quad \text{(A13)}$$

Equations (A12) and (A13) can be combined together to find the number of dry moles of product per kmole of fuel:

$$\frac{N_{dry}}{N_{fuel}}\left(\frac{mol}{kmol}\right) = 1 + \left(\frac{q-1}{\left(1+\frac{EA}{100}\right)*(1+r)}\right) \quad \text{(A14)}$$

Looking at Equation (A14), the ratio of dry product moles to moles of air will be less than one if q is less than one, which is applicable to most solid fuels. However, coal and biomasses have a q close to one and thus, the number of dry moles of product will be approximately equal to the number of moles of air. One further simplification can be made to determine the maximum value the ratio could handle. This will occur when the flame is stoichiometric and thus the excess air is 0:

$$\left(\frac{N_{dry}}{N_{air}}\right)_{maximum}\left(\frac{mol}{kmol}\right) = 1 + \left(\frac{q-1}{1+r}\right) \tag{A15}$$

It is possible to predict the percentage of CO2 that should be formed when a solid fuel is completely burned. From this calculation, it is possible to determine the ratio of number of moles of CO3 formed relative to the number of kmoles of fuel burned:

$$\frac{N_{CO_2}}{N_{fuel}}\left(\frac{mol}{kmol}\right) = q * \nu_{O_{2,stoichiometric}} \tag{A16}$$

and the percentage of CO_2 formed is:

$$CO_2(\%) = \frac{q*100}{\frac{x}{100}+q+r*\left(1+\frac{x}{100}\right)} \tag{A17}$$

It is common for q to be very small relative to the other terms in the denominator in Equation A.3.10 and thus be ignored:

$$CO_2(\%) = \frac{q*100}{\frac{x}{100}+r*\left(1+\frac{x}{100}\right)} \tag{A18}$$

Equation (A18) is graphed in Figure A-2.

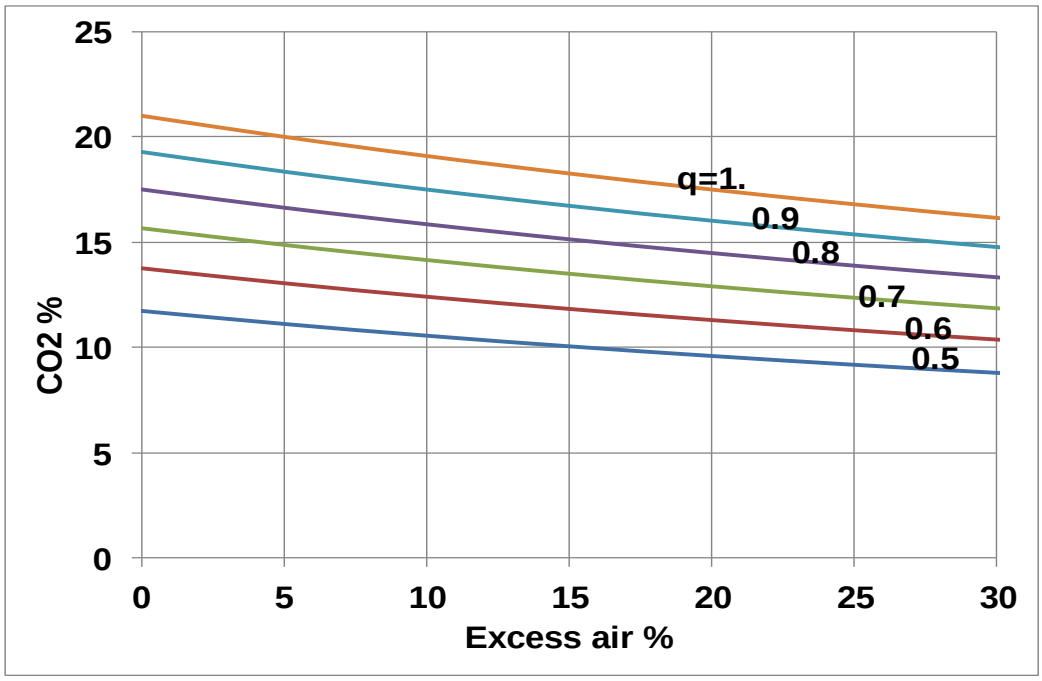

Figure A-2 Variation of CO_2 produced with Excess Air percentages for a range of q values.

Finally, if the fuel is not completely burnt, then the maximum amount of CO_2 will not be formed. It is safe to approximate the ratio of actual CO_2 formed to theoretical maximum CO_2 formation as being equal to the ratio of the measured q to the theoretical q. This provides a fast method to approximate the burnt fraction:

$$\frac{CO_{2_{measured}}}{CO_{2_{theoretical}}} \cong \frac{q_{measured}}{q_{theoretical}} = BF \qquad \text{(A19)}$$

APPENDIX B

TEMPERATURE PROFILES

Because of thermal NO_x's strong temperature dependence, it is necessary to monitor temperature profile throughout the furnace. Temperature was measured using type K shielded ungrounded thermocouple placed in 0.1524 m (6 inch) intervals along the axial length of the furnace measuring the centerline temperature. The third thermocouple was removed from service to accommodate the arm OFA staging and thus there is an abnormally large gap between the second and third data points in the figures. Sometimes thermocouples burn up, and cannot be repaired until the furnace cools. It was undesirable to cease experimentation when a thermocouple had burned, so not all data sets have a complete temperature profile. Figure B-1 presents the peak temperature for all experimental cases investigated.

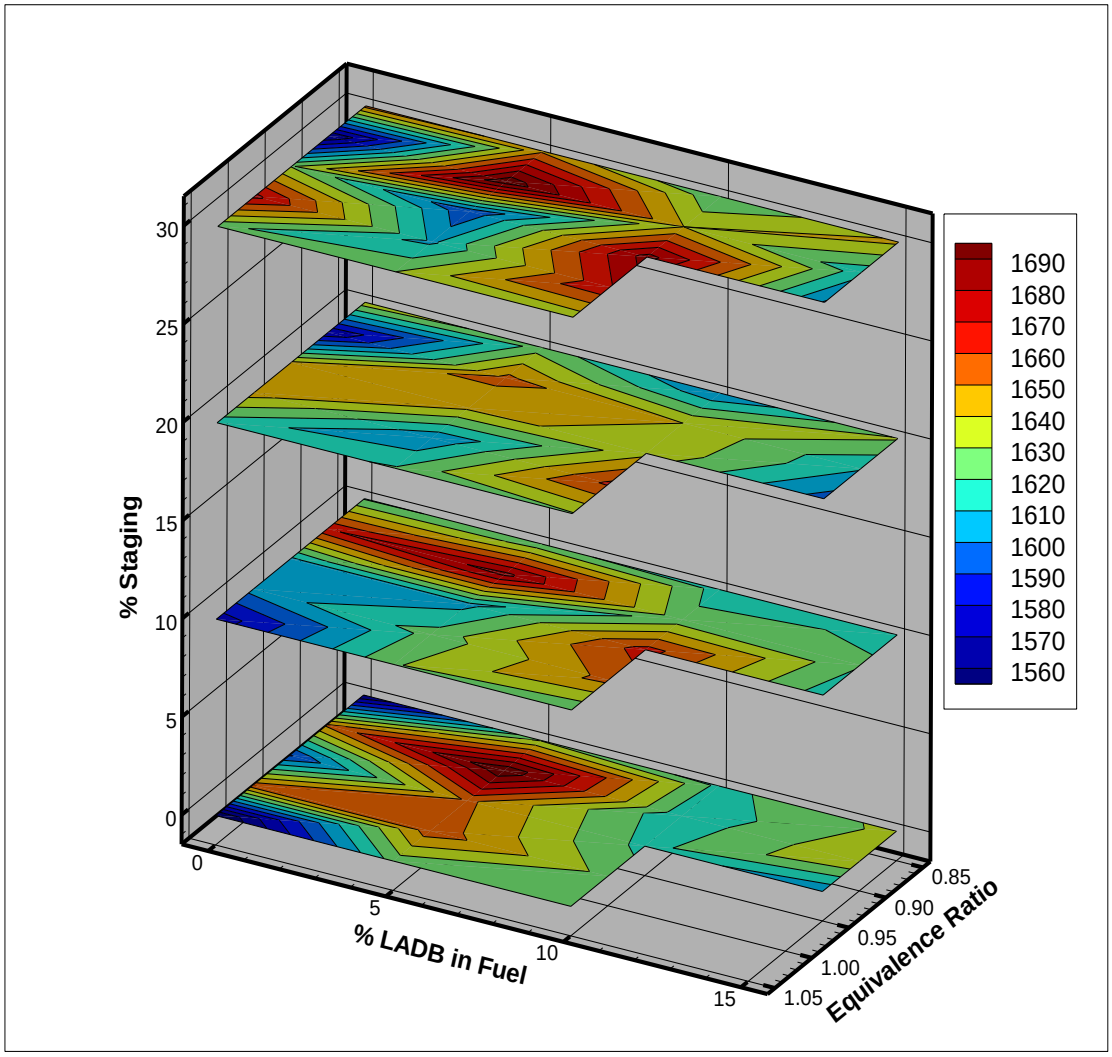

Figure B-1 Peak temperature for all experimental cases investigated.

APPENDIX C

NO and NH_3 PARTITIONING DURING VOLATILE MATTER PYROLYSIS

This appendix is adapted from the information available in Duo et al. (1992), Thien et al. (2012), and Spear (2012). Thermal NO production is typically low at temperatures below 1600 K. Typical temperatures measured in the furnace were 1589 K (2400 F). If the NO would have been dominated by thermal NO, then increasing excess air (i.e., decreasing temperature), may have decreased NO due to the lowered temperature effect. on the other hand, the fuel N conversion efficiency would increase with excess air because more oxygen is available for oxidation of the fuel N compounds, and fuel N oxidation is almost insensitive to temperature. When a CFB trips, NO production decreases because a portion of the coal feed burns under rich conditions. Thus less NH_3 is required to reduce NO and the residual NH_3 will slip. To facilitate quick and inexpensive predictions, two competitive reaction formulations have been used for modeling purposes. One may use an empirically based model which includes the following forward direction only competitive reactions:

$4NH_3 + 4NO + O_2 \rightarrow 4N_2 + 6H_2O$ Reaction C.1.

$4NH_3 + 5O_2$ □□$4NO + 6H_2O$ Reaction C.2.

$d[NO]/dt = k_B [NH_3] - k_A [NH_3] [NO]$ Equation C.1.

$d[NH_3]/dt = -k_B [NH_3] - k_A [NH_3] [NO]$ Equation C.2.

In order to use Equations C.1 and C.2, the kinetic constants are needed. They are given by: $k_A = 2.45 \times 1017 \exp(-29400/T)$ and $k_B = 2.21 \times 1014 \exp(-38130/T)$.

Under normal operating conditions, O_2 is typically compared to NH_3 in excess, and NO exists in trace amounts. Reaction C.1 represents the second-order reduction of NO to N_2 and Reaction C.2 represents the first order oxidation of NH_3. It can be seen from the values of the two activation energies and the overall rate constants how the simple model was able to predict the temperature window for NO reduction (1145 to 1480 K).

The following figures show plots of NO and NH_3 versus residence time at 1100 K for initial NO concentrations and various initial NH_3/NO ratios. Figures C-1 and C-2 show the change in NO ppm due to reduction reactions with NH_3 and as well as NH_3 concentration with time for several assumed initial NH_3/NO ratios and at T = 1100 K. When NO is deficient or NH_3 is in excess, there is residual NH_3 which is called NH_3 slip. At higher NH_3/NO or lower NO (rich conditions) NH_3 slip is high. Figures C-3 and C-4 show the corresponding figures at T=1000 K. It is apparent that NH_3 slip has increased at lower temperatures because of reduced NO reaction rates.

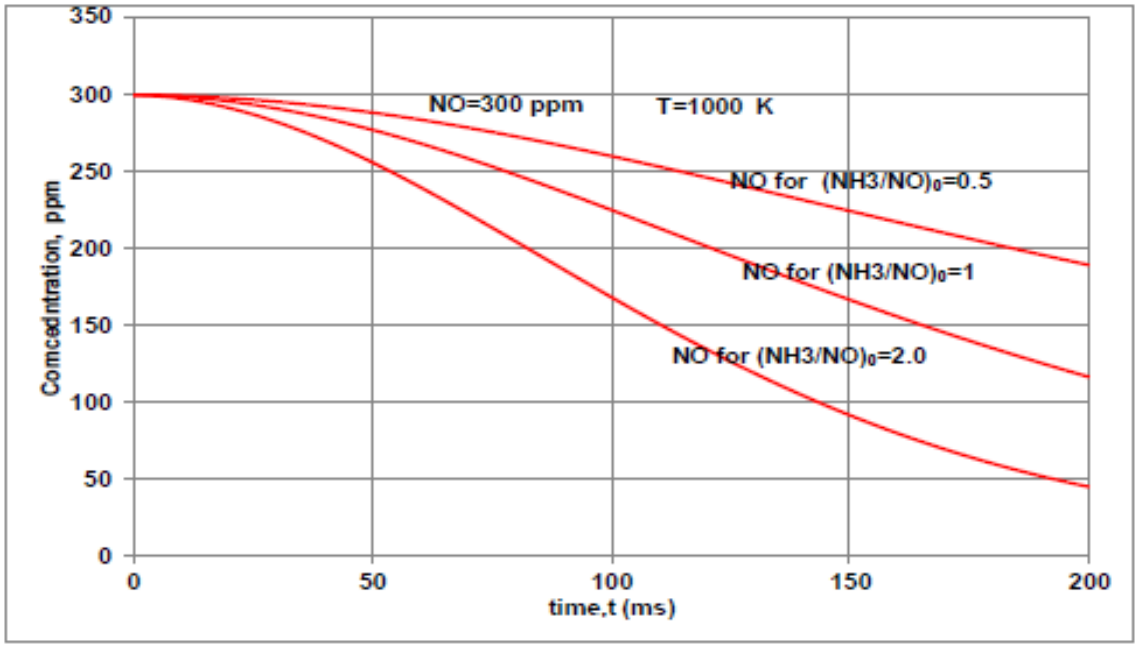

Figure C-1 Effect of initial NH_3/NO ratio on NO at 1000 K. A low NO concentration leads to a high NH_3 ratio which improves the degree of NO reduction.

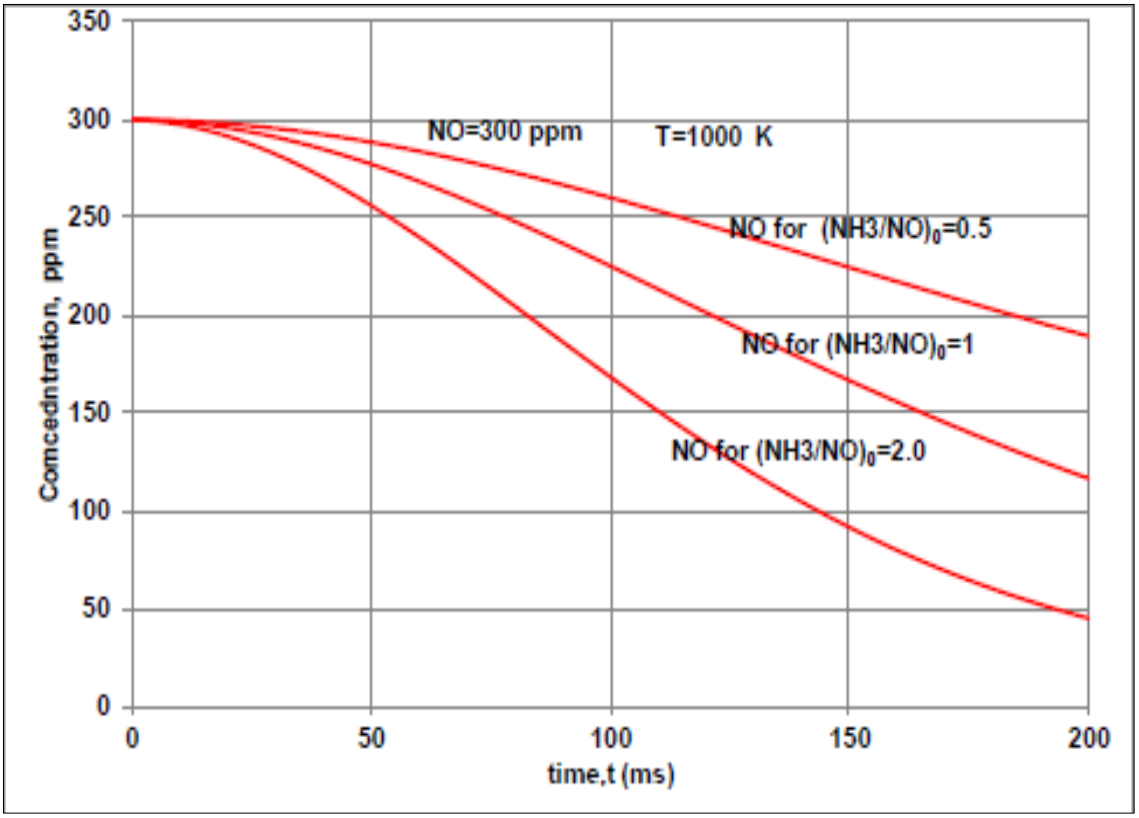

Figure C-2 Effect of initial NH_3/NO ratio on NH_3 at 1000 K. Low initial NO (rich conditions) leads to a high NH_3 ratio which leads to NH_3 slip.

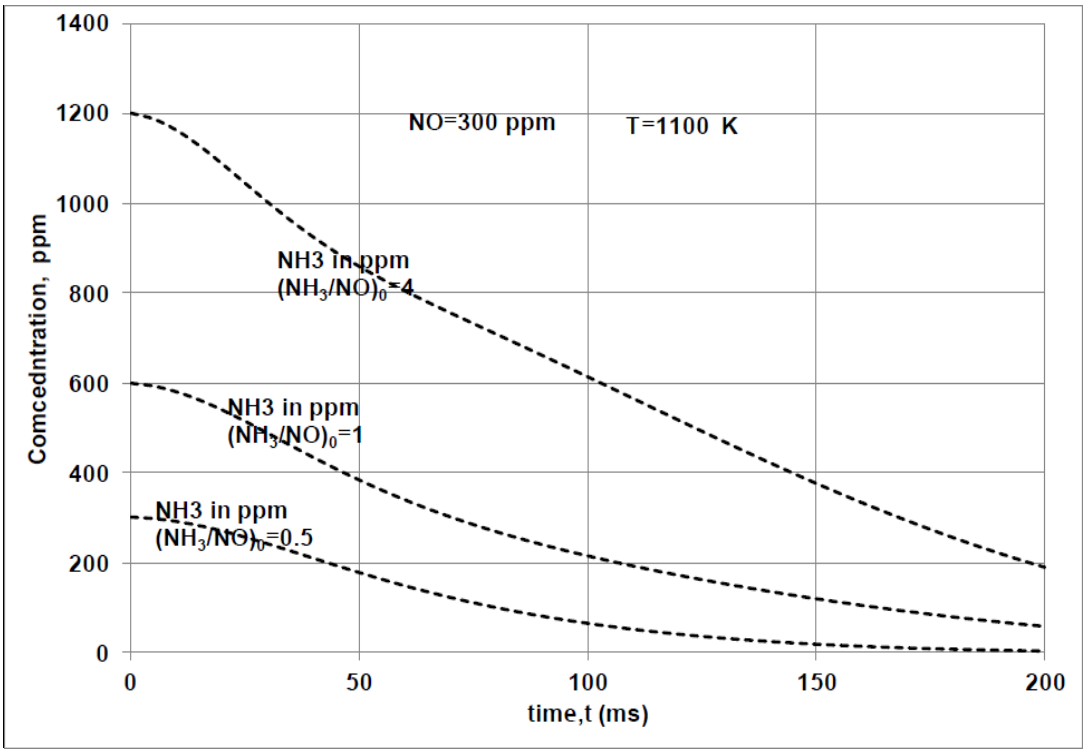

Figure C-3 Effect of initial NH_3/NO ratio on NO at 1100 K. A low NO concentration leads to a high NH_3 which improves the degree of NO reduction.

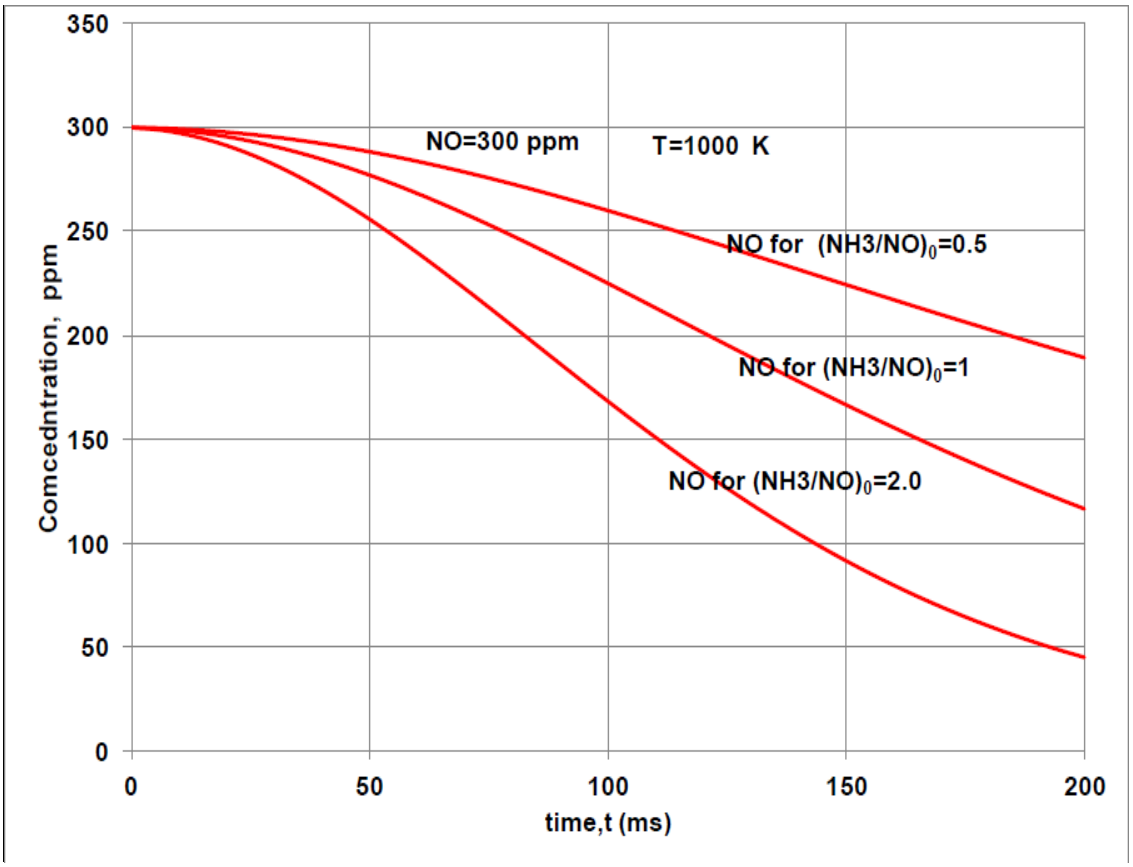

Figure C-4 Effect of initial NH_3/NO ratio on NH_3 at 1100 K. Low initial NO (rich conditions) leads to a high NH_3 ratio which leads to NH_3 slip (Spear, 2012).

APPENDIX D

GAS ANALYSES, BURNT FRACTION, AND RESPIRATION QUOTIENT

Problem 1: Consider a $CH_x Oy$ fuel reacting with O_2 and burning completely:

$$CH_x Oy + a\ O_2 + b\ N_2 \rightarrow c\ CO_2 + d\ H_2O + e\ O_2 + f\ N_2 \quad (A)$$

There are 8 unknowns: $_x$, y, a, b, c, d, e, and f.

Number of atom balances: 4.

Additional four equations: b/a= 3.7.

Wet analysis: H_2O%, CO2%, O_2%.

Thus, the solution can be obtained.

$$C{:}1 = c, \quad (B)$$

$$H{:}\times = 2\ d, \quad (C)$$

$$O{:}\ 2\ a + y = 2\ c + d + 2\ e, \text{ and} \quad (D)$$

$$N{:}\ 2\ b = 2f, \text{ where} \quad (E)$$

$$b/a = 3.76. \quad (F)$$

Percentage of $CO_2 = c \times 100 \div (c + d + e + f) = \%\ dry^*\{c + e + f)/(c + d + e + f\}$

$$= \%\ CO_2\ dry\ *\ dry\ mole/wet\ moles \quad (G)$$

Percentage of $O_2 = e \times 100 \div (c + e + d + f) = \%\ dry\ *\ \{c + e + f) / (c + d + e + f\}$

$$= \%\ dry\ *\ O_2{}^*\ dry\ mole/wet\ moles \quad (H1)$$

Percentage of $H_2O = d \times 100 \div (c + e + d + f)$ (H2)

Eight equations: (B throough H2); 8 unknowns: $_x$, y, a,b,c,d,e,f. Solve

c = 1, (I)

d = $_x$ /2, (J)

e = (2 a +y– 2 c-d)/2 = a +y/2– 1– $_x$ /4, (K)

f = b = 3.76 a, (L)

%CO_2 / %O2 = c / e = 3.6 / 15.70 = 0.229, e = 4.361

% H_2O / %CO_2 = 0.062 / 0.036 = d / c = 1.722, d = 1.722

$_X$ = 2 * d = 3.444

Wet moles = c + d + e + f = c / CO_2 mole fraction

wet = c / 0.036 = 27.778

F * 100 / wet moles = N_2% or f = N_2% / CO_2% or N_2% 100-CO_2%-O_2%-H_2O%

F = b = {c + d + e + f}-{c + e + d} = 27.778-1-4.361-1.722 = 20.695

b / a = 3.76; so a = b / 3.76 = 20.695 / 3.76 = 5.504,

from (K)

e = a + y / 2-1-$_x$ / 4,

4.361 = 5.504 + y / 2-1-0.861 = 3.64 + (y / 2)

y = 1.436,

$CH_{3.444}\,O_{1.436} + 5.504\,O_2 + 5.504 \times 3.76\,N_2 \rightarrow 1\,CO_2 + 1.722\,H_2O + 4{,}361\,O_2 + 20.695\,N_2$,

Dry moles / wet moles = CO_2% wet / CO2% dry = 0.036 / 0.0384 = 0.938

Problem 2: Consider a $CH_x\,O_y$ fuel reacting with O_2 and partially burnt; x is known (but not y), dry analysis of CO_2%, O_2% as well as measured equivalence ratio.

If ε is the bunt fraction, then

$$CH_x\,O_y + aO_2 + bN_2 \rightarrow \varepsilon CO_2 + (_x / 2)\,\varepsilon\,H_2O + (a - a_{stoich} * \varepsilon)O_2 + 3.76N_2 + (1-\varepsilon)CH_x\,O_y$$

Exact Method

$$CO_2\% = \varepsilon * 100 / N_{dry,\varepsilon},$$

$$N_2\% = 100 - CO_2\% - O_2\% = 3.76a * 100 / N_{dry,\varepsilon}$$

$$O_2\% = \{a - a_{stoich} * \varepsilon) * 100 / N_{dry,\varepsilon}$$

$$O_2\% / \{N_2\%\} = \{a - a_{stoich} * \varepsilon) / 3.76a\} = \{1 - \varepsilon\phi) / 3.76$$

So $\varepsilon\phi = \phi'$, a pseudo equivalence ratio lower than measured equivalence ratio based on air and fuel flows due to incomplete combustion

$$\phi' = 1 - [O_2\% * 3.76 / \{N_2\%\}] \text{ and } \varepsilon = \phi'/\phi$$

$$BF = \varepsilon = \frac{1}{\phi}\left\{1 - 3.76\frac{O2\%}{N2\%}\right\} = \frac{1}{\phi}\left\{1 - \left(\frac{1 - X_{O2a}}{X_{O2a}}\right)\frac{O2\%}{N2\%}\right\} = \frac{1}{\phi}\left\{1 - \left(\frac{1}{X_{O2a}} - 1\right)\frac{O2\%}{N2\%}\right\} \quad (M)$$

$N_2\% / CO_2\% = f / \varepsilon$

$f = \varepsilon * N_2\% / CO_2\%$

$O_2\% / CO_2\% = e / \varepsilon$

$e = \{O_2\% / CO_2\%\} * \varepsilon$

$N_{dry,\varepsilon} = \varepsilon * 100 / CO_2\%$

Approximate Expression for Burnt Fraction

$N_{dry,\varepsilon} = \varepsilon + (a\text{-}a_{stoich} * \varepsilon) + 3.76a = \varepsilon + (a\text{-}\{1 + {}_x / 4\text{-}y / 2) * \varepsilon) + 3.76a =$

$(4.76a\text{-}\{{}_x / 4\text{-}y / 2) * \varepsilon) \approx 4.76$

$O_2\% = (a\text{-}a_{stoich} * \varepsilon) * 100 / N_{dry,\varepsilon} = \{a\text{-}a_{stoich} * \varepsilon) * 100 / 4.76a = \{1\text{-}\phi * \varepsilon) *$

$100 / 4.76$

So $BF = \varepsilon \approx \frac{1}{\phi}\left\{1 - \left(\frac{X_{O2}}{X_{O2a}}\right)\right\}$ where 1 / X O_2a = 4.76, X O_2a= ambient O_2 mole fraction (Lawrence et al. 2009).

When $\varepsilon = 1$, measured O_2 % is low and when $\varepsilon < 1$, measured O_2 % is high.

Note that measured or theoretical RQ is unaffected because less fuel is burnt less O_2 is used and hence RQ remains the same.

$RQ = CO_2 / O_2 = 1 /\{1 + d / 2\} = 1 / \{1 + 0.5\% H_2O\%wet / O_2\%wet\}$

APPENDIX E

PROOF OF RESPIRATION COEFFICIENT AND GAS ANALYSIS

HHV_{O2} is defined to be the heat value of the fuel divided by the amount of oxygen required to combust the fuel stoichiometrically. This value is approximately constant for most fuels. For proof of this statement, begin with the Boie Equation (Annamalai and Puri, 2005) which is an empirical calculation of higher heating value based upon ultimate analysis:

$$HHV\ \left(\frac{kJ}{kg}\right) = 422{,}272 * C + 117{,}387 * H - 155{,}371 * O + 100{,}480 * N + 335{,}508 * S \quad \text{(E1)}$$

Equation (E1) can be rearranged by factoring the C out to obtain:

$$HHV\ \left(\frac{kJ}{kg}\right) = C\left(422{,}272 + 117{,}387 * \frac{H}{C} - 155{,}371 * \frac{O}{C} + 100{,}480 * \frac{N}{C} + 335{,}508 * \frac{S}{C}\right) \quad \text{(E2)}$$

However, to obtain the Boie Equation in a form that is useful in conjunction with Ultimate Analysis, it is necessary to get the coefficients in terms of mass fractions like reported in Ultimate Analysis:

$$HHV\ \left(\frac{kJ}{kg}\right) = \left(\frac{Y_C}{12.01}\right)\left(422{,}272 + 117{,}387 * \frac{H}{C} - 155{,}371 * \frac{O}{C} + 100{,}480 * \frac{N}{O} + 335{,}508 * \frac{S}{O}\right) \quad \text{(E3)}$$

The hydrogen to carbon ratio can also be replaced in terms of mass fractions:

$$\frac{H}{C} = \frac{12.01Y_H}{1.01Y_C} \quad \text{(E4)}$$

Similar substitutions can be made with the other variables in the Boie Equation. The stoichiometric amount of oxygen needed to combust a fuel can be found using:

$$\nu_{O_2} = 32\left(C + \frac{H}{4} - \frac{O}{2} + S\right) = 32C\left(1 + \frac{H}{4C} - \frac{O}{2C} + \frac{S}{C}\right) \quad \text{(E5)}$$

Equation E.2 and E.5 can now be combined together to determine the higher heating value per unit of stoichiometric oxygen:

$$HHVO2\ \left(\frac{kJ}{kg\ of\ O2}\right) = \frac{422{,}272+117{,}387*\frac{H}{C}-155{,}371*\frac{O}{C}+100{,}480*\frac{N}{C}+335{,}508*\frac{S}{C}}{32\left(1+\frac{H}{4C}-\frac{O}{2C}+\frac{S}{C}\right)} \quad \text{(E6)}$$

Because nitrogen and sulfur exist is solid fuels in trace amounts, it is acceptable to ignore their contributions and treat the fuel as if it was exclusively C-H-O. Making this assumption, Figure E-1 plots HHVO2 vs. H/C with O/C as parameter (with N and S as trace species) are approximately constant and have a value of 14,250 kJ/kg of stoichiometric oxygen or 18.6 kJ/standard L of oxygen. Considering that air is 20.9% oxygen, this can also be calculated to give 3,280 kJ/kg of stoichiometric air or 3.9 kJ/standard L of stoichiometric air. As an example, literature states that HHV per unit of stoichiometric oxygen of methane is 13,550 kJ/kg (17.7 kJ/standard L of oxygen) and the Boie Equation yields 13,934 kJ/kg. For n-octane the literature value is 13,640 kJ/kg (17.82 kJ/standard L) and the Boie Equation yields 13,730 kJ/kg.

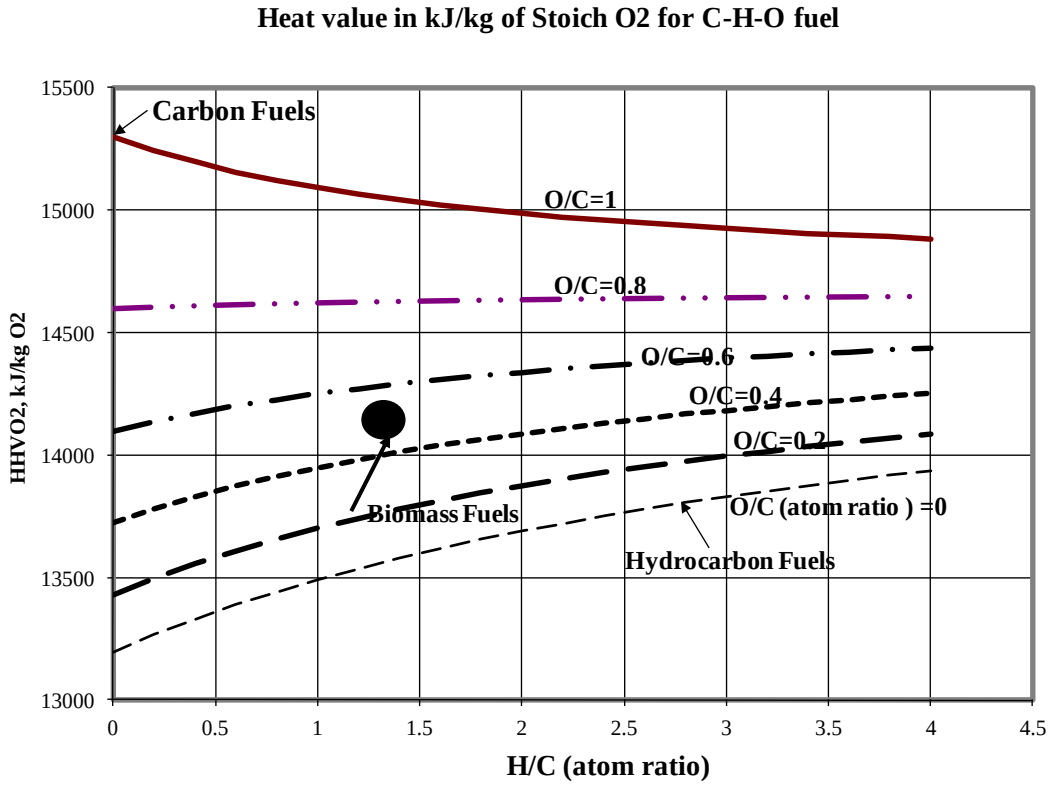

Figure E-1 Boie-based HHV_{O2} vs.. H/C with O/C atom ratio as parameter; S and N are trace species Interesting results are obtained for burnt gases when using the ratio of the number of moles of CO_2 produced per mole of stoichiometric oxygen.

This ratio is most commonly encountered in biology. With the introduction of the respiratory ratio, the number of moles of CO2 produced per kmole of fuel can be calculated by:

$$\frac{N_{CO_2}}{N_{fuel}}\left(\frac{mol}{kmol}\right) = q * \nu_{O_2} \qquad \text{(E7)}$$

Figure E-2 shows the variation of q with H/C and O/C based upon the Boie Equation.

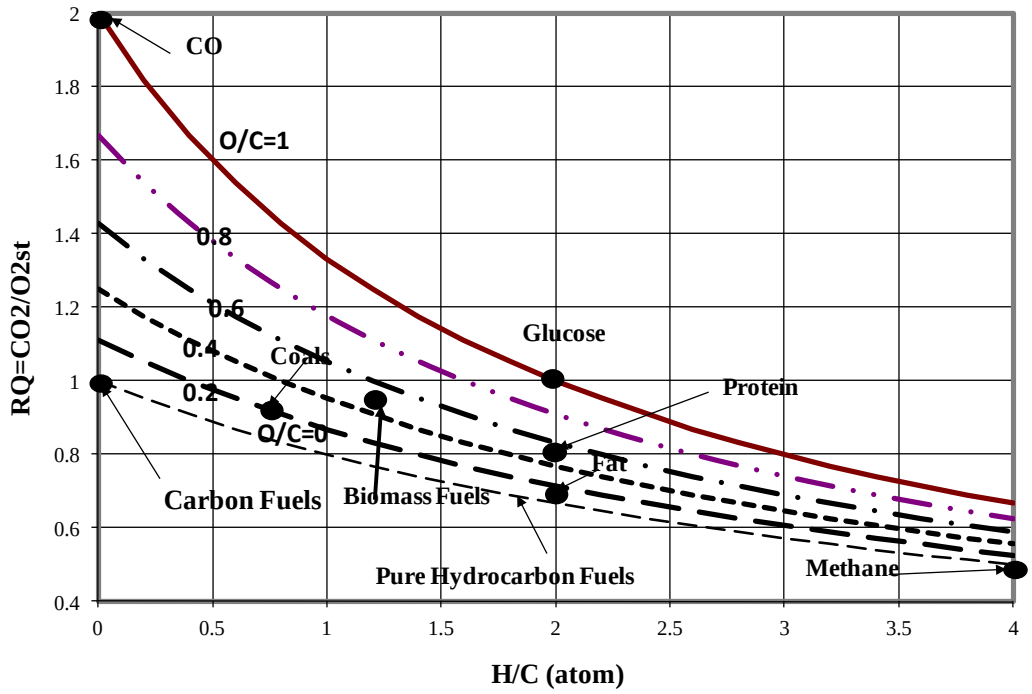

Figure E-2 Variation of CO_2/O_{2st} with H/C and O/C in C-H-O fuels; CO has high RQ ratio.

Because CO is produced mainly from C with RQ=0, and CO has RQ of 2, then the sum ($C+1/2\ O_2 \rightarrow CO$, $CO+1/2\ O_2 \rightarrow CO_2$; on adding $C+O_2 \rightarrow CO_2$) will be equal to 1 when CO_2 is produced from C. Fat RQ=0.7; HC has lower RQ values compared to alcohols. Ethanol with O/C=0.5, H/C=3 has RQ=0.7, but it is a renewable fuel.

Table E-1 presents the value and range of one for several different fuels. For most biomass fuels, q ranges from 0.94-0.97 and for coals it ranges from 0.92-0.93. Animal wastes typically fall in the range 0.92-0.95. Thus, most solid fuels will be somewhere in the range 0.92-0.97. The RQ values for renewable biomass fuels are not of concern to this research. Methane has lowest RQ while pure carbon/coal has the highest

RQ values. For comparative purposes, most liquid or gaseous fuels are in the range 0.50-0.80.

Table E-1 Values and range of respiratory ratio for various fuels

	q	Range of q	Remarks
Paraffins, C_nH_{2n+2}	$q = \frac{1}{\left\{1+\left(\frac{1}{2}+\frac{1}{2n}\right)\right\}}$	½<q<(2/3)	q increases slightly with n; q=1/2 for CH_4 and q→(2/3) as n→∞
Olefins, Napthenes or Cycloparafin, C_nH_{2n}	$q = \frac{2}{3}$	$q = \frac{2}{3}$	q constant
Diolefins, C_nH_{2n-2}	$q = \frac{1}{\left\{1+\left(\frac{1}{2}-\frac{1}{2n}\right)\right\}}, \quad n \geq 2$	4/5<q<(2/3)	q decreases slightly with n
Aromatics, C_nH_{2n-6}	$q = \frac{1}{\left\{\left(\frac{3}{2}-\frac{3}{2n}\right)\right\}}, \quad n \geq 6$	4/5<q<(2/3)	q decreases slightly with n
Alcohols, $C_nH_{2n+1}O$	$q = \frac{2}{3}$	$q = \frac{2}{3}$	q constant
Glucose $C_6H_{12}O_6$	1	1	
Palmitic Acid $C_{16}H_{32}O_2$	0.68	0.68	
Proteien $CH_2O_{0.5}$	0.8	0.8	
Mesquite, $CH_{1.3582}O_{0.5779}N_{0.0122}S_{0.0003}$	0.95	0.95	
Juniper $CH_{1.3708}O_{0.5637}N_{0.0049}S_{0.0001}$	0.94	0.94	
Rice Straw $CH_{1.414}N_{0.0147}O_{0.638}S_{0.0004}$	0.97	0.97	
PRB $CH_{0.71}N_{0.014}O_{0.18}S_{0.0014}$	0.92	0.92	
Texas Lignite $CH_{0.678}N_{0.0157}O_{0.0.194}S_{0.00615}$	0.93	0.93	
Feedlot Biomass $CH_{1.287}N_{0.04991}O_{0.532}S_{0.0057}$	0.95	0.95	
Dairy Biomass $CH_{1.06}N_{0.047}O_{0.41}S_{0.0045}$	0.94	0.94	
Litter Biomass $CH_{1.55}O_{0.60}$	0.92	0.92	

It will be shown now that RQ is related to CO_2 produced in kg/GJ of heat input for any fuel.

RQ = CO_2 production rate/O_2consumption rate= CO_2 production rate in kg/s/{Heat input rate in GJ/s)/(HHV_{O2} in GJ/kg O2)} CO_2 production in kg per GJ= RQ*HHV_{O2} in GJ/kg of oxygen

Because HHV_{O2} is constant for most fuels, then CO_2 in kg/GJ is proportional to RQ; thus RQ values were determined for various fuels and they are summarized in table Flue gas analyses can now be performed in terms of RQ. Ignoring NO_x and SO_2 formed in combustion, the theoretical amount of oxygen in the exhaust is:

$$X_{O_2} = \frac{EA}{0.01*EA+RQ+r*(1+0.01*EA)} \quad \text{(E8)}$$

Additional simplification can be made with the assumption that RQ is much smaller than r. With this simplification applied, exhaust O_2 concentration is insensitive to RQ even RQ ranges through as wide a range of values as 0.5 to 1.00, as demonstrated by Figure E-3. Thus, with a fixed excess air percentage, most fuels will have the same percentage of O_2 in the exhaust.

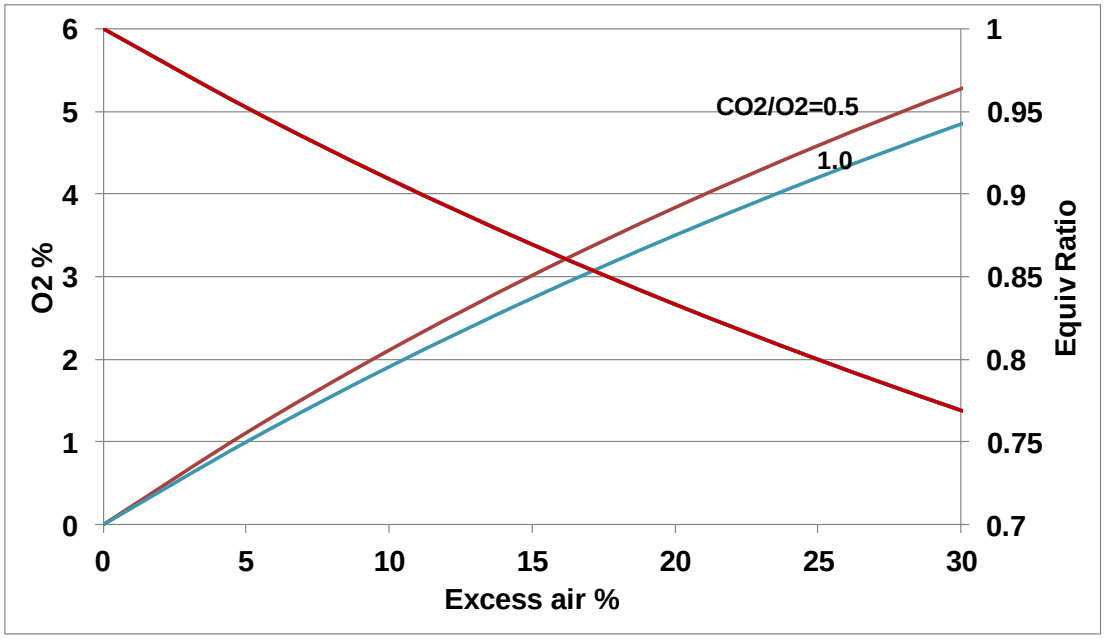

Figure E-3 Exhaust O_2 concentration and equivalence ratio when excess air percentage is varied for q = 0.5 and RQ= 1.0.

The number of moles of air per kmole of fuel can be found by:

$$\frac{N_{air}}{N_{fuel}}\left(\frac{mol}{kmol}\right) = \nu_{O_{2,stoichiometric}} * \left(1+\frac{EA}{100}\right) + \nu_{O_{2,stoichiometric}} * r * \left(1+\frac{EA}{100}\right)$$

$$= \nu_{O_{2,stoichiometric}} * (1+r)\left(1+\frac{EA}{100}\right) \quad \text{(E9)}$$

Equations (E8) and (E9) can be combined together to find the number of dry moles of product per kmole of fuel:

$$\frac{N_{dry}}{N_{fuel}}\left(\frac{mol}{kmol}\right) = 1 + \left(\frac{RQ-1}{\left(1+\frac{EA}{100}\right)*(1+r)}\right) \quad \text{(E10)}$$

Looking at Equation (E10), the ratio of dry product moles to moles of air will be less than one if q is less than one, which is applicable to most solid fuels. However, coal and biomasses have a q close to one and thus the number of dry moles of products will be approximately equal to the number of moles of air.

$$\frac{N_{CO_2}}{N_{fuel}}\left(\frac{mol}{kmol}\right) = RQ * \nu_{O_{2,stoichiometric}} \quad \text{(E11)}$$

$$CO_2(\%) \approx \frac{q*100}{\frac{x}{100}+r*\left(1+\frac{x}{100}\right)} \quad \text{(E12)}$$

Equation (E12) is graphed in Figure E.4.

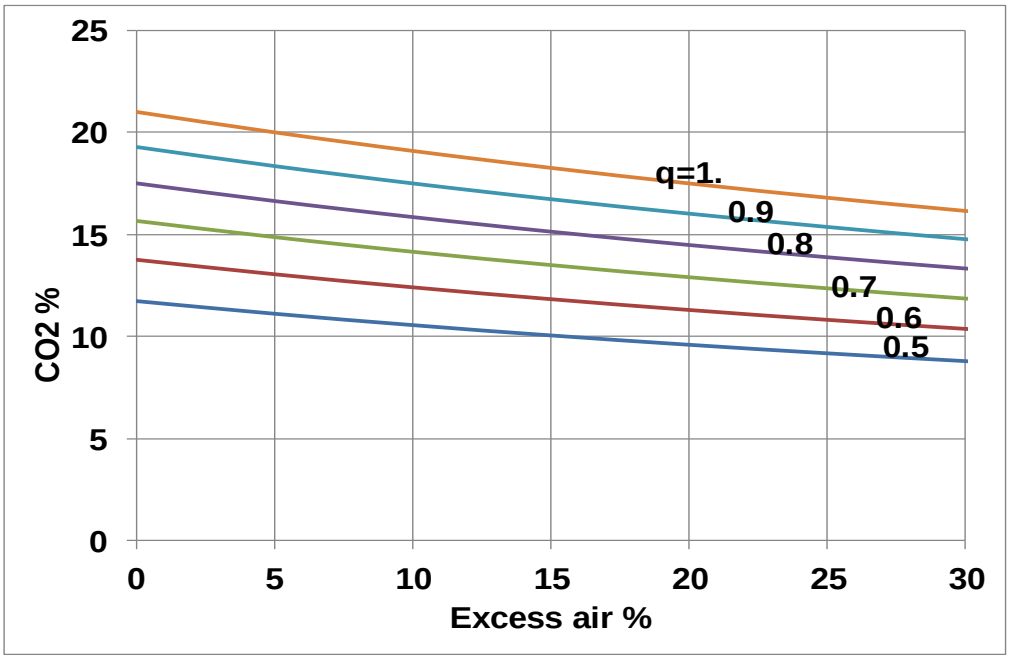

Figure E-4 Variation of CO_2 produced with Excess Air percentages for a range of q (same as RQ) values.

Finally, if the fuel is not completely burnt, then the maximum amount of CO_2 will not be formed. It is safe to approximate the ratio of actual CO_2 formed to theoretical maximum CO_2 formation as being equal to the ratio of the measured RQ to the theoretical RQ. This provides a fast method to approximate the burnt fraction:

$$\frac{CO_{2_{measured}}}{CO_{2_{theoretical}}} \cong \frac{RQ_{measured}}{RQ_{theoretical}} = BF \quad \text{(E13)}$$

APPENDIX F

EXPERIMENTAL RESULTS TABLES

Table F-1 presents the measured exhaust concentrations for unstaged combustion from the experimental work.

Table F-1 Measured exhaust concentrations for unstaged combustion from experimental work

Fuel	Equivalence Ratio	% LADB in Fuel	% Staging	O2 (%)	CO2 (%)	NOx (ppm)	CO (ppm)	NOx (g/GJ)
PRB	0.85	0%	0%	3.1	16.9	661	740	381
PRB	0.90	0%	0%	2.2	16.9	653	1070	377
PRB	0.95	0%	0%	1.9	17.5	549	2445	304
PRB	1.00	0%	0%	1.8	17.1	439	2280	248
PRB	1.05	0%	0%	1.3	17.2	427	2792	239
95-5 PRB-LADB	0.85	5%	0%	3.3	16.7	711	725	415
95-5 PRB-LADB	0.90	5%	0%	2.3	16.6	673	910	395
95-5 PRB-LADB	0.95	5%	0%	2.0	16.9	642	960	370
95-5 PRB-LADB	1.00	5%	0%	1.8	17.3	562	2220	314
95-5 PRB-LADB	1.05	5%	0%	1.2	16.2	475	2510	283
90-10 PRB-LADB	0.85	10%	0%	3.2	17.1	838	638	478
90-10 PRB-LADB	0.90	10%	0%	2.3	16.9	687	1015	397
90-10 PRB-LADB	0.95	10%	0%	1.9	16.5	670	1325	395
90-10 PRB-LADB	1.00	10%	0%	1.8	17.8	653	2072	354
90-10 PRB-LADB	1.05	10%	0%	1.2	16.4	483	2872	283
85-15 PRB-LADB	0.85	15%	0%	3.2	17.5	885	514	494
85-15 PRB-LADB	0.90	15%	0%	2.3	16.8	691	940	400
85-15 PRB-LADB	0.95	15%	0%	1.9	16.6	683	1030	400

Table F-2 presents the measured exhaust concentrations for 10% staged combustion from the experimental work.

Table F-2 Measured exhaust concentrations for 10% staged combustion from experimental work

Fuel	Equivalence Ratio	% LADB in Fuel	% Staging	O2 (%)	CO2 (%)	NOx (ppm)	CO (ppm)	NOx (g/GJ)
PRB	0.85	0%	10%	3.3	17.3	663	257	376
PRB	0.90	0%	10%	2.1	17.1	572	3031	321
PRB	0.95	0%	10%	1.1	17.7	532	4363	287
PRB	1.00	0%	10%	0.8	16.5	426	4800	246
PRB	1.05	0%	10%	0.8	15.8	307	5350	184
95-5 PRB-LADB	0.85	5%	10%	3.3	17.2	670	239	381
95-5 PRB-LADB	0.90	5%	10%	2.1	18.6	607	2175	316
95-5 PRB-LADB	0.95	5%	10%	1.1	17.7	537	2786	293
95-5 PRB-LADB	1.00	5%	10%	0.9	18.0	470	2916	252
95-5 PRB-LADB	1.05	5%	10%	1.0	16.0	382	4650	227
90-10 PRB-LADB	0.85	10%	10%	3.3	17.2	677	257	386
90-10 PRB-LADB	0.90	10%	10%	2.3	18.5	613	2613	319
90-10 PRB-LADB	0.95	10%	10%	1.2	17.7	585	3012	318
90-10 PRB-LADB	1.00	10%	10%	0.7	16.6	442	4075	254
90-10 PRB-LADB	1.05	10%	10%	0.8	16.2	384	5300	225
85-15 PRB-LADB	0.85	15%	10%	3.1	16.9	802	324	464
85-15 PRB-LADB	0.90	15%	10%	2.3	18.5	679	2525	354
85-15 PRB-LADB	0.95	15%	10%	1.2	17.5	617	3001	340

Table F-3 presents the measured exhaust concentrations for 20% staged combustion from the experimental work.

Table F-3 Measured exhaust concentrations for 20% staged combustion from experimental work

Fuel	Equivalence Ratio	% LADB in Fuel	% Staging	O2 (%)	CO2 (%)	NOx (ppm)	CO (ppm)	NOx (g/GJ)
PRB	0.85	0%	20%	3.4	17.3	405	2506	226
PRB	0.90	0%	20%	1.7	17.5	451	2440	249
PRB	0.95	0%	20%	0.8	17.8	352	3854	189
PRB	1.00	0%	20%	0.8	17.8	306	5134	164
PRB	1.05	0%	20%	0.7	17.1	310	5660	172
95-5 PRB-LADB	0.85	5%	20%	3.2	17.4	580	1923	322
95-5 PRB-LADB	0.90	5%	20%	2.0	17.1	521	2660	293
95-5 PRB-LADB	0.95	5%	20%	0.8	17.5	387	4628	211
95-5 PRB-LADB	1.00	5%	20%	0.7	17.9	421	5378	224
95-5 PRB-LADB	1.05	5%	20%	0.8	16.1	365	7900	212
90-10 PRB-LADB	0.85	10%	20%	3.3	17.0	595	1707	338
90-10 PRB-LADB	0.90	10%	20%	2.1	17.4	545	1746	304
90-10 PRB-LADB	0.95	10%	20%	0.9	17.5	420	4206	230
90-10 PRB-LADB	1.00	10%	20%	0.9	17.7	409	5309	220
90-10 PRB-LADB	1.05	10%	20%	0.6	17.7	409	8309	216
85-15 PRB-LADB	0.85	15%	20%	3.2	16.3	721	651	431
85-15 PRB-LADB	0.90	15%	20%	2.2	17.2	546	2280	306
85-15 PRB-LADB	0.95	15%	20%	0.9	17.3	484	4257	267

Table F-4 presents the measured exhaust concentrations for 30% staged combustion from the experimental work.

Table F-4 Measured exhaust concentrations for 30% staged combustion from experimental work.

Fuel	Equivalence Ratio	% LADB in Fuel	% Staging	O2 (%)	CO2 (%)	NOx (ppm)	CO (ppm)	NOx (g/GJ)
PRB	0.85	0%	30%	3.3	17.4	441	579	247
PRB	0.90	0%	30%	2.0	17.0	255	4922	142
PRB	0.95	0%	30%	1.2	16.9	344	1083	198
PRB	1.00	0%	30%	0.7	17.8	267	2380	145
PRB	1.05	0%	30%	0.6	17.5	30	3290	16
95-5 PRB-LADB	0.85	5%	30%	3.1	15.4	480	530	304
95-5 PRB-LADB	0.90	5%	30%	2.4	17.2	352	3020	197
95-5 PRB-LADB	0.95	5%	30%	0.9	17.8	331	1134	181
95-5 PRB-LADB	1.00	5%	30%	0.7	16.3	308	2340	182
95-5 PRB-LADB	1.05	5%	30%	0.8	15.8	284	4300	171
90-10 PRB-LADB	0.85	10%	30%	3.4	16.0	585	1603	354
90-10 PRB-LADB	0.90	10%	30%	2.0	17.5	577	1833	319
90-10 PRB-LADB	0.95	10%	30%	1.1	16.6	360	2256	210
90-10 PRB-LADB	1.00	10%	30%	0.8	18.2	350	7100	181
90-10 PRB-LADB	1.05	10%	30%	0.8	17.3	347	3295	193
85-15 PRB-LADB	0.85	15%	30%	3.1	15.9	573	1009	351
85-15 PRB-LADB	0.90	15%	30%	2.0	17.6	644	2167	354
85-15 PRB-LADB	0.95	15%	30%	0.9	16.3	384	7300	221